REPORT SERIES IN AEROSOL SCIENCE
N:o 232 (2020)

OBSERVATIONAL INSIGHTS ON THE EVOLUTION OF ORGANIC AEROSOL IN THE BOREAL ENVIRONMENT

LIINE HEIKKINEN

Institute for Atmospheric and Earth System Research (INAR) / Physics
Faculty of Science
University of Helsinki
Helsinki, Finland

Academic dissertation

To be presented, with the permission of the Faculty of Science of the University of Helsinki, for public criticism in Athena, Hall 107, Siltavuorenpenger 3A, on December 8th, 2020, at 16 o'clock.

Helsinki 2020

Author's Address: Institute for Atmospheric and Earth System Research / Physics
P.O. Box 64
FI-00014 University of Helsinki
liine.heikkinen@helsinki.fi

Supervisors: Associate professor Mikael Ehn, Ph.D.
Institute for Atmospheric and Earth System Research / Physics
University of Helsinki

Senior researcher Matthieu Riva, Ph.D.
Univ Lyon, Université Claude Bernard Lyon 1
CNRS France

Mikko Äijälä, Ph.D.
Institute for Atmospheric and Earth System Research / Physics
University of Helsinki

Reviewers: Professor Miikka Dal Maso, Ph.D.
Aerosol Physics Laboratory
Tampere University of Technology

Senior researcher Tomi Raatikainen, Ph.D.
Climate System Research
Finnish Meteorological Institute

Opponent: Professor Christopher Cappa, Ph.D.
Department of Civil and Environmental Engineering
University of California Davis

ISBN 978-952-7276-45-7 (printed version)
ISSN 0784-3496
Helsinki 2020
Unigrafia Oy

ISBN 978-952-7276-46-4 (pdf version)
http://www.atm.helsinki.fi FAAR
Helsinki 2020

Acknowledgements

The research conducted within this thesis was performed at the Institute for Atmospheric and Earth System Research (INAR) at the Faculty of Science of the University of Helsinki. I thank the heads of the Department of Physics and INAR, especially Academician Professor Markku Kulmala, for providing me the working facilities.

I thank Professor Miikka Dal Maso and senior researcher Tomi Raatikainen for reviewing my thesis and Professor Christopher Cappa for agreeing to serve as my opponent.

I thank my main supervisor, Associate Professor Mikael Ehn for guidance leading to the completion of this thesis. Thank you for always being available and your solid logic, which makes everything seem more simple.

I thank my supervisor senior researcher Matthieu Riva for showing me how much fun science can be and for believing in me.

I thank my supervisor Dr Mikko Äijälä for teaching me most of the skills I needed for this thesis and for his patience and kindness.

I thank Professor Douglas Worsnop and others at Aerodyne for the mass spectrometers and for bringing the instrument users together.

I thank the SMEAR II staff for the great summer in 2013 and for taking such good care of the ACSM. I also thank the INAR technical staff, especially Frans Korhonen, Pasi Aalto, Erkki Siivola and Pekka Rantala for all their work.

I thank all my co-authors, colleagues and friends: Otso Peräkylä, Kaspar Daellenbach, Krista Luoma, Olga Garmash, Lauriane Quéléver, Lisa Beck, Jenni Kontkanen, Kukka-Maaria Kohonen, Yanjun Zhang, Frans Graeffe, Diego Aliaga, Federico Bianchi, Minttu Tuononen, Veronika Pospisilova and Ian Chen among many others. I also thank Antoine Guillou and Leslie Brügger from the French office.

Finally, I thank my family and Charline for their love and support.

Observational insights on the evolution of organic aerosol in the boreal environment

Liine Heikkinen
University of Helsinki, 2020

Abstract

Aerosol particles, which are solid or liquid particles suspended in the air reduce air quality as well as influence Earth's radiative balance through their direct and indirect interactions with solar radiation. The sensitivity of Earth's climate to aerosol particles has remained elusive despite a wealth of studies conducted. Some of this uncertainty arises from the highly dynamic manner the physicochemical properties of aerosol particles evolve in the atmosphere. Recent advances in mass spectrometric measurement techniques have helped to assess the aerosol chemical (trans)formation altering many climate-relevant aerosol properties such as aerosol particle size, volatility and water affinity.

The scope of my thesis is the formation and evolution of organic aerosol (OA) in the boreal environment. Boreal forests emit a wide variety of volatile organic compounds (VOCs), which can form secondary organic aerosol (SOA) after oxidation. Notably, the mechanisms behind the VOC to SOA conversion is not straightforward and depends highly on the type of VOC, oxidants and ambient conditions, such as relative humidity (RH) and temperature (*T*) among others. This process can therefore be sensitive to the changes projected to take place within the boreal biome along with the changing climate. Changes regarding tree species can alter the composition and relative abundances of the emitted VOCs, which can further influence boreal SOA formation. Anthropogenic emissions can also affect natural VOC to SOA conversion and further SOA processing (aging) even in the pristine regions of the boreal biome. Due to attempts in air quality improvements in several locations worldwide, many anthropogenic species have shown declining trends with potential consequences in SOA formation and aging. Therefore, both boreal vegetation changes and anthropogenic emission regulations subject possible perturbations in both regional and global climate through SOA.

The studies conducted within this thesis can be divided into two categories: 1) examining the accumulated OA composition and its seasonal dynamics in the boreal forest to understand the present state of boreal OA (field studies), and 2) zooming in on the early stages of SOA formation and evolution and the potential impacts of anthropogenic emissions on them (laboratory studies). The measurements were conducted via online mass spectrometry. Obtaining results from the field required the retrieval of prevailing structures in the aerosol mass spectra recorded in real time (multidimensional data). This led to the development of an analysis framework utilising machine-learning tools for OA classification. The results highlight the importance of aged low-volatility oxygenated OA (LV-OOA) within the boreal environment throughout the year, with highly season-dependent sources. The LV-OOA production was found to be extremely sensitive to meteorological conditions, such as heat waves. In the laboratory, we examined the volatilities and fates of highly oxygenated organic molecules (HOMs), which form in boreal VOC oxidation. HOMs were shown to be primarily of low volatility and therefore good candidates as SOA precursors. In the presence of nitrogen oxides, which imply anthropogenic influence, HOMs of relatively higher volatilities were formed, potentially reducing HOM condensate formation. HOM condensate has been previously shown to be labile, and fragment quickly after formation. In our studies, this reaction was boosted in the presence of acidic aerosol particles. SOA formation was influenced by aerosol acidity also by significantly enhancing the SOA yield from semi- or intermediate volatility precursors and simultaneous oligomerisation reactions. The formation of high molecular weight oligomers significantly reduced SOA volatility.

The suite of studies conducted in this thesis succeeded in both the characterisation of the accumulated ambient OA and gaining new insight on the initial SOA formation and processing with and without anthropogenic influence in the boreal forest. However, the difference observed between the ambient LV-OOA and fresh laboratory SOA composition underlines the importance of photochemical aging needed for the formation of the highly oxidised ambient OA.

Keywords: OA, SOA, OA aging, aerosol chemical composition, aerosol acidity, monoterpenes, HOMs, volatility, AMS, CIMS, PMF, data classification.

Abbreviations

ACSM	Aerosol Chemical Speciation Monitor
AMS	Aerosol Mass Spectrometer
BC	Black carbon
BBOA	Biomass burning organic aerosol
CCN	Cloud condensation nuclei
CI-APi-TOF	Chemical Ionisation Atmospheric Pressure interface Time-of-Flight mass spectrometer
CIMS	Chemical Ionisation Mass Spectrometer
COALA	Comprehensive Molecular Characterisation of Organic Aerosol Formation in the Atmosphere
COA	Cooking-like organic aerosol
ELVOC	Extremely low volatility organic compound
FIGAERO	Filter Inlet for Gases and AEROsols
HOA	Hydrocarbon-like organic aerosol
HOM	Highly oxygenated organic molecule
IVOC	Intermediate-volatility organic compound
LVOC	Low volatility organic compound
m/Q	Mass-to-charge ratio
NR-PM_1	Non-refractory particulate matter with diameter less than 1 µm (mass concentration)
OA	Organic aerosol
PM	Particulate matter (mass concentration)
PM_x	Particulate matter with diameter less than x µm (mass concentration)
PMF	Positive Matrix Factorisation
POA	Primary organic aerosol
RH	Relative humidity
SMEAR II	Station for Measuring Ecosystem – Atmosphere Relations II
SOA	Secondary organic aerosol
SVOC	Semi-volatile organic compound
TOL	Time over land
UV	Ultra-violet
VOC	Volatile organic compound

Contents

List of publications

This thesis consists of an introductory review, followed by five research articles. In the introductory part, the papers are cited according to their roman numerals. All the research articles are reproduced under the Creative Commons Attribution 3.0 or 4.0 International Licenses.

I **Heikkinen, L.**, Äijälä, M., Riva, M., Luoma, K., Daellenbach, K.R., Aalto, J., Aalto, P., Aliaga, D., Aurela, M., Keskinen, H., Makkonen, U., Rantala, P., Kulmala, M., Petäjä, T., Worsnop, D., and Ehn, M.: Long-term sub-micrometer aerosol chemical composition in the boreal forest: inter- and intra-annual variability, *Atmos. Chem. Phys.*, https://doi.org/10.5194/acp-20-3151-2020, 2020.

II **Heikkinen, L.**, Äijälä, M., Daellenbach, K.R., Gang, C., Garmash, O., Aliaga, D., Graeffe, F., Räty, M., Luoma, K., Aalto, P., Kulmala, M., Petäjä, T., Worsnop, D., Ehn, M.: Eight years of organic aerosol composition data from the boreal forest characterized using a machine learning approach. *Atmos. Chem. Phys. Discuss.*, https://doi.org/10.5194/acp-2020-868, in review, 2020.

III Äijälä, M., **Heikkinen, L.**, Fröhlich, R., Canonaco, F., Prévôt, A. S. H., Junninen, H., Petäjä, T., Kulmala, M., Worsnop, D., and Ehn, M.: Resolving anthropogenic aerosol pollution types – deconvolution and exploratory classification of pollution events, *Atmos. Chem. Phys.*, https://doi:10.5194/acp-17-3165-2017, 2017.

IV Peräkylä, O., Riva, M., **Heikkinen, L.**, Quéléver, L., Roldin, P., and Ehn, M.: Experimental investigation into the volatilities of highly oxygenated organic molecules (HOMs), *Atmos. Chem.Phys.*, https://doi.org/10.5194/acp-20-649-2020, 2020.

V Riva, M., **Heikkinen, L.**, Bell, D.M., Peräkylä, O., Zha, Q., Schallhart, S., Rissanen, M.P., Imre, D., Petäjä, T., Thornton, J.A., Zelenyuk, A., Ehn, M.: Chemical transformations in monoterpene-derived organic aerosol enhanced by inorganic composition. *npj Clim Atmos Sci*, https://doi.org/10.1038/s41612-018-0058-0, 2019.

1 Introduction

The English word '*atmosphere*' originates from the Ancient Greek words for vapour (ἀτμός [atmós]) and sphere (σφαῖρα [sphaîra]). Vapours are gases, which can relatively easily undergo phase transitions, mainly through condensation (gas → liquid). Examining the composition of the atmosphere, we can see that 99% of it is made up of nitrogen and oxygen molecules (N_2 and O_2). Neither of these gases can be defined as vapours under any natural atmospheric condition. While such a statement could make us question the preciseness of the word '*atmosphere*', the importance of the existing vapours in the atmosphere speaks for the choice of name.

Water vapour is the most abundant vapour in the atmosphere. It acts as a natural greenhouse gas, which accounts for a large fraction of the natural warming of the atmosphere. Without the naturally occurring greenhouse effect, Earth's average surface temperature would be only -19 °C (Le Treut et al., 2007). The ability of water to undergo phase transitions also provides other extremely crucial effects sustaining life on Earth. The hydrological cycle ties together the atmosphere, land and ocean via a global water circulation loop. While not attempting to give a full detailed review on the cycle, the atmospheric part of it could be alternatively called as the cloud life cycle. It consists of the following basic principles: evaporation of water from the Earth's surface, lifting of humid air from the surface to a higher altitude and simultaneous cooling of the air, when condensation of water vapour onto cloud seeds takes place. The process then continues by the growth of the cloud droplets, which finally precipitate down to the surface.

The formation of clouds influences the Earth's radiation budget. This happens through the reflection of incoming solar radiation, which causes a cooling effect, as well through trapping of longwave (infrared) radiation, which causes a warming effect. Importantly, as an average these opposing phenomena do not cancel each other out and clouds provide a net cooling effect of clouds to the Earth-atmosphere system. The extent of this cooling effect is sensitive to the number of cloud seeds. In fact, through cloud seeding, cloud formation may take place at significantly lower water vapour supersaturation than cloud formation would require in particle free air. By increasing the number of cloud seeds and thus cloud droplets, clouds become brighter and their precipitation efficiency reduces (Twomey, 1974;Twomey, 1977;Albrecht, 1989;Lohmann and Feichter, 2005;Boucher et al., 2013). As a result, clouds comprising numerous small cloud droplets introduce a longer lasting cooling effect on climate compared to a cloud containing fewer and larger cloud droplets (e.g. Lohmann and Feichter, 2005; Boucher et al., 2013).

The cloud life cycle is influenced also by other vapours than just water vapour. This is linked to the cloud seeds, which consist of atmospheric particulate matter (PM), i.e. solid or liquid aerosol particles suspended in the air. The importance of these other vapours comes into play when PM is formed in the atmosphere, either in the process forming new particles or via growing pre-existing ones. The biosphere is a significant source of volatile organic compounds (VOCs; e.g. Guenther et al., 2012; Li et al 2020a; Li et al., 2020b), which yield condensable organic vapours in atmospheric oxidation processes (Peräkylä, 2020). Ozone

(O_3), OH radical (OH) and nitrate radical (NO_3) represent the most influential atmospheric oxidants (Seinfeld and Pandis, 2016). The condensation and/or uptake of the produced organic vapours form secondary organic aerosol, SOA (Ziemann and Atkinson, 2012).

Approximately 50% of the tropospheric fine particulate matter is organic (Murphy et al., 2006;Zhang et al., 2007;Jimenez et al., 2009). The total atmospheric organic aerosol (OA) comprises the directly emitted primary OA (POA) and SOA. Most of the mass has been connected to SOA (Zhang et al., 2007). While several inorganic aerosol species can be relatively easily connected to various sources, determining OA formation pathways and distinguishing biogenic processes from anthropogenic ones remains elusive (Hallquist et al., 2009;Shrivastava et al., 2017). This is e.g. due to the long distances aerosol particles can travel, the high number of POA sources and the complexity of SOA formation processes from possibly tens of thousands of precursors (Goldstein and Galbally, 2007). In addition, estimating biogenic SOA formation can be challenging due to influence of anthropogenic emissions, such as those of sulphur dioxide (SO_2), nitrogen oxides (NO_x) or amines, which can significantly influence SOA formation and properties (Shrivastava et al., 2017;Xu et al., 2015;Marais et al., 2016). Last, but not least, the composition of nearly any OA type hardly stays constant. These physical and/or chemical transformations of OA composition further influence OA physicochemical properties such as particle size, water affinity (hygroscopicity), volatility and viscosity (e.g. Jimenez et al., 2009; Riva et al., 2019a).

The growth of particles through condensation of organic and inorganic vapours is important, because this way small particles can reach climate-relevant sizes (Scott et al., 2014;Riipinen et al., 2012). While large particles facilitate cloud formation under ambient supersaturations, they also interact with incoming solar radiation more efficiently (Boucher et al., 2013;Seinfeld and Pandis, 2016). In addition to the size of aerosol particles, also their chemical composition influences aerosol-radiation interplay either directly or via clouds. For example, if PM consists of hygroscopic material, such as inorganic salts, cloud droplet formation is favoured over a scenario, where PM comprises hydrophobic material such as soot (McFiggans et al., 2006;Petters and Kreidenweis, 2007). In addition, light-coloured salt crystals scatter radiation efficiently, whereas dark-coloured soot particles absorb it (Boucher et al., 2013).

During the industrialised era, humankind has drastically altered the composition of the air (Stocker et al., 2013). The Intergovernmental Panel for Climate Change (IPCC) has been founded to assess the extent to which these anthropogenic emissions influence the future climate. In these estimates, where the warming effect of greenhouse gases is predicted with high confidence in various projected future emission scenarios, the cooling effect of aerosols, especially that related to clouds, has remained the most uncertain factor (Stocker et al., 2013). Therefore, in order to improve projections of the future climate these aerosol effects must be carefully assessed (e.g. Seinfeld et al., 2016; Ghan and Schwartz, 2007). This is where aerosol measurements become crucial (Ghan and Schwartz, 2007;Kulmala, 2018). Comparisons between long-term measurement data and a global climate model or a chemical transport model outputs can be used as tools to evaluate a model performance and accuracy or to pinpoint processes not well replicated by the model. These comparisons could be most useful among the most important aerosol parameters such as aerosol size distribution,

chemical composition, and other physicochemical properties (Ghan and Schwartz, 2007). Importantly, to ensure good comparability among ambient data sets and models, long-term measurement data are needed with clear measurement and data processing guidelines. Luckily, a majority of the long-term measurements are nowadays conducted as parts of large research networks, such as Global Atmospheric Watch (GAW), the Research Infrastructure for the observation of Aerosol, Clouds and Trace Gases (ACTRIS) or the Interagency Monitoring of Protected Visual Environments (IMPROVE), with these specific aims of improving data comparability between sites. Due to the high amounts of data collected, utilisation of data-driven machine learning techniques might further lead also the analyses to yet more streamlined directions in the future.

The necessity of long-term measurements can be argued with multiple points. One of them is that they reduce the weight given by abnormal conditions, such as extreme weather phenomena, on the model comparisons. Furthermore, only long-term measurements help capture the inter- and intra-annual variabilities of e.g. the measured aerosol properties at the measurement location. Still, the high number of atmospheric chemical constituents and the myriad of reactions they can undergo hampers resolving key atmospheric chemical processes from ambient measurements. Therefore, mapping of potential processes is/should be conducted via laboratory studies using atmospheric reaction chambers. The significance of discovered processes should be further evaluated with modelling efforts (Ghan and Schwartz, 2007). Such assessment could help narrowing down the detail of aerosol properties or processes needed to be incorporated in global models (Boucher et al., 2013).

Although a global spatial coverage of long-term measurements of key aerosol properties is much desired, the initial measurements should be prioritised to take place in environments showing vulnerability to the changing climate and/or anthropogenic emissions (Kulmala, 2018). The measurements conducted at the boreal Station for Measuring Ecosystem Atmosphere Relations (SMEAR II) serve as a forerunner in the comprehensive measurements tracking the boreal Earth-Atmosphere interface (Hari and Kulmala, 2005;Kulmala, 2018). In addition, SMEAR II provides crucial information of the biosphere-atmosphere exchange in the boreal forest, where major changes are projected with the changing climate. These include e.g. the vegetation zones' spanning to the North as a result of Arctic greening as well as the spread of southerly tree species to the southern parts of the biome (Prăvălie, 2018;Settele et al., 2014). Such disturbances can further lead to changes in the composition of the atmosphere, for example through changes in concentrations and relative abundances of emitted VOCs. Currently, the monoterpenes, such as α-pinene, represent the dominantly emitted VOCs in the boreal forest (Rinne et al., 2009). If southerly tree species were to spread to the boreal biome, this could enhance the relative abundance of isoprene in the boreal air. Changes in the relative proportions of these vapours can further propagate to changes in SOA formation potential (McFiggans et al., 2019) and ultimately influence both regional and global climate.

1.1 Thesis aims

The potential of boreal forests producing significant amounts of climate-relevant SOA motivated the OA focus of this thesis. The studies conducted here comprise both long-term OA data from SMEAR II and laboratory experiments. The measurements were conducted via online mass spectrometry, which has been a popular approach for studying near real-time evolution of both OA and oxidised organic vapours (Canagaratna et al., 2007;Thornton et al., 2020;Bianchi et al., 2019). As the OA detected in the field contains unknown fractions of various OA constituents, a suite of statistical tools including machine learning applications were applied for the OA classification. Process-level studies related to biogenic SOA formation and evolution, and in particular the effects of anthropogenic emissions on those, were conducted in the laboratory. The scientific goals to be addressed are:

(1) Develop a statistical analysis framework for OA classification in rural or remote regions (**Papers II** and **III**).
(2) Determine the driving constituents of boreal OA and their inter- and intra-annual variabilities in the boreal forest (**Papers I** and **II**).
(3) Assess the volatilities of condensable vapours in the boreal forest (**Paper IV**).
(4) Assess the influence of anthropogenic pollutants in boreal SOA formation (**Papers IV** and **V**).
(5) Determine the types of chemical transformations taking place in fresh boreal SOA with or without anthropogenic influence (**Paper V**).

2 Organic aerosol life cycle

This chapter summarises the basic scientific understanding of OA formation (Sect. 2.1) and evolution (Sect. 2.2) in the atmosphere, which provides the most crucial background to the thesis work. In addition, atmospheric aerosol dilution, scavenging and sink mechanisms including dispersion (Sect. 2.3), deposition (Sect. 2.4) and cloud droplet formation (Sect. 2.5) are briefly described.

2.1 Formation

The emissions of OA (Sect. 2.1.1) and formation through secondary processes (Sect. 2.2.2) is a highly studied topic in atmospheric sciences. This section introduces the major OA constituents originating from primary emissions, and then focuses on SOA formation emphasising the description of the formation of highly oxygenated organic molecules (HOMs), the discovery of which serves as one of the most recent advances in atmospheric chemistry. In general, the content given in this section is written so that it supports the topics of this thesis. Therefore, details regarding SOA formation in urban environments or deciduous forests such as the Amazon have been given only little if any attention. Thus, for a more comprehensive SOA formation overview on a global scale, I direct the reader to Hallquist et al. (2009) and Shrivastava et al. (2017).

2.1.1 Primary organic aerosol (POA)

The directly emitted POA originates from a wide range of sources. Based on current knowledge, the most significant ones are biomass burning and fossil fuel combustion (Bond et al., 2004). The POA emitted from biomass burning is typically referred to as biomass burning OA (BBOA) and the POA emissions from fossil fuel combustion are characterised as hydrocarbon-like OA (HOA). While primary biological particles such as pollen, bacteria and viruses could also be categorised as POA and represent important POA sources within the boreal forest, they are not discussed within this thesis. Still, these particles have shown climate relevance e.g. through acting as seeds for cloud droplets or ice crystals (Schnell and Vali, 1976;Ariya et al., 2009) and therefore, further understanding of their roles in the climate system is important.

BBOA can be distinguished by its high mass fractions of various sugars, such as levoglucosan, originating from cellulose pyrolysis (Schneider et al., 2006;Alfarra et al., 2007;Simoneit et al., 1999). Globally, the highest BBOA emissions come from open wild and agricultural fires taking place most intensely at low latitudes (Bond et al., 2004;De Gouw and Jimenez, 2009). BBOA concentrations also exhibit high values in various residential areas, where domestic wood burning takes place (Bond et al., 2004;Jiang et al., 2019). These emissions can be transported even up to the high Arctic (Winiger et al., 2017). Black carbon (BC) and carbon monoxide (CO) are typically produced in all biomass burning events whereas the simultaneously emitted vapours largely depend on the burning material (e.g. Coggon et al., 2016). The significance of these co-emitted vapours is discussed in section 2.2.

HOA comprises mostly hydrocarbons and its concentrations are typically high near roads with heavy traffic (e.g. Zhang et al., 2005, 2007) as a large fraction of it presumably originates from diesel exhaust (Canagaratna et al., 2010;Jiang et al., 2019). Therefore, it typically correlates well with other traffic emissions, such as NO_x or black carbon (BC) and several aromatic VOCs such as benzene and toluene.

2.1.2 Secondary organic aerosol (SOA)

The large role of biogenic VOCs in atmospheric chemistry, especially in processes forming (blue) haze, have been first discussed already in the 1960s (Went, 1960). In his paper, Dr. Went proposed the formation of submicroscopic particles from terpene oxidation by ozone, which interacted with solar radiation resulting in blue haze. Similar formation of secondary organic aerosol (SOA) has been the focus of wealth of studies ever since (Hallquist et al., 2009;Shrivastava et al., 2017). While the budgets of anthropogenic SOA might be still heavily underestimated, natural sources are believed to surpass the anthropogenic ones (e.g. De Gouw and Jimenez, 2009, and references therein).

Atmospheric VOC oxidation has been extensively studied and documented (Atkinson and Arey, 2003;Vereecken and Francisco, 2012;Ziemann and Atkinson, 2012;Orlando et al., 2003). However, atmospheric autoxidation of VOCs yielding highly oxygenated species was discovered to be atmospherically relevant only recently (Bianchi et al., 2019;Ehn et al., 2014). HOMs are defined as products formed via atmospheric autoxidation involving peroxy radicals (RO_2; Bianchi et al., 2019; Crounse et al., 2013).

Figure 1 summarises the formation and chemical reactions that RO_2 typically undergo in the atmosphere (Atkinson and Arey, 2003;Ziemann and Atkinson, 2012). In brief, RO_2 radicals form fast after the initial oxidation steps between VOCs and the most common atmospheric oxidants such as OH, O_3 or NO_3. The oxidation first yields an alkyl radical (R), which then forms a peroxy radical (RO_2) upon addition of molecular oxygen (O_2). RO_2 radicals represent one of the key intermediates in the oxidation of organic compounds along with alkoxy radicals (RO), which can form in the reaction between RO_2 and nitrogen monoxide (NO) or another RO_2, for example (Fig. 1).

Under the autoxidation mechanism yielding a HOM, an RO_2 undergoes an intramolecular shift of a loosely bound hydrogen atom (H-shift). The H-shift moves the H-atom to the peroxy radical centre, which yields both a new hydroperoxide functionality, where H is added, and a carbon-centred radical, where H is abstracted. This step enables the addition of molecular oxygen (O_2) to the carbon-centred radical unit without making changes in the number of carbon or hydrogen. The addition of O_2 to the compound transforms the species back to RO_2, however now possessing two more oxygen atoms. If the new form of the RO_2 is suitable, the same steps (H-shift and O_2 addition) can reoccur several times in the gas phase before the autoxidation is terminated via uni- or bimolecular reactions.

The unimolecular termination refers to the fragmentation of a small radical, such as OH, from the RO_2 yielding a closed-shell product. In the bimolecular pathway, the closed-shell

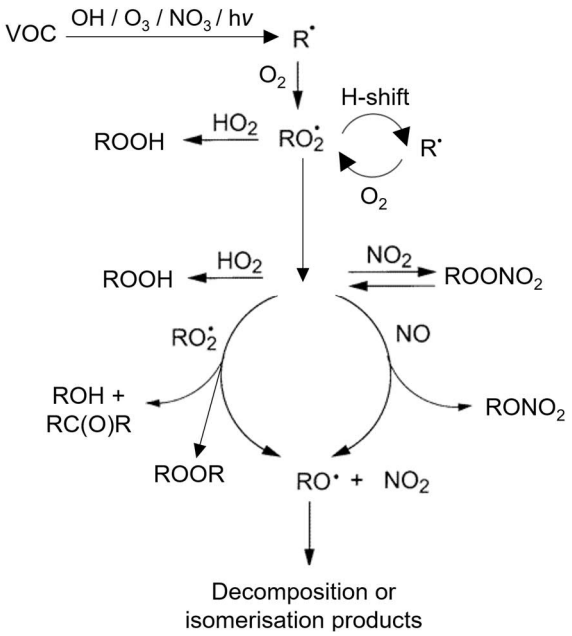

Figure 1. A diagram simplifying the major VOC oxidation pathways in the atmosphere. The figure is adapted from Atkinson and Arey (2003) and Ziemann and Atkinson (2012) by adding the autoxidation loop (H-shift + O_2 addition; Bianchi et al., 2019) in connection to the initially formed RO_2 and the formation of dimers (ROOR) upon RO_2 + RO_2 reaction (Berndt et al., 2018).

product forms in the reaction between the autoxidised RO_2 and NO, HO_2 or another RO_2 (Crounse et al., 2013;Bianchi et al., 2019). Importantly, as mentioned before, such bimolecular reactions can also yield RO. The RO can further undergo H-shifts and O_2 additions ultimately yielding yet another RO_2 (Orlando et al., 2003;Crounse et al., 2013;Bianchi et al., 2019).

The composition of the closed-shell product strongly depends on the termination pathway. For example, the autoxidation termination with NO can yield an organic nitrate (Ehn et al., 2014) whereas termination with another RO_2 can produce a covalently bound dimer (Berndt et al., 2018). In the case of autoxidation following α-pinene ($C_{10}H_{16}$) ozonolysis, these dimers can compose of 20 carbons, whereas the NO termination would not change the carbon number unless fragmentation of the carbon skeleton takes place.

The volatilities of the oxidised VOCs (OVOCs incl. HOMs) determine their abilities to condense and form SOA. While some of the OVOCs have too high volatilities to be found in significant mass fractions in the particle phase, others possess volatilities so low that they can even nucleate to form new particles (Kirkby et al., 2016). The OVOCs are typically grouped in the following classes as suggested by Donahue et al. (2012b;2006): intermediate-volatility VOCs (IVOCs), semi-volatile VOCs (SVOCs), low-volatility VOCs (LVOCs) and extremely low-volatility VOCs (ELVOCs). Each of these classes is characterised by volatility, or more precisely in terms of effective saturation vapour concentration (C^*; saturation vapour pressure converted to concentration; Donahue et al., 2006; Epstein et al., 2010), which is temperature-dependent (resulting from the Clausius-Clapeyron equation; e.g. Sandler, 2017). These classes, as defined by Donahue et al. (2012b), spread in the C^* ranges of $300 < C^* < 3\times10^6$ µg m^{-3} (IVOCs), $0.3 < C^* < 300$ µg m^{-3} (SVOCs), $3\times10^{-4} < C^* < 0.3$

μg m^{-3} (LVOCs), $C^* < 3\times10^{-4}$ μg m^{-3} (ELVOCs), respectively. Notably, also other divisions do exist (e.g. Pye and Seinfeld, 2010). As it can be spotted e.g. from the Donahue (2012b) C^* divisions, the volatility bins are spread in powers of 10 and therefore the volatility distribution spreads over several orders of magnitude. ELVOCs can be expected to be found almost entirely in the condensed phase under any atmospheric condition, whereas SVOCs can be found in significant concentrations in both phases and for IVOCs, the gas phase presence is highly dominating.

The species resulting from autoxidation commonly contain high O:C ratios (even up to ~1) and are defined as HOMs in case the number of oxygen atoms exhibits six (Bianchi et al., 2019). Due to the high number of oxygen atoms present in the various polar functional groups, the volatilities of HOMs are expected to be low or extremely low (Bianchi et al., 2019). Hence, they are suggested to significantly contribute to SOA formation via condensation despite the relatively small monoterpene-HOM molar yields (≤ 17% for the systems studied; Bianchi et al., 2019; Ehn et al., 2014; Jokinen et al., 2015).

A simplified schematic of α-pinene autoxidation in an oxidation state ($\overline{OS_c} \approx 2 \times O{:}C - H{:}C$) vs. the effective saturation vapour concentration (C^*) space is visualised in Figure 2. It shows how functionalisation taking place in the traditional step-wise oxidation not including autoxidation (red dashed arrows) leads to less oxidised species compared to the functionalisation via the autoxidation mechanism (red solid arrow). While the accretion reactions between the step-wise formed oxidation products can form covalently bound higher molecular weight species (ester formation) in the particle phase, their volatilities remain above those of the dimers yielded via $RO_2 + RO_2$ autoxidation termination reaction (Barsanti et al., 2017). The figure highlights importance of the HOM discovery, which yields oxidised low-volatility species much more efficiently than the step-wise chemistry (Barsanti et al., 2017).

Due to the relatively high concentration of monoterpenes, especially α-pinene, in the boreal forest (Hakola et al., 2012), HOMs are ubiquitous in the boreal air (e.g. Ehn et al., 2012; Yan et al., 2016). These HOMs have been shown to play an important role explaining the growth of newly formed particles (Mohr et al., 2019;Tröstl et al., 2016;Riipinen et al., 2011;Öström et al., 2017). In addition, they presumably explain a significant mass fraction of summertime boreal OA (Roldin et al., 2019). However, not all biogenic SOA is HOM condensate. SVOCs form substantial amounts of SOA via condensation onto larger particles as well as via multiphase chemistry involving their reactive uptake (Jang et al., 2002). Reactive uptake could potentially occur also on the smallest particles contributing to the nanoparticle growth (Wang et al., 2010).

Despite the large amount of various mechanisms yielding SOA in the atmosphere, SOA is typically grouped into two bins based on its volatility and degree of oxygenation: low-volatility oxygenated OA (LV-OOA) and semi-volatile oxygenated OA (SV-OOA) (Fig. 3). This grouping method originates from Aerosol Mass Spectrometer (AMS; Sect. 3.2) data interpretation, which is known to preserve only little chemical detail due to molecular fragmentation (Sect. 3.2), disconnecting the observations from the actual SOA formation mechanisms. Therefore, this OA description can be linked to instrumental limitations of separating various SOA types. Due to a strong presence of LV-OOA being observed all over the

Northern Hemisphere (Zhang et al., 2007), questions regarding the stability of freshly emitted or of the formed OA composition began to rise. Hints of OA transformations were provided e.g. by the more volatile and less oxygenated SOA formed in chambers mismatching the field observations and the increasing amounts of LV-OOA in urban outflows and the simultaneous decreases in POA concentrations not explainable by atmospheric dilution. This brings us to the next section, which examines the dynamic behaviour of OA composition and loading in the atmosphere.

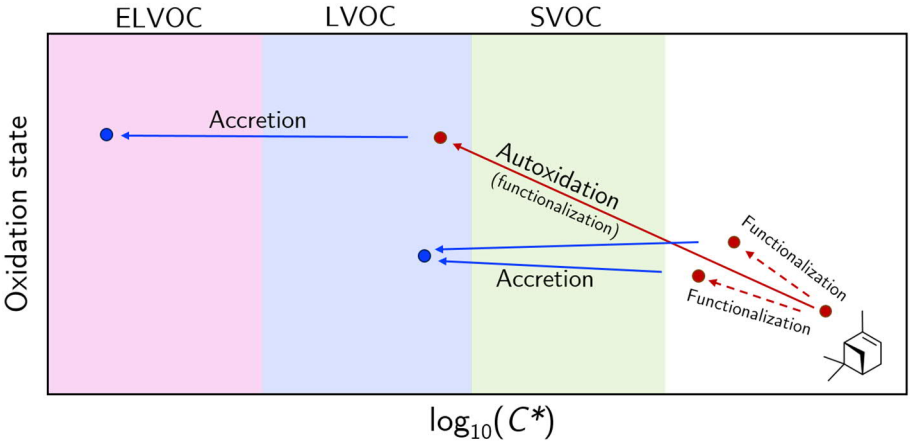

Figure 2. A simplified diagram of the production of condensable vapours from α-pinene (molecule drawn in the lower right corner) oxidation in the gas phase visualised in an oxidation state ($\overline{OS_c} \approx 2 \times O{:}C - H{:}C$; Kroll et al., 2011) vs $\log_{10}(C^*)$ space. The schematic illustrates how functionalisation via RO_2 autoxidation yields low volatility vapours, which can yield even extremely low volatility products upon accretion reactions between two autoxidised RO_2 radicals. The figure is redrawn based on Barsanti et al. (2017).

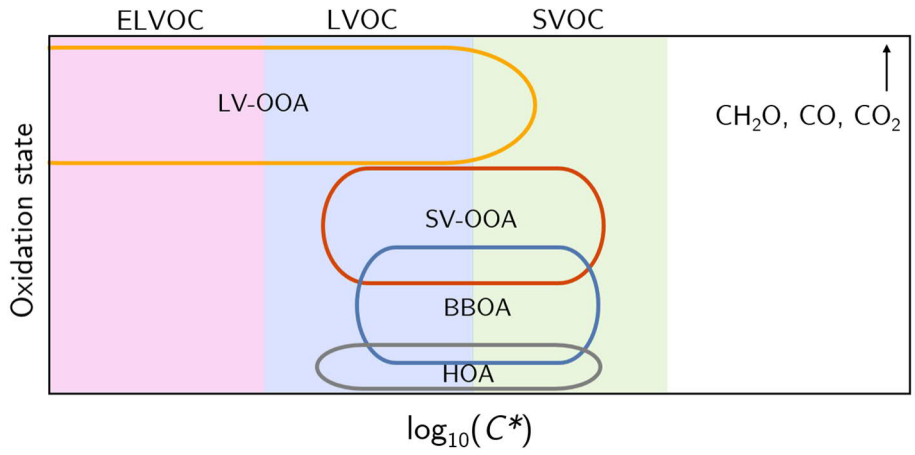

Figure 3. Volatilities and oxidation states ($\overline{OS_c} \approx 2 \times O{:}C - H{:}C$) of common OA constituents: low-volatility oxygenated OA (LV-OOA), semi-volatile oxygenated OA (SV-OOA), BBOA and HOA. LV-OOA is of lowest volatility and most oxidised of these types, whereas HOA is the most volatile and least oxygenated OA species (e.g. Cappa and Jimenez, 2010). The final oxidation products of organics (CH_2O, CO and CO_2) are located beyond the top right corner of the graph (highest oxidation state and volatility), towards which also atmospheric oxidation processes regarding organic matter also move. The figure is adapted and redrawn based on Donahue et al. (2012b).

2.2 Aging

While SOA formation has achieved plenty of scientific focus, the sinks of SOA, including chemical transformation (i.e. aging), have remained a far less studied topic. The concentration and composition of OA are highly dynamic in the atmosphere. The mechanisms altering OA properties with aging are categorised as functionalisation, fragmentation and accretion/oligomerisation reactions (e.g. Jimenez et al., 2009). Typically, fresh OA evolves in the atmosphere towards higher oxidation states ($\overline{OS_c} < -0.5 \rightarrow \overline{OS_c} > 0$) and lower volatilities. In Figure 3, this shifts the various fresh SOA and POA types towards the region where LV-OOA is located (Jimenez et al., 2009). A recent study, which tracked the composition of both gas and particle phases upon OA evolution further reported that upon the formation of the low-volatility SOA (i.e. LV-OOA), significant changes took place also in the gas phase. Two major carbon reservoirs were formed: one of condensed low volatility SOA and one of oxidised high volatility gases (Fig. 4; Isaacman-VanWertz et al., 2018). The next sections discuss the major processes explaining these phenomena including both gas-phase and heterogeneous OA aging processes.

2.2.1 Homogeneous aging through gas phase

In order to elaborate on the gas phase photochemical OA processing, it is important to denote that fresh SOA or POA have been typically characterised as semi-volatile (Cappa and Jimenez, 2010). Fluxes of vapours between the gas and condensed phases tend to move the aerosol system towards equilibrium. Some studies suggest low kinetic limitations in gas-to-particle equilibration rates for common OA types (Liu et al., 2019;Saleh et al., 2013), but others suggest it can be significantly hindered by particle phase state or viscosity (Shiraiwa and Seinfeld, 2012;Cappa and Wilson, 2011). Still, perturbations in one phase on certain species' loading will make the system drift from the equilibrium state, which can trigger phase transitions to rebuild the balance if kinetic limitations are minimal. The sensitivities of SOA and POA to changes in the gas phase composition have been demonstrated and further linked to their chemical transformations (Donahue et al., 2012a;Robinson et al., 2007;Hennigan et al., 2011).

Let us investigate first fresh SOA from α-pinene oxidation due to the boreal focus of this thesis. The oxidation of α-pinene yields several OVOCs, such as pinonaldehyde (C^* ca. 10^4 μg m^{-3} at 300 K) or pinic acid (C^* ca. 10 μg m^{-3} at 300 K). Pinonaldehyde represents the major α-pinene oxidation product with yields up to 25–50% (Hatakeyama et al., 1991). The first generation oxidation products of α-pinene can be found in both gas and particle phases. The extent to which they are found in the particle phase is much linked to their C^*. The lifetimes of these α-pinene first generation oxidation products are significantly shorter than the lifetime of α-pinene-derived SOA. For example, in a summer day the lifetime of pinonaldehyde is in order of hours (Vereecken and Peeters, 2002), whereas the lifetime of aerosol particles can be up to a week (Wagstrom and Pandis, 2009). Pinonaldehyde is efficiently consumed in the gas phase by photolysis or oxidation (Finlayson-Pitts and Pitts Jr, 1999;Glasius et al., 1997). These losses disturb the equilibrium achieved between phases. The equilibrium perturbation can then trigger evaporation of the corresponding molecules,

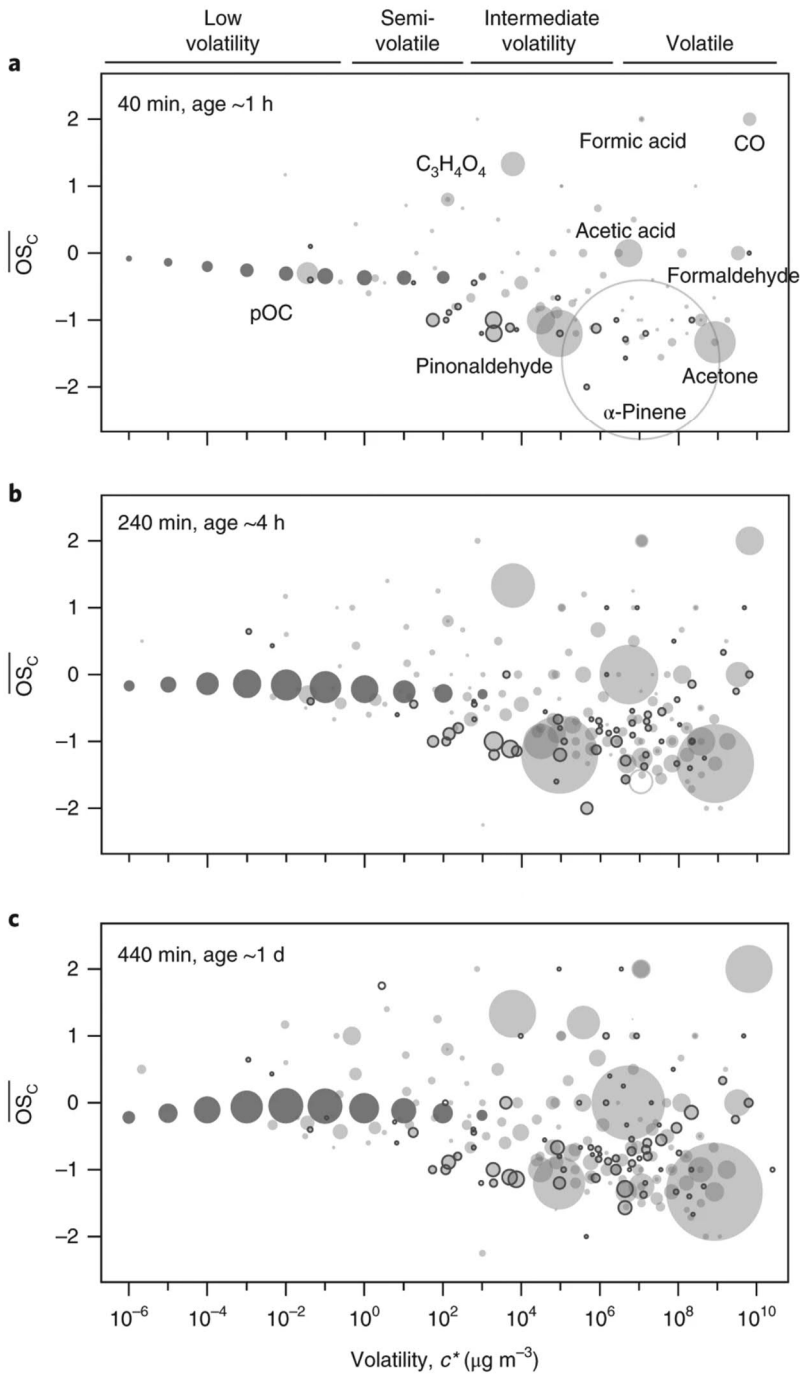

Figure 4. Photo-oxidation products of α-pinene in the gas and particle phases visualised in the oxidation state vs. volatility space. The panels represent the product distributions after 40 minutes, 4 hours and 7 hours of oxidation, respectively. These conditions are equivalent of ca. 1 hour, 4 hours and 1 day of aging in the atmosphere, respectively. The size of the markers depicts the carbon concentrations. The α-pinene concentration is shown with a hollow circle in panel **a**. Its absence in the following panels indicates its depletion. Other gas phase species are shown in light grey. Some of them, such as pinonaldehyde, are formed in the beginning of the experiment and then depleted in the end. Others, such as CO, become gradually more significant over the course of time. Particle phase products are printed in dark grey. The rapid increase in the oxidation state and decrease in volatility are visible when comparing panel **a** to panels **b** and **c**. Reprinted with permission from Isaacman-VanWertz et al. (2018). Copyright © 2018 Springer Nature.

such as pinonaldehyde, from the aerosol particle. Upon the gas phase OH (or NO_3) oxidation of α-pinene first generation oxidation products, it is likely that the oxidation products are of lower volatility and condense to the particle phase (Chacon-Madrid et al., 2013;Donahue et al., 2012a). These phase transitions and chemical reactions result in more oxygenated SOA and lowers its volatility.

Equivalent transformations of semi-volatile POA types, such as diesel exhaust HOA or BBOA have been highlighted (Robinson et al., 2007;Hennigan et al., 2011). For example, Robinson et al. (2007) described partial evaporation of POA due to atmospheric dilution (Shrivastava et al., 2006) and substantial generation of SOA through the particle phase partitioning of the oxidation products of the initially evaporated species. This functionalisation mechanism yielded more regionally distributed OA and its incorporation to models generated an improved agreement with observations from urban environments (Tsimpidi et al., 2010). In the case of biogenic SOA, similar modelling efforts tend to overshoot the SOA concentrations (Lane et al., 2008;Pai et al., 2020;Shrivastava et al., 2015), which indicates the importance of incorporating also fragmentation processes. Fragmentation of gas phase species, such as pinonaldehyde due to photolysis reduce the SOA yield and the degree of functionalisation from multigenerational oxidation significantly (Chacon-Madrid and Donahue, 2011).

Shrivastava et al. (2015) performed a modelling exercise, where the initial POA or SOA were considered non-volatile, but the gas phase multigenerational oxidation (functionalisation) and fragmentation processes were both incorporated. The SOA yielded upon aging was treated either semi-volatile or non-volatile. A key message from this study was that if the oxidation of IVOCs and SVOCs co-emitted with POA was taken into account, especially in the case of BBOA, the yielded SOA burden could surpass that of biogenic SOA in both scenarios (Fig. 5 for the non-volatile scenario). Moreover, the agreement between aircraft measurements and the model output improved significantly when the BBOA-derived SOA yield was considered. Interestingly, over areas rich with biogenic SOA, the best agreement with ground-based measurements and the model was obtained when the SOA formed upon aging was treated as non-volatile. The authors related this to the potential importance of particle phase aging through oligomerisation (Shiraiwa et al., 2013).

While the results given by Shrivastava et al. (2015) are highly interesting and promote the importance of multigenerational aging in the atmosphere, it should be remembered that they carry large uncertainties. Some of them can be linked to the assumption of POA being non-volatile upon emission, which can lead to SOA overestimation, and some link to the magnitudes of the co-emitted SVOC and IVOC concentrations, for example. In addition, in the real atmosphere the aging processes are potentially strongly affected by the highly complex heterogeneous and condensed phase OA processing, which can influence both OA concentration and volatility in various ways (George and Abbatt, 2010). These processes can further disturb any thermodynamic equilibria and thus alter also the partitioning from the gas phase.

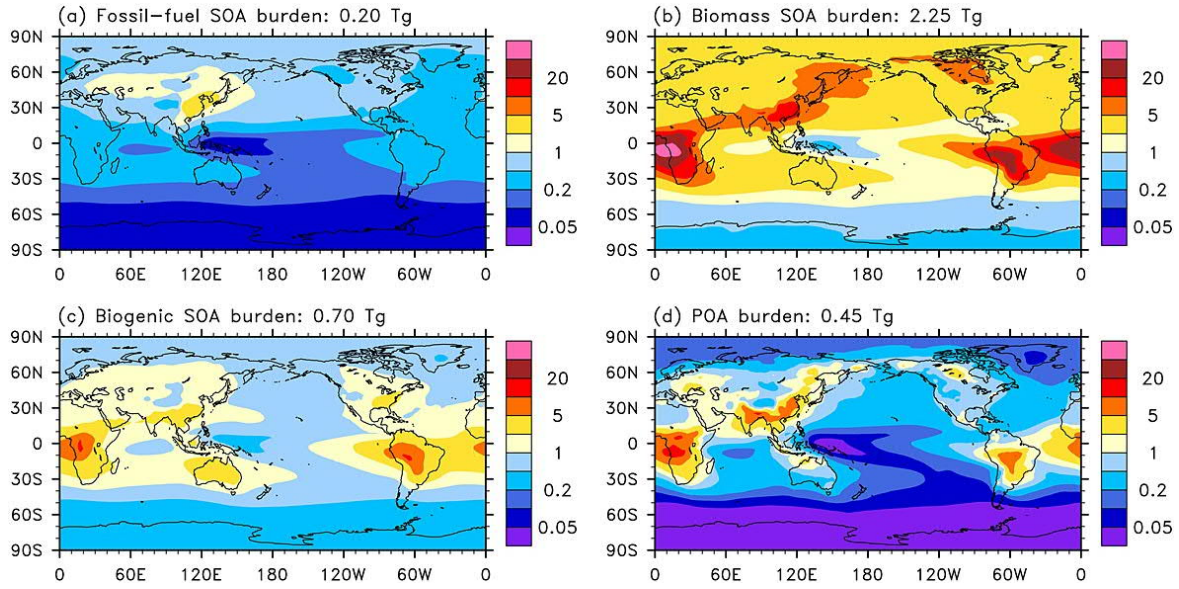

Figure 5. A snapshot of results from a modelling study performed by Shrivastava et al. (2015). The panels **a-c** depict the global SOA production from fossil fuel, biomass burning and biogenic (S)OA, when multigenerational gas phase aging including both functionalisation and fragmentation reactions, has been incorporated in the modelling framework. Importantly, these scenarios visualised are following the assumptions of non-volatile POA (fossil fuel emissions + biomass burning emissions, panel **d**) upon emission and non-volatile SOA condensate formation upon aging. The figure highlights the high potential of SOA formation from biomass burning, potentially surpassing that of biogenic SOA. Still, the complexity of the atmospheric aging requires more research for the final quantifications of atmospheric aging on e.g. biomass burning SOA burden. Reprinted with permission from Shrivastava et al. (2015). Copyright © 2015 John Wiley and Sons.

2.2.2 Heterogeneous aging

While the reaction rate between gas phase OH (or NO_3) and particulate species is several times slower than the reaction between OH (or NO_3) and the same compound in the gas phase (Lambe et al., 2009), it is still much shorter than typical life times of OA. It is therefore highly likely that some fraction of the aging occurs through OH (or NO_3) uptake upon collisions and subsequent oxidation in the particle phase (Donahue et al., 2012a;George and Abbatt, 2010;Kroll et al., 2015). The heterogeneous oxidation of hydrocarbons happens somewhat similarly as in the gas phase (Fig. 1), however the relative importance between pathways might be different in the condensed phase and the likelihoods of reactions can be affected by the particle phase state or viscosity (George and Abbatt, 2010).

Importantly, the heterogeneous oxidation-driven functionalisation reactions compete with fragmentation reactions (Henry and Donahue, 2012;Kroll et al., 2009). This competition leads to further competition in the direction of OA mass evolution: functionalisation aims on increasing it and fragmentation the opposite. Kroll et al. (2009) acknowledged the importance of fragmentation especially among particle phase compounds with O:C-ratios > 0.4. The empirically suggested O:C-ratio –dependent branching ratios between heterogeneous functionalisation and fragmentation would suggest more significant fragmentation for multifunctional biogenic SOA compared to POA (Kroll et al., 2009;Donahue et al., 2012a;Robinson et al., 2007). This O:C-dependence of fragmentation also explains the observed tendencies, where fragmentation reactions eventually surpass functionalisation (Lambe et al., 2012;Isaacman-VanWertz et al., 2018). Notably, this refers to a time, when significant functionalisation has already taken place. The phenomenon is visible in Figure

4, where the particulate organic carbon became less volatile in time; however, also fragmentation products in the gas phase become more and more evident over the course of the experiment as revealed by increased concentrations of the oxidised volatile vapours such as CO (Isaacman-VanWertz et al., 2018).

Alternatively, some fragmentation reactions have been shown to take place mostly within fresh SOA. These reactions include SOA photo-degradation (Presto et al., 2005). The photolysis reactions occur among similar functional groups as in the gas phase: functional groups able absorb solar radiation at wavelengths ca. $\lambda \geq 290$ nm (i.e. chromophores) have high tendency to fragment. Upon their decomposition, volatile species can be yielded and their evaporation can result in a reduction in SOA mass. Importantly, the degree SOA fragmentation depends on the availability/concentration of chromophores. A recent study focusing on α-pinene-derived SOA illumination suggests that ~10–30% of the SOA particulate mass is sensitive for photo-degradation and these chromophores are presumably consumed exponentially making the SOA totally photo-recalcitrant after 4 days (O'Brien and Kroll, 2019). The fact that hydroperoxide functional groups can act as chromophores could to some extent explain the observed decomposition of HOMs in the particle phase (Knopf et al., 2011). Hydroperoxide-containing HOMs and HOM organonitrates ($RONO_2$) have been shown to have short post-condensation life times (Knopf et al., 2011;Pospisilova et al., 2020;Lee et al., 2016). Their decomposition could trigger further condensed phase transformations including the production of reactive oxygen species influencing also the toxicity of PM or oligomers (Zhang et al., 2015;Krapf et al., 2016;Riva, 2016).

Within this work, oligomers are referred to as particle phase products with high molecular weights. Their formation decreases OA volatility. Significant oligomer-contents have been reported within SOA (e.g. Kalberer et al., 2004) and their formation has been shown to frequently coincide with SOA formation upon acid catalysed reactive uptake of (semi/intermediate)volatile epoxides or carbonyls (e.g. Surratt et al., 2007; Gao et al., 2004; Herrmann et al., 2015; Hallquist et al., 2009; Shiraiwa et al., 2013). Hallquist et al. (2009) and Herrmann et al. (2015) provide comprehensive reviews on the proposed oligomerisation/accretion reactions, such as aldol condensation or hemiacetal formation, yielding high molecular weight compounds observed in atmospheric aerosol.

2.3 Dispersion

Understanding and modelling of the transport of species in the atmosphere from a place to another serves as one of the great mathematical challenges in atmospheric science because of the chaotic nature of the atmosphere. While this section does not aim at describing any of the common mathematical or statistical tools currently used for this purpose, I aim at explaining some of the phenomena, which take place in the transport process. As exemplified by several studies showing for example the presence of Saharan dust over the Amazon basin (e.g. Swap et al., 1992), black carbon at polar regions (e.g. Hansen and Nazarenko, 2004; Wolff and Cachier, 1998), hazy layers over marine areas exposed to urban outflows (e.g. Yu et al., 2008), or acid rain over pristine boreal forest (e.g. Likens et al., 1972), atmospheric PM can travel long distances in the atmosphere. Therefore, accounting for distant

sources of air pollution, especially from the outflows of wild fires or urban areas, is important also regarding rural regions.

The spatial spread of a plume of air pollutants is affected by the initial emission conditions, turbulence and horizontal wind characteristics and even larger scale circulation patterns (e.g. Oke et al., 2017; Seinfeld and Pandis, 2016). Let us consider a point source, a factory smokestack for example, releasing PM to the air. This plume is transported by the wind and gradually widening. Such spreading (dispersion) of the plume takes place nearly without exceptions. The dispersion process in the atmosphere can be referred to as *turbulent* dispersion, which indicates the turbulence-driven mixing of the emitted substance with air along the plume (e.g. Seinfeld and Pandis, 2016). Dispersion always dilutes the initial plume meaning that it will never re-concentrate (e.g. Seinfeld and Pandis, 2016). However, it is important to keep in mind that these plumes can be rich in VOCs, and as discussed earlier (Sect. 2.2.1), and the oxidation of these VOCs as well as OA aging can yield SOA along the transport.

Turbulent dispersion in the atmosphere are regulated by atmospheric stability. For example, in a case where emissions are ejected to a stable nocturnal boundary layer, the plume does not mix much vertically and the horizontal transport of the plume is only controlled by horizontal winds. Similarly, the continuous production of monoterpene-derived SOA within the nocturnal boundary layer yields high concentrations due to the weak vertical mixing. As the sun rises and starts heating the surface, convection starts to take place leading to vertical dilution of the accumulated species. While atmospheric dispersion introduces a diluting effect on atmospheric particulate matter concentrations causing e.g. strong diurnal cycles in monoterpene-derived SOA concentrations in the boreal environment, it does not take part in actual particle removal processes. Therefore, these processes also strongly influencing particle concentrations are discussed in the next sections.

2.4 Deposition

Dry and wet deposition mechanisms (including sedimentation) represent the key removal mechanisms of PM from the atmosphere (e.g. Seinfeld and Pandis, 2016). Dry deposition of aerosol particles means the loss of the particles onto surfaces in processes not involving precipitation. It is greatly influenced by turbulence at the atmospheric surface layer as these turbulent eddies define the efficiency in which the particles are potentially deposited on the Earth's surface. The surface roughness also influences the deposition efficiency in terms of particle adsorption or absorption. Natural (rough) surfaces, such as vegetation, generally provide a good surface for dry deposition whereas smooth surfaces can promote particle bounce from it.

Wet deposition includes below-cloud scavenging of PM by hydrometeors (rain, fog, snow, ice crystals) and in-cloud scavenging (impaction and cloud droplet activation). While the below-cloud scavenging of aerosol particles has been mostly studied in connection with rain, also snow has shown great removal potential (Graedel and Franey, 1975), which ought to be further studied to understand the influence of climate change on this particle removal pathway at high latitudes (Paramonov, 2015). The in-cloud scavenging of aerosol particles occurs via collisions between particles and cloud droplets and the activation of CCN to cloud

droplets (described later in Sect. 2.5). The in-cloud scavenging of particles of this kind is known not to be as effective removal mechanism as cloud droplet activation (Seinfeld and Pandis, 2016). Importantly, the removal mechanisms includes also the washout of the scavenged PM through precipitation from the air.

Atmospheric aerosol populations are often classified by their size distributions. The aerosol particles is sink mechanisms are sensitive to these sizes. The aerosol size distribution generally holds the following modes: nucleation mode (diameters up to 10 nm), Aitken mode (10 nm–100 nm), accumulation mode (100 nm–2.5 μm) and coarse mode (>2.5 μm). Schutgens and Stier (2014) give a detailed overview of processes influencing the number and mass concentrations in different modes of the aerosol size distribution. Condensational growth and coagulation (i.e. collision → accretion) processes represent important mechanisms influencing especially the nucleation and Aitken mode concentrations (Schutgens and Stier, 2014). The significance of wet and later the dry deposition as removal mechanisms starts to increase from Aitken mode onwards (Schutgens and Stier, 2014). Indeed, in the coarse mode, both wet and dry deposition as well as sedimentation dominate the particle sinks (Schutgens and Stier, 2014). As the loss mechanisms are most efficient for the smallest and biggest modes of the aerosol size distribution, the life times for accumulation mode particles in the atmosphere are the longest (Seinfeld and Pandis, 2016), ca. one week (Wagstrom and Pandis, 2009).

2.5 Activation

The growth of aerosol particles to cloud droplets (activation of cloud condensation nuclei, CCN) followed by precipitation can be considered as a sink of aerosol particles. The activation and the subsequent formation of cloud droplets typically occur higher up in the atmosphere and it is triggered by supersaturated air. Through the updrafts and the subsequent cooling of rising air, critical supersaturations can be achieved causing CCN runaway growths to droplets by water vapour condensation. The critical supersaturation enabling the CCN activation for a given CCN size can be estimated via Köhler theory (Köhler, 1936). The Köhler curve composes of two competing effects termed as the Kelvin effect and Raoult's law, which detail the size and composition dependencies of the equilibrium vapour pressures of water around the potential CCN, respectively (McFiggans et al., 2006). While the Kelvin effect describes the equilibrium vapour pressures (of water) being higher over curved surfaces compared to flat ones, which in other words means that (water) molecules from curved surfaces can escape easier to the gas phase, the Raoult's law explains the lower equilibrium vapour pressures over solutions compared to pure water. The composition-dependence is typically parameterised in models using a single hygroscopicity (i.e. water affinity) parameter κ (Petters and Kreidenweis, 2007), which in case of SOA increases with oxidation state (Jimenez et al., 2009). While the dominance of aerosol size over composition in CCN activation is acknowledged (Dusek et al., 2006), and the activation of inorganic CCN (such as sea salt) is well understood and modelled via κ-Köhler theory, the complexity introduced by organic species (both in gas and particle phases) in cloud droplet formation certainly serves as one of the major complex questions to be studied in detail in the future.

3 Measurements

In this chapter, I describe the main analytical tools used in this thesis. The description includes the basic working principles of mass spectrometry as well as brief overviews of the instrumentation applied: the Aerosol Mass Spectrometer (AMS; **Papers III** and **V**), the Aerosol Chemical Speciation Monitor (ACSM; **Papers I–II**) and Chemical Ionisation Mass Spectrometers (CIMS) including nitrate (NO_3^-) or iodide (I^-) reagent ion chemistries (**Papers IV** and **V**, respectively). The final part of this chapter includes the descriptions of the measurement environments, e.g. the Station for Measuring Ecosystem-Atmosphere Relations (SMEAR II; **Papers I–III** and **V**) and the Comprehensive Molecular Characterisation of Secondary Organic Aerosol Formation in the Atmosphere (COALA) chamber (**Papers IV–V**).

3.1 Basic principles in mass spectrometry

Mass spectrometers measure mass-to-charge ratios (m/Q) meaning they only detect charged species (i.e. ions). In this work, we have assumed one charge per ion (i.e. Q = 1 C). Therefore, in order to detect neutral species in the samples, they need to be charged first. Various charging methods exist, but they can be categorised to soft and hard ionisation techniques. While hard techniques tend to break up the molecules resulting in a loss of chemical information, soft techniques, despite of preserving the chemical integrity of the analyte due to the gentler charging, are often selective and less sufficient in sample quantification.

After sample charging, the ions are guided to the mass analysers. There are various types of mass analysers, but here I briefly introduce the quadrupole and time-of-flight (TOF) mass analysers due to their utilisation in the instrumentation applied within this work. Quadrupole mass analysers consist of four rods and electric fields between them. By altering these fields, it is possible to enable the pass-through of a single m/Q ratio at the time. In a TOF mass analyser, the ions, all given kinetic energy of equal quantity, are accelerated in a TOF chamber, which is kept under high vacuum. The chosen trajectory shape, typically a parabola, for ions in the TOF chamber is defined by an electric field. The speed obtained by the ions traveling on this route is dependent on their m/Q.

TOF mass analysers have typically much higher mass resolving power and time resolution than quadrupoles. This means that ions possessing similar m/Q can be more easily distinguished with the TOF along with their temporal variabilities.

In the case of any mass analyser, the relationship between the m/Q and the time the ions spent either traveling through the quadrupole rods or the TOF chamber, needs to be calibrated. This is referred to as the m/Q calibration and a mass spectrum can be yielded as a result of it. A mass spectrum has m/Q on the x-axis and the number of ion counts in a unit of time in the y-axis. Nearly all the results of this thesis are yielded by analysis of such mass spectra. Mass spectra recorded from the boreal forest air via the different instrumentation used in this thesis are shown in Figure 6.

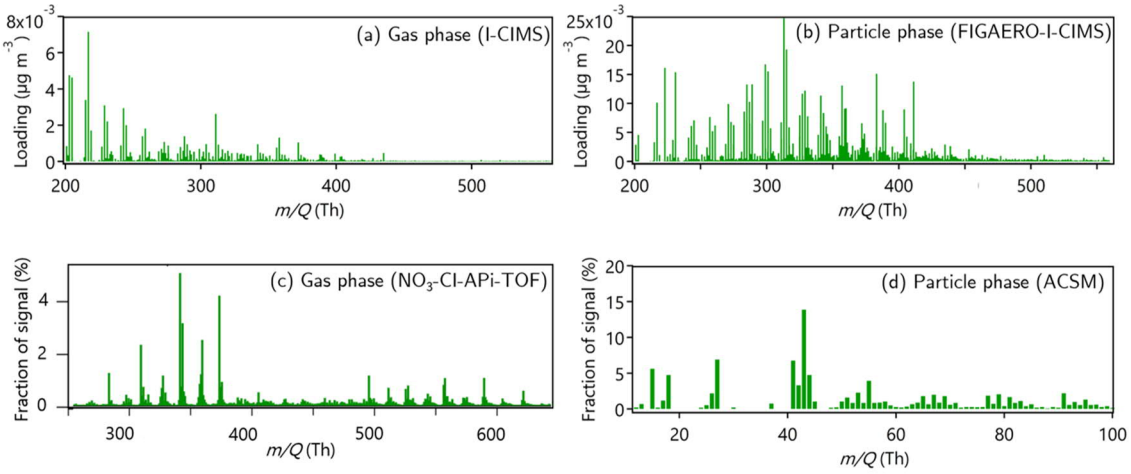

Figure 6. Panels **a**–**b**: Mass spectra measured of gas and particle phase, respectively, at SMEAR II with a FIGAERO-I^--CIMS in 2014 (e.g. Lopez-Hilfiker et al., 2014; Mohr et al., 2017; Lee et al., 2020). I thank Assist. Prof. Claudia Mohr and Dr Wei Huang for sharing these data. Panel **c**: A mass spectrum measured with a NO_3^--CI-APi-TOF at SMEAR II. The figure is adopted from Ehn et al. (2012). Panel **d**: The SMEAR II SV-OOA and mass spectrum factorised from ACSM data in **Paper II**.

3.2 Aerosol mass spectrometry

The development of the AMS started already more than two decades ago (Jayne et al., 2000). Since then, many different variations of the AMS have been developed and commercialised by Aerodyne Research Inc., USA (Canagaratna et al., 2007;Ng et al., 2011b;Fröhlich et al., 2013;Xu et al., 2017). The compact time-of-flight AMS (i.e. the C-TOF-AMS; Drewnick et al. (2005); **Paper III**), the long time-of-flight AMS (i.e. the L-TOF-AMS; **Paper V**), and the ACSM (Ng et al. (2011b); **Papers I–II)** were used in this thesis work.

All of these instruments sample ambient air with ca. 0.1 Lpm flow rate through a critical orifice, which has a diameter of 100 µm. Inside the instrument, the air sample travels through an aerodynamic lens system, which concentrates the aerosol particles in a beam while injecting them to the vacuum environment inside the instrument. It efficiently transmits particles in vacuum aerodynamic diameters between ca. 75 and 750 nm and passes particles up to 1 µm albeit less efficiently (Liu et al., 2007). Due to this cut-off at approximately 1 µm, these AMS applications are classified as PM_1 instruments. While focusing the PM_1 particle beam deeper to the instrument, a large fraction of the air of the sample flow is pumped out providing a high vacuum environment. The instruments are therefore equipped with several vacuum pumps.

After the lens system, the particle beam enters the particle-sizing chamber. The feature is only available in the AMS. The AMS has a rotating chopper with a slit (or slits). By knowing the rotation frequency and the length of the sizing chamber, the size of the particles passing the slit and travelling through the sizing chamber can be calculated based on their time of flights. This way, the AMS can provide size-segregated aerosol chemical composition. While information of this kind is highly valuable, such data were not collected within this work mostly due to challenges in AMS operation in the particle-sizing mode (the chopper spinning caused mechanical stress on the chopper wiring resulting in AMS hardware damages). Therefore, instead of spinning the chopper, it was only moving interchangeably to

either block (closed) or move away from the particle beam (open). A background-subtracted signal was determined based on the difference between the open and closed signals. As the ACSM does not have a chopper unit, the background signals were determined frequently through the regular sampling of particle-filtered ambient air. For this purpose, the ACSM has a 3-way valve at its inlet, which automatically switches between the ambient and particle-filtered sampling.

After the sizing chamber, the particle beam encounters a vaporiser, which is operated at 600 ºC. While it enables fast vaporisation of several species, its operation at 600 ºC prevents efficient quantitative detection of heat resistant material such as soot or sea salt (Drewnick et al., 2015). These heat resistant species are referred to as refractory species, and therefore the traditional AMS application-based measurements only report the non-refractory (NR) chemical species' concentrations in the submicrometer size range (i.e. NR-PM_1). The vaporised molecules are charged via electron impact ionisation (70 eV, hard ionisation). Both the vaporisation and the ionisation process lead to severe fragmentation of the molecules forming the PM. The charged fragments then travel to the final, mass analyser part of the instrument.

The three AMS applications, i.e. the C-TOF-AMS, L-TOF-AMS and ACSM, presented here all have different mass analysers. As the names suggest, the C-TOF-AMS and L-TOF-AMS are both based on TOF technology. The ACSM on the other hand has a quadrupole mass analyser. The more sophisticated TOF analysers further require better detectors and data acquisition cards. Therefore, the data obtained with TOF mass spectrometers are better both in terms of time and mass resolution compared to quadrupole mass spectrometers. However, due to the length of the L-TOF chamber and the compactness (shortness) of the C-TOF, the mass resolving power of the L-TOF-AMS is much greater than that of the C-TOF, which is only slightly better than that of the ACSM. Still, the significantly cheaper cost and robustness have led to the high popularity of the ACSM. The ACSM measurements have become more and more streamlined and in Europe, for example, long-term ACSM measurements are performed in several locations (e.g. Fröhlich et al., 2015; Zhang et al., 2019; Poulain et al., 2019; **Papers I – II** from SMEAR II).

The AMS or ACSM measurements provide initially signal intensities per m/Q. To convert these numbers to meaningful mass concentrations, calibrations are conducted (Allan et al., 2003). The ionisation efficiency calibration represents one of them. It is conducted using size-selected ammonium nitrate particles and a condensation particle counter is used as a reference instrument. Other ammonium salts can also be used to obtain sulphate or chloride relative ionisation efficiencies (using ammonium sulphate and ammonium chloride, respectively). The relative ionisation efficiency of organics is determined from a suite of laboratory samples. A constant value (of 1.4), reported by Canagaratna et al. (2007) is typically utilised without additional organic calibrations performed by the user. The suitability of a constant value to represent the wide variety of organic species has been argued sufficient fue to its low degree of observed variability among organic species samples (Canagaratna et al., 2007;Jimenez et al., 2016). These relative ionisation efficiencies are needed when the signals are speciated to organics, nitrate, sulphate, ammonium and chloride using a fragmentation table (Allan et al., 2004) to achieve mass

concentration for each species distinguished also from air signals. The fragmentation table is the most complex for unit mass resolution data, such as data retrieved via C-TOF-AMS or ACSM measurements. In the case of high resolution data, i.e. data collected with the L-TOF-AMS, the signals at each unit mass region are relatively easily separated during high resolution peak fitting.

After obtaining the species' mass concentration, the data still need to be corrected for collection efficiency (CE) which is reduced from 100% mainly due to solid particles bouncing from the vaporiser. This typically reduces the CE to ca. 50% (Middlebrook et al., 2012).

3.3 Chemical ionisation mass spectrometry

The CIMS applications discussed here refer to the CIMS systems involving an atmospheric pressure interface time-of-flight mass spectrometer (APi-TOF; Junninen et al., 2010). The APi-TOF samples air through a pinhole to a pair of quadrupoles placed one after another behind the instrument inlet to filter out gas and passing through mainly ions. The filtering (in better words pumping) of the gas reduces the pressure several orders of magnitude before the TOF mass analyser part of the instruments starts. The TOF mass analysers utilised here are similar to the one deployed in the L-TOF-AMS (i.e. long TOF). While the APi-TOF itself could be used to sample naturally charged ions and clusters, we focused on chemical ionisation via nitrate or iodide reagent ion chemistries to capture neutral molecules.

The nitrate-CIMS, i.e. NO_3^--CIMS, also referred to as the NO_3^--CI-APi-TOF (i.e. the chemical ionisation APi-TOF; Jokinen et al., 2012), uses a chemical ionisation inlet prior to the APi-TOF. The inlet is similar to those applied earlier by Eisele and Tanner (1993) or Kurtén et al. (2011). The air sampled with the NO_3^--CI-APi-TOF is first reacted with nitrate ions, which are produced in the inlet sheath flow by gaseous nitric acid radiation. By letting the sample react with the nitrate ions for few hundred milliseconds, adduct formations between the sample molecules and nitrate ions may occur yielding sample molecule clusters with nitrate ions or nitrate ion clusters with nitric acid. In the NO_3^--CI-APi-TOF, the ionisation occurs under ambient pressure and the sample is then guided through a critical orifice to the APi-TOF, with a flow rate of 0.8 Lpm, and afterwards to a TOF mass analyser.

In the iodide-CIMS, i.e. I^--CIMS (Lee et al., 2014), the ionisation happens in the ion-molecule reaction chamber (IMR), held at pressures lower than atmospheric pressure (ca. 100 mbar) under a fixed temperature (ca. 40 ºC). The IMR is connected to the instrument prior to the pair of quadrupoles. The main difference between the NO_3^--CI-APi-TOF and I^--CIMS is simply the sampling and ionisation method, the mass spectrometer part of the instruments being identical. The iodide ions were generated using a permeation tube holding methyl iodide, the outflow from which was mixed with the sample at the IMR while being radiated. The sample molecule iodide adducts then travelled through the critical orifice to the quadrupoles and finally to the TOF mass analyser.

Importantly, in this work the I^--CIMS measurements were conducted using a FIGAERO-I^--CIMS inlet (Lopez-Hilfiker et al., 2014;Thornton et al., 2020). The FIGAERO inlet col-

lects particles on a Teflon® filter while the gas phase is being sampled via the above described I^--CIMS technique. This simultaneous sampling was conducted for 45 minutes during our experiments. Then, the filter was exposed to a heated nitrogen flow, the temperature of which was ramped up 15 ºC a minute from room temperature to 200 ºC while the iodide adducts of the evaporated species were measured with the TOF-CIMS. The temperature was kept at 200 ºC an additional 30 min to ensure full cleaning of the filter before the next sampling circle started. As the evaporated molecules can be measured as a function of their evaporation temperature (i.e. thermograms), the FIGAERO-I^--CIMS can also give information regarding the volatilities of the evaporated species (Lopez-Hilfiker et al., 2014;Mohr et al., 2017). However, these thermograms can occasionally be highly spread or multimodal, which can result from various isomers of different volatilities and/or molecular fragmentation (Lopez-Hilfiker et al., 2015;Stark et al., 2017 ; **Paper V**).

The various CI techniques can be selective and lead to the detection of a wide variety of species. The most commonly used techniques in atmospheric OVOC measurements were compared by Riva et al. (2019b). In this study, the I^--CIMS was shown to be more efficient in detecting the less oxidised (yet still oxygen-containing) species than the NO_3^--CI-APi-TOF, which is optimal for measuring HOM and RO_2. These experimental observations agree with the theory suggesting strong bonding affinity between nitrate ions and strong acids as well as highly oxygenated compounds (Hyttinen et al., 2015), while iodide adduct formation has been shown to be more broadly sensitive to any polar compound (Iyer et al., 2016).

3.4 Ambient measurements (SMEAR II)

The Station for Measuring Ecosystem – Atmosphere Relations (SMEAR) II (Hari and Kulmala, 2005;Kulmala, 2018) serves as the key measurement site of this thesis (**Papers I –III** and **V**). It is the most comprehensive measurement station of its kind (Kulmala, 2018), located in the boreal forest of Finland (61°51’N, 24°17’E, 181 m above sea level). The station is surrounded by a roughly uniform, nearly 60-year-old forest, mostly comprising of Scots pine (*Pinus Sylvestris*). While the station has been recognised as a rural, emissions from various distant locations such as the city of Tampere (60 km to the NW), industrialised areas in Southern Finland, Saint Petersburg (Russia) or continental Europe are often detected at the site (Patokoski et al., 2015;Riuttanen et al., 2013;Yttri et al., 2011;Tunved et al., 2006). Two sawmills, located just 6–7 km to the SE from SMEAR II likely represent the largest local pollution source (e.g. **Papers I–III**). Due to the emissions originating from wood processing, their chemical composition highly resembles biogenic SOA (Pospisilova et al., 2020). Luckily, winds from the NE bring air with little anthropogenic influence to the station enabling investigation of several natural processes, representable of the north-western quadrat of the boreal forest (Tunved et al., 2006). However, it should be kept in mind that most (90%) of the forested areas of Fennoscandia are influenced by anthropogenic activities via forest management (Gauthier et al., 2015) and do not therefore represent a boreal forest in a fully natural state.

All the mass spectrometry measurements conducted at SMEAR II were performed below the forest canopy from air-conditioned measurement containers. Further details can be found in **Papers I – III** and **V**.

3.5 Chamber measurements (COALA)

The COALA chamber was installed at the University of Helsinki laboratory facilities in conjunction with a European Research Council funded project titled COALA: Comprehensive Molecular Characterisation of Secondary Organic Aerosol Formation in the Atmosphere, and named after it. **Papers IV** and **V** utilise experiments conducted in this chamber. **Paper IV** holds the most comprehensive descriptions of the chamber operation and dynamics.

The chamber is a two cubic metre Teflon® bag held under room temperature. It was operated in a continuous flow mode, which means injections of clean air and reactants at the same rate as the chamber was being flushed out (primarily sampled with instruments). The turnover time in the chamber was ca. 50 minutes. The flow going in the chamber comprised clean and dry air, gaseous α-pinene and ozone as well as in some experiments NO_2, which underwent photolysis triggered by LED lights to yield NO. Four types of seed particles, all 80 nm in dry diameter, were used in the experiments: effloresced ammonium sulphate (AS), dried ammonium bisulphate (ABS), and deliquesced AS and ABS aerosol particles. The deliquescence was attained by exposing the dried and size-selected seed particles to a humidifier (RH > 80%) prior to the chamber injection. The experiments were conducted either in a dry chamber (RH < 1%) or in a humid chamber (relative humidity (RH) ca. 40%). While the dried seed particles were utilised in both dry and humid chamber, the deliquesced seed particles were injected invariably to the humid chamber in order to maintain the deliquescence.

4 Statistical methods

The ability to measure aerosol mass spectra in real time provides challenges in the sector of data analysis. Several mathematical tools, such as factorisation or clustering, exist to aid the analysis and ease the interpretation of complex data. This chapter holds brief descriptions of the Positive Matrix Factorisation (PMF) algorithm and the Multilinear Engine (ME-2) PMF solver including commonly used approaches in the so-called "constrained PMF" runs, where known information is introduced to the PMF modelling process. The PMF section is followed by introduction of K-Means clustering, which is used within this work to sort PMF output profiles. The developed methodologies for such K-Means applications are introduced in the last section, where also the utilisation of the clustering output in a Chemical Mass Balance (CMB) –like PMF run is described.

4.1 Positive Matrix Factorisation (PMF) and the Multilinear Engine (ME-2)

Positive Matrix Factorisation (PMF; Paatero 1997) is a statistical algorithm commonly used in chemometrics. The goal of PMF analysis is to obtain a simplified picture of multidimensional measurement data. For example, in the case of online mass spectrometry, hundreds of *m*/*Q* are recorded simultaneously with a fine time resolution (typically in order of seconds to minutes). Investigation of these *m*/*Q* individually and manually gaining insight of which of them co-vary and whether several sources contribute to each *m*/*Q* is laborious and arriving at a comprehensive understanding of the data in this way is typically not feasible. PMF, on the other hand, assigns the measured variables into factors with static profiles and varying abundances (time series). The grouping is done so that the measured data matrix ($\mathsf{X}_{i\times j}$) is approximated by a linear combination the profiles ($\mathsf{F}_{k\times j}$) and time series ($\mathsf{G}_{i\times k}$). The residual matrix ($\mathsf{E}_{i\times j}$) is the difference between the measured and the PMF model output. In matrix element notation, the PMF model is written as follows:

$$x_{i,j} = \sum_{k=1}^{p} g_{i,k} f_{k,j} + e_{i,j} \tag{1}$$

In the modelling process, the PMF algorithm minimises the following quantity *Q:*

$$Q = \sum_{i=1}^{n}\sum_{i=1}^{m}\left(\frac{e_{i,j}}{\sigma_{i,j}}\right)^2 \tag{2}$$

in various iterations in the factorisation process. As $\sigma_{i,j}$ refers to the measurement uncertainty of variable *j* at time point *i*, *Q* can be considered as the uncertainty-weighted residual. To ensure a global (uncertainty-weighted) residual minimum, conducting PMF from several starting points (seeds) is necessary. These steps are nowadays conducted with the Multilinear Engine (ME-2) PMF solver. Its popularity has partially arisen from the possibilities to reduce the rotational ambiguity of PMF (PMF yields similar *Q*-values with various G and F

combinations; Paatero and Hopke., 2009). This is performed by forcing PMF towards atmospherically meaningful results (Canonaco et al., 2013). The ME-2 solver includes the possibility of introducing known (mass spectral) profiles or time series to PMF upon initialisation (Canonaco et al., 2013). Due to these fixed anchors, the PMF then solves either the unknown time series or factor profile pair of the output. Importantly, deploying such PMF anchors should only be conducted when the presence of the constrained factor has been verified in the measurement environment.

The constraining can be conducted in different ways. Currently, constraining PMF with known profiles (mass spectra) is more widely used than time series constraints. Therefore, the following text discusses only constraining mass spectra. However, all the methods given also work for time series constraints in a similar manner. A so called *a*-value approach (Canonaco et al., 2013) is a commonly used technique among AMS data analysis. In this approach, a reference mass spectrum, typically retrieved near some OA source being clean of other sources, is introduced. PMF is forced to retrieve a profile resembling this reference spectrum. The degree of allowed difference between the reference spectrum and PMF output is given by a scalar $a = [0, n]$, corresponding to variability of 0 to n times the original signal. The higher the *a*-value is, the more the PMF output profile is allowed to differ from the anchor. Typically, not all factors are constrained and the *a*-value approach is typically most useful when trying to explain contributions of sources making up a minimal mass fraction of the OA, which would not be resolved in the unconstrained PMF. Indeed, PMF can be considered to have a "detection limit" (5% of variation (Ulbrich et al., 2009), 7% estimated in **Paper II**). In the case of fixing all the profiles of the PMF output, and giving no room for variability, we talk about performing chemical mass balance (CMB; Watson et al., 1984).

More and more PMF analyses on OA mass spectra measured by an AMS or ACSM contain constraint factors (*a*-value approach) to account for OA sources with low signal contributions. These source profiles used for anchoring the PMF run, as well as the applied *a*-values are typically defined by the PMF user. Therefore, the decision of utilising certain reference profile is often not data-driven but subjective which gives rise to several risks, potentially lowering the atmospheric relevance of the constrained PMF result. BBOA, for example, is known to possess significant mass spectral variability depending on its source (Weimer et al., 2008). Moreover, BBOA is known to be efficiently subjected to chemical transformations upon transport (Grieshop et al., 2009;Cubison et al., 2011). Accounting for such chemical complexity upon the selection of suitable mass spectral reference profile is commonly overlooked.

Within this thesis work, we applied K-Means clustering to conduct data-driven determination of suitable reference profiles for PMF-ME-2 analysis. The scientific background for K-Means clustering is presented in the next section (Sect. 4.2).

4.2 K-Means clustering

K-Means clustering (Steinhaus, 1956;Ball and Hall, 1965;MacQueen, 1967) is one of the most, if not the most popular unsupervised machine learning technique used worldwide (Jain, 2010), and applied also in the context of atmospheric sciences including air pollution studies (Govender and Sivakumar, 2020) with a goal to explore unknown structures in the data set(s). The structures of multidimensional data sets, such as time-dependent mass spectra, are challenging to capture with manual data exploration. With clustering techniques, such as the K-Means, the similarities between samples can be quantified and the data can be classified. Moreover, by reporting the mean structures (centroids) of each class (cluster), the information within the data set can be condensed. Such a summarising method can ease further steps in data analysis.

K-Means was developed nearly half a century ago, but only recent advances in the algorithm development (e.g. the development of the K-Means ++; Arthur and Vassilvitskii, 2007) have led to more robust clustering outputs. Figure 7 visualises (in a simplified manner) the main working principles of K-Means utilising random data. The algorithm works as follows: first, the algorithm selects random seeds (i.e. cluster centroids), the number of them is given by the algorithm user. This initialisation is optimised with the K-Means ++ algorithm.

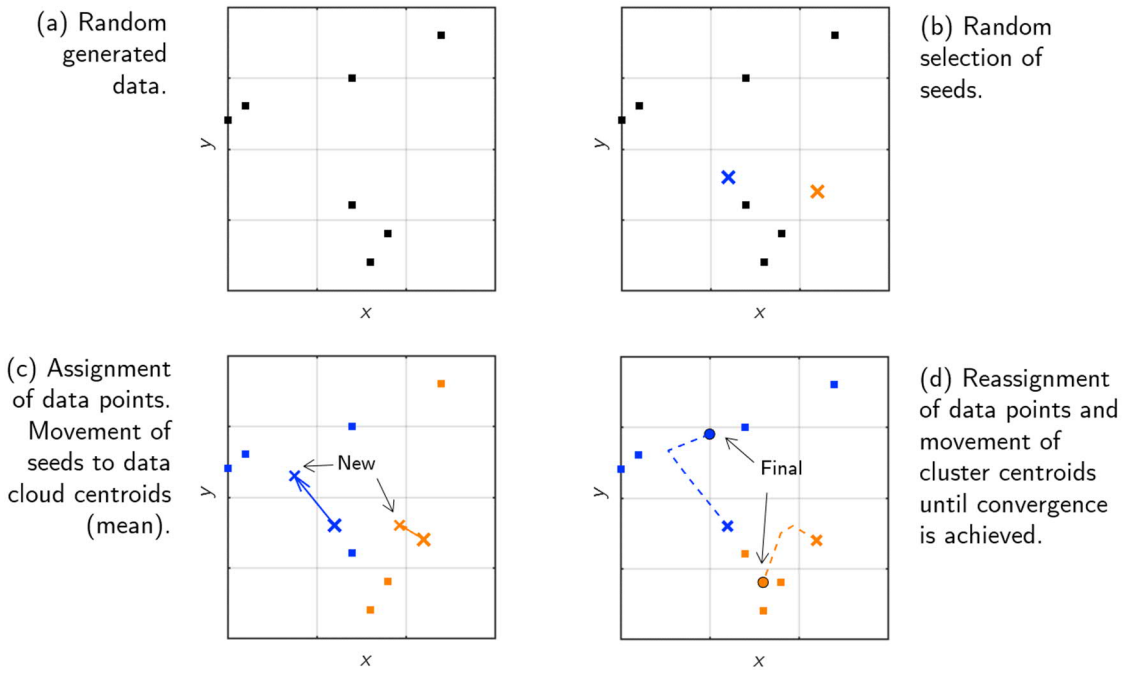

Figure 7. Visualisation of the working principles of the K-Means algorithm via random data. The data are visualised in panel **a**. Panel **b** shows the locations of the randomly chosen seeds (i.e. initial "centroids", crosses). Panel **c** shows where each data point was assigned to and the movement of the cluster centroid after recalculation. Panel **d** shows the final assignment of data points and the final cluster centroids (circles). It also shows the trajectories (dashed lines) of the cluster centroids upon iterations before convergence was achieved.

Hereafter, the distances (typically squared Euclidean distance, but other metrics can be used equally) between each data point and each centroid are calculated and the data points are assigned to the closest centroid's cluster. This is followed by the calculation of new centroids (mean of the data belonging to each cluster) and the centroid is moved to its new coordinates. Due to shifts in the centroids' locations, the distances between them and each data point need to be recalculated. This step sometimes moves data from one cluster to another as some of the data points are closer to another centroid due to the previously occurred shift of cluster centroids. After these possible reassignments, new centroids are once again calculated. If the centroid locations changed, the distances between centroids and data points are recalculated and possible movements of data between clusters can again take place. This kind of reassignment of data points and the subsequent movements of cluster centroids are performed until convergence is achieved, which means that the solution is stable and the centroids no longer relocate.

4.3 Data-driven OA classification

This section holds the description of the data-driven OA classification methodology, i.e. the first scientific goal of the thesis (**Papers II** and **III**). The idea of the method is to first determine the main OA constituents by performing K-Means clustering on a large number mass spectra retrieved from several unconstrained PMF runs and then perform a regular constrained (*a*-value approach) or a fully constrained PMF run with these constituents and their observed mass spectral variabilities. The latter option is referred to as *relaxed* CMB (rCMB) due to being *fully* anchored (CMB), yet with some allowed factor variability ($a \neq 0$).

In practise, the unconstrained PMF could be performed for example through a pollution episode at the time over long sampling periods possessing many of them (**Paper III**) or a (short) measurement campaign at the time if many campaigns have taken place at the measurement site (Äijälä et al., 2019). Alternatively, in the case of long-term measurements (≥ 1 year), unconstrained PMF can be performed a short time window (≥ 14 days) at the time (**Paper II**), which is shifted a short time step (≥ 1 day) at the time over the full measurement period (rolling PMF; Parworth et al., 2015;Canonaco et al., 2020). All the factor profiles retrieved from these PMF analyses, can be combined and clustered using K-Means. **Paper III** holds detailed information regarding e.g. K-Means input data weighting, distance metric selections and clustering solution quality inspections to be considered in order to maximise the information gain of the prevailing OA types within the PMF solutions.

The information from the clustering can be finally compressed via calculation of cluster centroids and intra-cluster variabilities for further utilisation in regular semi-constrained PMF or (rolling) rCMB (**Paper II**) analyses. This way, the choice of reference profiles is proven to be appropriate based on the data and is therefore less prone to subjective bias. The methodologies, presented in detail in **Papers II** (for long-term data) and **III** (for pollution episodes), should be applicable also to measurement sites other than SMEAR II.

5 Results

This chapter contains the main scientific results of the thesis describing boreal OA composition from long-term measurements (Sect. 5.1), the assessment of HOM volatilities and the influence of anthropogenic NO_x to those (Sect. 5.2) and finally the effect of aerosol acidity on SOA (trans)formation (Sect. 5.3).

5.1 Aerosol chemical composition in the boreal forest

While previous measurements have revealed a large organic mass fraction of the fine particulate matter in various regions within the boreal biome (Äijälä et al., 2019;Mikhailov et al., 2017;Williams et al., 2007), the data collected within this work at SMEAR II since 2012 by the ACSM represents the longest *in situ* measurements of aerosol chemical composition ever conducted in the boreal environment. The analysis of these time series therefore provides a missing piece of fundamental scientific understanding of the boreal aerosol populations not only at SMEAR II but also within the boreal biome. The analysis regarding SMEAR II aerosol phenomenology yielded three publications (**Papers I–III**). Consistent with previous studies (e.g. Äijälä et al., 2019), the sub-micrometre aerosol mass at SMEAR II was mostly organic (**Paper I** & Fig. 8a). Multiple sources contribute to this mass fraction and it should not be mistaken as solely biogenic aerosol despite the rather homogeneous boreal forest, where the measurements took place. Due to the long lifetime of aerosol particles especially in the accumulation mode, they can travel long distances.

Determining whether the measured OA, of which LV-OOA, SV-OOA and POA were deconvolved, was of natural or anthropogenic in origin is challenging, especially regarding the OOA aerosol types. SV-OOA and LV-OOA are categorised by their volatilities, which are reflected in their diurnal cycles rather than their sources. On the other hand, various POA types, such as BBOA or HOA, can be linked to their emission sources. Inorganic species measured at SMEAR II, such as ammonium sulphate or ammonium nitrate, can also be easily connected to anthropogenic activities which emit SO_2 or NO_x. These were present at highest concentrations and mass fractions in winter making up ca. half of the sub-micrometre aerosol mass concentration (**Paper I** & Fig. 8a).

The wintertime NR-PM_1 maximum was observed at SMEAR II during February. Many meteorological conditions likely promoted such February maximum. It is likely that February, being the driest month in terms of precipitation, facilitated the more efficient (i.e. less wet deposition) transport of pollutants from faraway urban and industrialised areas to SMEAR II. Wintertime LV-OOA peaked in February, similarly to sulphate (Fig. 8b, **Papers I– II**). The reduced biogenic activity in wintertime speaks for the anthropogenic origin of the wintertime LV-OOA. As multiple OA types from various sources age to yield a mass spectral structure of LV-OOA (Jimenez et al., 2009), it remains an open question which sources most contributed to its wintertime mass. However, as residential wood combustion represents one of the largest wintertime OA sources in Europe (Jiang et al., 2019) and BBOA has further been shown to efficiently age to OOA (Grieshop et al., 2009), we could speculatively

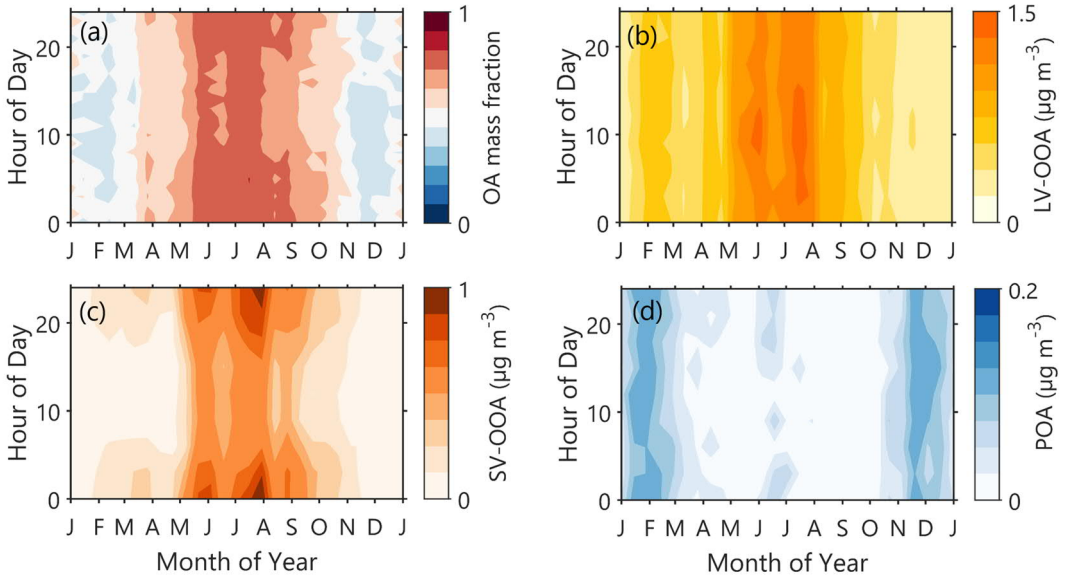

Figure 8. Panel **a**: The seasonal variability of OA mass fraction. The *x*-axis represents the time of the year and the *y*-axis the time of the day (UTC+2). The colour coding represents the OA mass fraction, where red indicates that majority of the NR-PM_1 is organic, whereas blue colours indicate dominance of inorganics. The data utilised in this plot spans between April 2012 and April 2020. The figure is unpublished, but drawn utilising data from **Papers I** and **II**. Panels **b–d**: The seasonal variabilities in LV-OOA, SV-OOA and POA concentrations (in µg m^{-3}), respectively. The data utilised spans between April 2012 and October 2019. They are adopted from **Paper II**.

attribute the detection of such transported and aged wood-burning POA emissions. The similar wind direction and speed dependency of LV-OOA to those of the POA detected at SMEAR II in relatively fresh state (**Paper II**) could also support the hypothesis of anthropogenic, and perhaps wood burning-related origin of wintertime LV-OOA.

The POA reported in **Paper II** is likely a mix of several (anthropogenic) POA types such as relatively fresh HOA and BBOA. Unlike in cities, the POA diurnal cycles did not follow typical HOA cycles tracking traffic rush hours nor BBOA diurnals with a clear evening maximum. This is not surprising, as the majority of the detected POA was not locally produced and its arrival and subsequent observation at the site was delayed and depended on source distances and wind speeds. The seasonal cycle of POA was nearly a reverse of the seasonal cycles of temperature, radiation or the planetary boundary layer height and actually, all of those could influence POA lifetime favouring higher wintertime loadings compared to summer. The concentration and mass fraction of POA at SMEAR II during the 8-year ACSM measurement period was significantly lower than those reported from two to four years earlier studies conducted with the C-TOF-AMS (Äijälä et al., 2019). While the decreasing BC loading at SMEAR II (Luoma et al., 2020) would suggest also decaying POA concentrations, possibly due to EU legislation aiming for better air quality, it is also likely that the ACSM did not capture well short-term pollution plumes, which were averaged out even more due to the 3-hour averaging of data used.

The several anthropogenic POA (and OOA) types, extracted before 2012 with a C-TOF-AMS from pollution plumes and episodes at SMEAR II revealed the presences of HOA and cooking-related organic aerosol (COA) as well as anthropogenic LV-OOA (resembling aged BBOA), SV-OOA from nearby sawmills and other anthropogenic SV-OOA within the SMEAR II NR-PM_1 (**Paper III**). In addition, several amine-linked aerosol types were

found, but their presence in the ambient air still needs further validation due to their potential formation within the instrument. In order to visualise the variety of OA species detected at SMEAR II, the mass fractions of different *m/Q* are visualised in various projections in Figure 9. The SMEAR II-specific values are accompanied with BBOA, HOA, LV-OOA and SV-OOA averages calculated from 27 Northern Hemispheric locations (Ng et al., 2010).

In Figure 9a, the organic mass fractions of *m/Q* 44 and 43 Th (f_{44} and f_{43}, respectively) are visualised from all the mass spectra. As f_{44} is approximately proportional to OA O:C-ratio (Canagaratna et al., 2015) and f_{43} related to the H:C (Ng et al., 2011a), this panel shows the presence of a full spectrum of less and more oxidised species detected. However, as depicted in Figure 8b, most of the mass concentration lies on the top of the Figure 9a triangle.

The POA extracted in **Paper II** shows up as more oxidised (higher f_{44}) compared to the HOA deconvolved in **Paper III** (Fig. 9b), yet less oxidised than the anthropogenic LV-OOA presumably containing aged BBOA (**Paper III**). Importantly, the difference between POA or anthropogenic LV-OOA and the BBOA average from Ng et al. (2010) is striking in terms of f_{60}, which is a marker for levoglucosan-like sugars released in cellulose pyrolysis (Simoneit et al., 1999;Alfarra et al., 2007). The low f_{60} at SMEAR II spectra strongly indicates the absence of fresh BBOA. If assuming the city of Tampere (ca. 60 km from SMEAR II) as a significant wintertime source of BBOA, this would indicate BBOA aging or removal within time scales of hours if assuming moderate wind speeds transporting pollutants to SMEAR II (ca. 4–5 m s^{-1}). Further analysis and collaboration with chemical transport models could provide further insight into wintertime OA (trans)formation, while also estimating the magnitude of the urban (or suburban) plume dispersion and deposition processes. Due to the length of the data set, it provides a good scientific basis for further in-depth analysis and collaboration with the atmospheric modelling community.

The summertime OA at SMEAR II was nearly exclusively OOA (**Paper II** & Fig. 8b) the sources of which presumably were mostly biogenic and influenced by the nearby sawmills (**Papers I–III**). The sawmill influence observed especially with South-easterly winds can be spotted mainly by the plume-like structures of the elevated OA (**Paper III**) and monoterpene signals (Liao et al., 2011). The importance of the sawmills in SOA production should not be mistaken as biogenic SOA formation. The striking resemblance of the sawmill-OA with laboratory-generated monoterpene-SOA has been shown by Pospisilova et al. (2020). Thus, the separation of sawmill-OA by any chemical fingerprints from the forest-generated (biogenic) monoterpene-SOA will remain a challenge not at least easily solvable by increasing the chemical resolving power of the measurement tools, but rather via data-analytical tools such as PMF analyses over pollution episodes (**Paper III**). The biogenic influence in summertime OA loading was visible from the strong temperature-driven OA bursts (**Paper I**). The measurement period contained two summers (2014, 2018) significantly warmer than others (others termed as mild summers). The median OA loading obtained during the warm summers was nearly double to the median of the mild summers (Fig. 10a). While the temperature anomaly also affected the monoterpene mixing ratio in a similar manner to OA, it is possible that not the entire enhancement was due to enhanced biogenic SOA production. This is because of boreal wild fires taking place in Siberia nearly every summer (and Sweden in 2018), and the potential of SOA production within BBOA

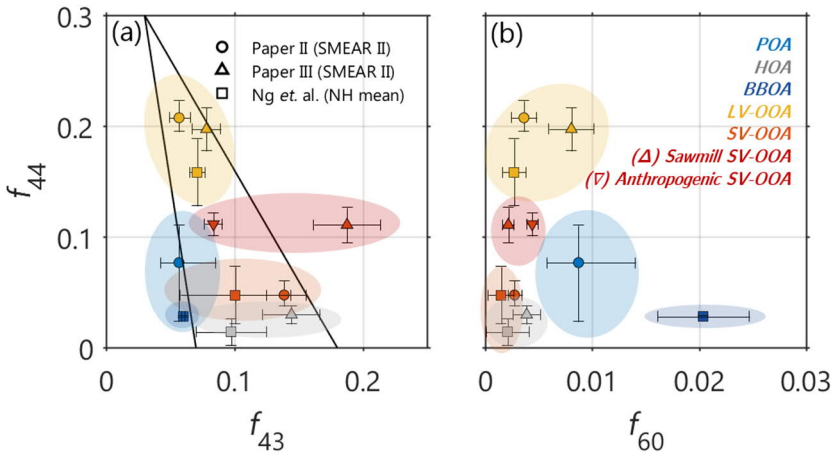

Figure 9. Panel **a**: f_{44} and f_{43} from various mass spectra from SMEAR II presented in **Papers II** and **III** with circle and triangle markers. The square markers represent a mean from various spectra factorised from 27 data sets collected within the Northern Hemisphere (NH). These are obtained from Ng et al. (2010). The f_{44} vs f_{43} projection, sometimes also referred to as the triangle plot typically holds the most aged OA components in the tip of the triangle (high f_{44}) and least oxidised constituents at the bottom (low f_{44}). Note that the **Paper III** spectra are obtained from pollution episodes exclusively, which explains the differences between **Paper III** and **Paper II** SV-OOAs, for example. Panel **b**: f_{44} vs f_{60} of the same spectra as in the previous panel. The higher the f_{60} and the lower the f_{44} the more the spectrum resembles that of fresh BBOA. Spectra obtained from other sources (such as HOA) or the OOAs have low f_{60}. This panel visualises the absence of fresh BBOA at SMEAR II as there are no spectra from **Papers II** or **III** that would overlap with the Ng. et al. (2010) BBOA spectra.

aging has been demonstrated (Shrivastava et al., 2015). However, the POA concentration was not much affected by the temperature anomalies (Fig. 10a), which on the other hand was not surprising knowing the speed of BBOA transformation to OOA in summertime air. Other, more inert species such as CO and black carbon were investigated in **Paper I**. Both showed elevated concentrations at SMEAR II under highest temperatures. Nonetheless, their accumulation in the air from their usual summertime sources is also a possibility during warm summers ruled by long-lasting (stationary) high pressure conditions (diminishing wet deposition and dispersion).

Tunved et al. (2009) introduced a clever method to evaluate natural SOA production over areas with little anthropogenic influence. They calculated the number of hours back trajectories had spent over land areas (time over land, TOL) in the clean north-western quadrat of the boreal forest, an area classified as clean without major anthropogenic sources. They further calculated the PM loading enhancement as a function of TOL and associated it with terpene-SOA production. We performed a similar exercise in **Paper II** and discovered that the LV-OOA loading responded most significantly to TOL. We estimated natural LV-OOA production of several tens of ng m^{-3} per hour over the boreal forest. During the warm summers of 2014 and 2018, the TOL-effect was greatest for LV-OOA (Fig. 10b&c). However, the LV-OOA production during warm summers (ca. 60 ng m^{-3} h^{-1}) was nearly four times greater than in mild summers (ca. 15 ng m^{-3} h^{-1}). Such high sensitivity of biogenic SOA to temperature suggests higher SOA production in the future climate due to the projected increase in the heat wave frequency in the area (Collins et al., 2013;Kim et al., 2018). On the other hand, such heat waves certainly promote wild fires in the Siberian areas of the boreal biome also contributing to the OA. Long-term measurements of aerosol chemical composition in other regions of the boreal forest would also greatly help mapping the spatial variability of the phenomena reported here.

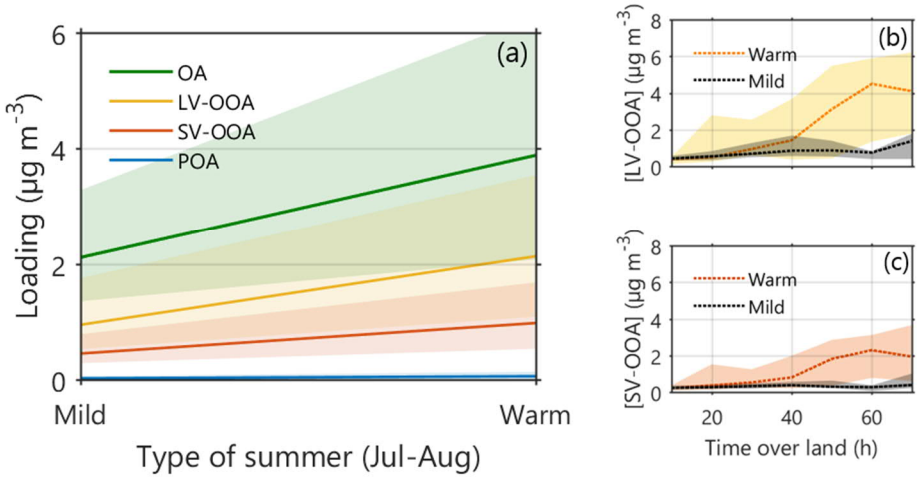

Figure 10. Panel **a**: The interquartile ranges (medians drawn with solid lines) of the concentrations of OA and the dominant OA types at SMEAR II in mild summers (mean temperature (T) < 15 ºC) and warm summers (T > 15 ºC). Panel **b-c**: The LV-OOA and SV-OOA concentrations in mild and warm summers, respectively as a function of time over land. The figure is drawn utilising from data presented in **Papers I** and **II**.

Even though the biogenic SOA production can be estimated via TOL-analyses, they still do not resolve the chemical processes behind initial SOA formation or aging. Therefore, also laboratory studies are broadly conducted to enhance understanding of these complex processes. The next sections in this thesis include experiments conducted in the COALA chamber, where conditions in the boreal forest were mimicked.

5.2 SOA formation via HOM condensation

HOMs have been suggested to play a major role in SOA formation (Ehn et al., 2014;Bianchi et al., 2019) and explaining a large fraction of boreal OA (Roldin et al., 2019). Importantly, some of these compounds have even been suggested to participate in the formation of new particles in the troposphere due to their extremely low vapour pressures (Kirkby et al., 2016). Accurate estimations of their vapour pressures, which drives their SOA formation potential, is not straightforward. Challenges arise due to the lacking knowledge of the structures of HOMs as the CIMS techniques currently give information just regarding the molecular formulas. Therefore large spread in HOM volatility estimates exists (Kurtén et al., 2016) not to mention the challenges arisen from the fact that HOM synthesis remain extremely challenging prohibiting HOM volatilities exploration through such channels (e.g. Kurtén et al. 2016).

The aim of **Paper IV** was to experimentally investigate the volatilities of HOMs at a molecular level. The experiments were conducted in the COALA chamber simulating the reactions taking place in the boreal atmosphere. As described earlier in Sect. 3.5, the chamber was operated in continuous flow mode, which meant constant flows of reactants going in the chamber and a constant outflow of the same volume. The average residence time of species in the chamber was ca. 50 minutes. The formation of HOMs in the COALA chamber was triggered by the injection of α-pinene and ozone. Once a steady state was achieved within the chamber, aerosol seed particles were injected. Similarly, to the gas phase species,

also aerosol seed particles were constantly injected. This way another steady state, now in the presence of seed, was achieved. When the seed injection was stopped, the chamber conditions returned to the previous steady state. A NO_3^--CI-APi-TOF was used to monitor HOM formation and behaviour under different conditions. As temperature strongly influences HOM formation and volatilities (Stolzenburg et al., 2018), the experiments within the COALA chamber were always conducted at room temperature (302 ± 2 K).

The switches between steady states led to different behaviours of different HOMs. Upon seed additions the signals of some HOMs dropped (due to HOM condensation onto seed particles) more than others. Figure 11 visualises the NO_3^--CI-APi-TOF mass spectrum having fraction remaining (FR) in the *y*-axis instead of the signal intensity typically presented. FR now reports the difference in the various OVOCs' (incl. HOMs) signals between the control steady state (absence of seed) and the steady state condition achieved in the presence of seed aerosol. A low FR indicates efficient condensation of the compound(s) whereas a high FR is associated with a volatile nature of the detected species. Figure 11 highlights the following observations: i) nearly all compounds possessing a molecular weight beyond ca. 350 Da (includes the NO_3^- charger ion mass) condensed and ii) compounds possessing an organic nitrate functional group condensed less efficiently than compounds without one at the same nominal mass. When comparing experiments conducted with and without NO_x, the sigmoid-like shape of the FR mass spectrum stayed the same with nearly one-to-one agreement between observations implying that NO_x did not influence the condensation of non-nitrates (Fig. 11b). However, the organonitrates would drop to low FR values ca. 45 Da later than the non-nitrates did (Fig. 11a). In the comparison of experiments conducted in a dry vs. humid chamber, a minor difference was observed: both non-nitrates and organonitrates were partitioning to the condensed phase more efficiently in the humid chamber, which might imply for example their solubility-driven partitioning to an aqueous phase (Fig. 11d).

To relate these observations to effective saturation vapour concentrations (C^*) modelling efforts were required. For this purpose, we utilised the ADCHAM model, developed by Roldin et al. (2014). The model is optimised to give information regarding C^* especially between the boundary of SVOCs and LVOCs (Roldin et al., 2014). After successfully modelling the OVOC and SOA behaviours from the COALA chamber experiments, the relationship between the C^* and the FR could be obtained. Next, a model was developed for OVOC volatility estimates. It was created using the molecular composition of detected OVOCs as input (i.e. numbers of carbon (n_C), hydrogen (n_H) and oxygen (n_O) to replicate the sigmoid-like FR curve:

$$\log_{10} C^* = 0.18 \times n_C - 0.14 \times n_H - 0.38 \times n_O + 0.80 \times n_N + 3.1. \quad (3)$$

Based on this equation, both the addition of carbon as well as nitrogen, increase the compound's volatility while additions of hydrogen and oxygen decrease it. It should be remembered that functionalisation of HOM occurs namely by addition of functional groups comprising often of two or more atoms present in Eq. (3). For example, the addition of a nitrate group (—ONO_2), which simultaneously adds three oxygen atoms to the compound. This leads to a net effect reducing the compound's

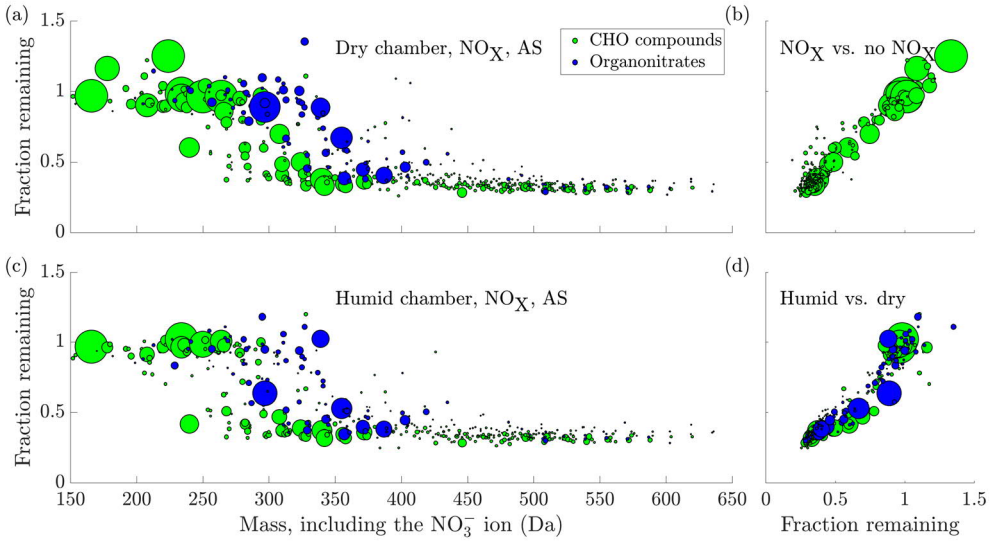

Figure 11. Panel **a**: Fraction of individual OVOCs remaining in the gas phase upon seed aerosol particle injections as a function of the OVOCs' mass (detected by the NO_3^--CI-APi-TOF, therefore the masses include the nitrate ions). The COALA chamber experiment was conducted in a dry chamber and the seed type was effloresced ammonium sulphate (AS). Panel **b**: Comparison of non-nitrate FR remaining curves retrieved in the presence and absence of NO_x. Panel **c**: A FR curve in a humid chamber with deliquesced AS seed. Panel **d**: Comparison between the FR curves presented in panels **a** and **c**. In Panels **c** and **d**, the *y*-axis has been cut at 1.5 for clarity, excluding the compound $C_5H_6O_6$ at mass 224 Da with a FR of 2.27. The figure is obtained from **Paper IV**.

effective saturation vapour concentration. Correspondingly, while Eq. (3) claims an increase of the compound volatility with increasing n_C, the carbon addition would commonly also add two hydrogen atoms (—CH_2). The addition of CH_2 results in a net reduction of volatility.

The results given by the parametrisation in Eq. (3) yield HOM volatility estimates similar to those derived in the past. In particular, these estimates fall between the existing ones of which highest estimates were given by Kurtén et al. (2016) and lowest by Bianchi et al. (2019). Based on these results, HOM monomers can be classified (with relatively high confidence) as mostly SVOCs or LVOCs, the ones containing the highest numbers of oxygen molecules belonging to the latter volatility class. Dimers on the other hand can be expected to be at least LVOCs, possibly even ELVOCs. As the conversion of FR to C^* might not have been performed exactly accurately for the ELVOC region more work should be conducted regarding the volatility estimates in the dimer region. Such work is crucial because at early stages in new particle formation the difference between LVOC and ELVOC becomes significant due to the Kelvin/curvature effect making evaporation easier from curved surfaces (Seinfeld and Pandis, 2016). However, for predicting the formation of HOM condensate onto larger particles Eq. (3) provides critical information and it should be applicable to systems other than α-pinene ozonolysis.

While gaining insight of HOM volatilities is crucial for predicting the amount of HOM condensate, the stability of HOMs in the particle phase arises questions mainly due to the high number of reactive functional groups they possess (e.g. Mentel et al., 2015; Krapf et al., 2016). Recent discoveries employing novel extractive electrospray ionisation (EESI) TOF

online mass spectrometry (Lopez-Hilfiker et al., 2019) reveal a decay in HOM concentrations to take place in fresh (first 6–7 hours) α-pinene-derived SOA (Pospisilova et al., 2020). Similarly to **Paper IV**, they observed depletion of all HOM dimers upon SOA formation in the gas phase. However, the similarity in HOM temporal behaviours, despite their similar C^* values, reduced in the particle phase. For example, some HOMs attained their maximum concentrations later than others, even at times when the gas phase production of HOM no longer occurred. All in all, most HOMs showed a decaying trend, some of them having particle phase half-life times of one to two hours and some more. After a careful analysis, Pospisilova et al. (2020) concluded that most of these observations might be explained by HOM decomposition in the particle phase. Without going to details, particle phase formation of ester and carboxyl functional groups from reactions between the highly reactive peroxycarboxyl or hydroperoxyl groups with carbonyls (Baeyer-Villiger reactions; Claflin et al., 2018) and subsequent hydrolysis of esters could well explain their observations (Pospisilova et al., 2020). Next, I will discuss the influence aerosol acidity on α-pinene-derived SOA formation and evolution bringing even more complexity to the discussion of HOM fate in the (boreal) atmosphere.

5.3 Effect of aerosol acidity on SOA formation and evolution

It is not only OVOC (incl. HOM) condensation or thermodynamic gas-to-particle transitioning that form and grow SOA in the boreal environment. However, many studies focus on these phenomena, due to the efficient production of condensable vapours from the oxidation of monoterpenes, which is able to explain high fractions of observed SOA. In other environments, notably in those where isoprene emissions overshadow those of monoterpenes, the effect of inorganic composition on SOA yields is a highly studied topic. In these environments, the OVOC volatilities are generally higher than in monoterpene-dominated regions and reactive uptake of OVOCs, especially those containing carbonyl functional groups or epoxides (such as the isoprene epoxydiols, IEPOX), plays an important role in SOA formation. These reactions, shown to be driven by particle acidity, involve reactive uptake of the abovementioned species yielding particle phase products of low volatility (Jang et al., 2002;Liggio and Li, 2006;Surratt et al., 2010). Despite the higher role in explaining SOA formation processes in isoprene-rich areas, such as acid-driven SOA generation should also affect monoterpene-derived SOA formation in a similar manner in monoterpene-rich areas according to strong evidence from several laboratory studies (e.g. Czoschke et al., 2003).

The low pH of aerosol particles has been shown to be commonplace (Pye et al., 2020). A decade-long analysis of $PM_{2.5}$ aerosol acidity from six Eastern Canadian measurement sites suggested strong seasonality in particle pH (Tao and Murphy, 2019). The pH was ca. 2 in summer while a ca. unit higher pH values were achieved in winter. The seasonality was mostly driven by changes in meteorological conditions (T, RH). The response of pH to changes in composition, such as varying ammonia concentrations, was also strongly temperature dependent in a way that summertime pH stayed less affected than in wintertime, making the latter time series less stable. Similar behaviour can be expected in the boreal forest. Despite the acidic particles likely existing in the boreal air at SMEAR II, where also

IEPOX production presumably takes place albeit its loading is much lower than in isoprene-rich areas, IEPOX-derived SOA has not been found at SMEAR II (**Paper II**). Based on this, one could argue that it does not represent a key SOA constituent at SMEAR II, but answering whether it is due to limited amounts of precursors, or other unsuitable conditions, requires further analysis. Nonetheless, monoterpenes emitted efficiently from the forest, yield several carbonyl-containing species including pinonaldehyde upon oxidation. As exemplified by Liggio and Li (2006), these factors already provide possibilities for SOA formation via acid-driven multiphase reactions.

These possibilities motivated a suite of studies conducted in the COALA chamber using various sulphate-containing aerosol seed particles, including crystallised, acidic and deliquesced particles, all comprising of ammonium sulphate (acidified ones spiked with sulphuric acid). The deliquesced particles were utilised to study the effects of aerosol liquid water on SOA composition, which is suggested to enhance formation of high molecular weight products, likely of low volatility, in the particle phase (Faust et al., 2017). While SOA precursors were generated via α-pinene ozonolysis in a similar manner under all experimental conditions (all of them described in Sect. 5.2), the highest SOA yields were always observed in the experiments where seed particles were acidic and RH < 1% (**Paper V**). Importantly, this coincided with a drop in the concentration of several gaseous aldehydes, including pinonaldehyde. This laboratory exploration was unique due to the use of the FIGAERO-I^--CIMS, which yielded critical insights on the behaviours on both gas and particle phase OVOCs.

The changes in particle phase composition upon seed injections relative to the control run are visualised in Figure 12, with the different seed types in the different panels. In the panels, the red colours indicate production of compounds and blue colours reductions. What can be seen by comparing the panels is that the colours, both red and blue, are much brighter in panels b&d, which belong to the experiments conducted with acidified seed aerosols. The blue colour spreads over the HOM monomer ($C_{9–10}H_xO_{>6}$) and dimer ($C_{17–20}H_xO_y$) regions indicating that their concentrations in the particle phase are reduced compared to the control run. In addition, the FIGAERO-I^--CIMS mass spectrum revealed an increase in the signals of several species with a short carbon skeleton and low number of oxygen atoms.

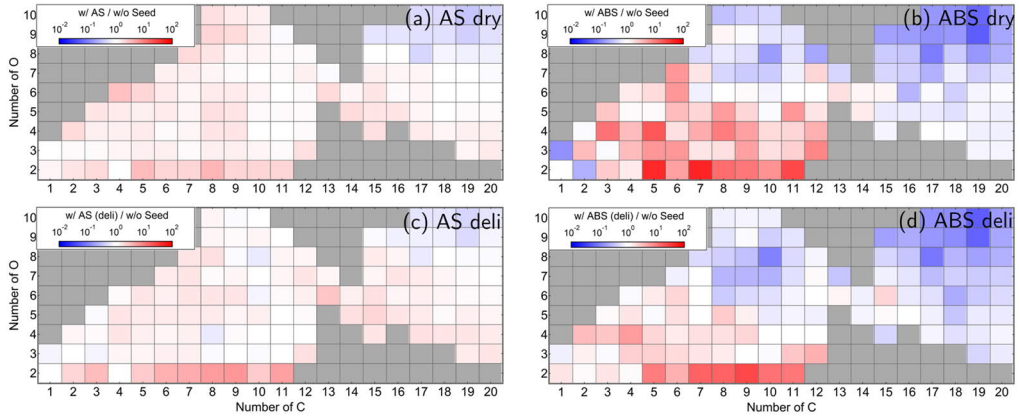

Figure 12. Relative differences in signal intensities between the steady states during seed injections and the control runs without seed (α-pinene ozonolysis in dry or humid chamber) prior to the seed injections. The figure is adopted from **Paper V** under creative Commons 4.0 Licence.

As the species should be volatile in nature, they should certainly show up in the gas phase measurements. Therefore, a similar figure to Figure 12 was drawn for the gas phase in **Paper V**. As it indicated no major differences between the different seed types, we suspected that these species originated from thermal decomposition of larger molecules, i.e. oligomers, during the FIGAERO-I^--CIMS heating cycle.

Oligomers (incl. dimers) can be produced in both gas and particle phases. According to the current understanding, dimers in the gas phase are produced by reactions between two RO_2 radicals (Berndt et al., 2018). Due to their (extremely) low vapour pressures (**Paper IV**), they condense fast and irreversibly to the particle phase yielding SOA. However, HOMs, likely to contain hydroperoxide functionalities (Mentel et al., 2015), are expected to decompose in the particle phase rapidly decreasing the HOM mass fraction of SOA as discussed already in the last section (Pospisilova et al., 2020;Krapf et al., 2016). We expect such reactions to also take place in our experiments in the COALA chamber, however in an acid-catalysed manner as reflected in the measurement data.

Importantly, the products originating from such particle phase HOM fragmentation reactions are different from those observed to accumulate in the acidic particle phase. Our results therefore indicated both accelerated HOM fragmentation and oligomerisation in the particle phase. Besides the signs of thermal decomposition of these other oligomers, also other signs of their presence in the acidic aerosols were found. Figure 13a shows an increasing presence of *m/Q* 500–800 Th signals with seed aerosol acidity. However, due to lack of external mass calibrants at such high mass range, the molecular composition of these ions remain undetermined in **Paper V**. A significant difference in terms of volatility can be expected for SOA (trans)formed under acid catalysed pathways compared to SOA yielded onto non-acidified systems. Figure 13b depicts the SOA volume fraction remaining as a function of time after the SOA has formed. It is undeniable that the SOA yielded onto acidified aerosol seed particles evaporated the least indicating SOA of lowest volatility (**Paper V**).

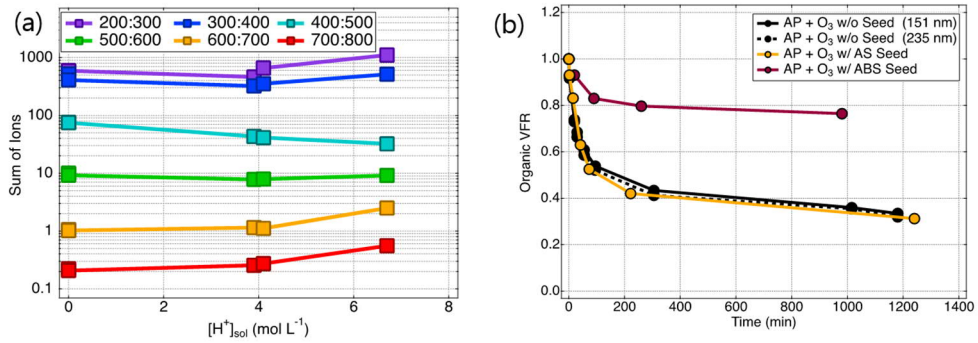

Figure 13. Panel **a**: Changes of the signals at different *m/Q* ranges of the mass spectrum representing of α-pinene-derived SOA as a function of seed aerosol acidity (in hydronium ion concentration in the solution used for seed generation) roughly estimated with thermodynamic model (E-AIM) calculations. Panel **b**: The volume fraction remaining (VFR) as a function of time under room temperature of α-pinene (AP)-derived SOA formed in the absence of seed and in the presence of AS or ABS. The higher the VFR stays over time, the less SOA has evaporated. The figures are adopted from **Paper V** under creative Commons 4.0 Licence.

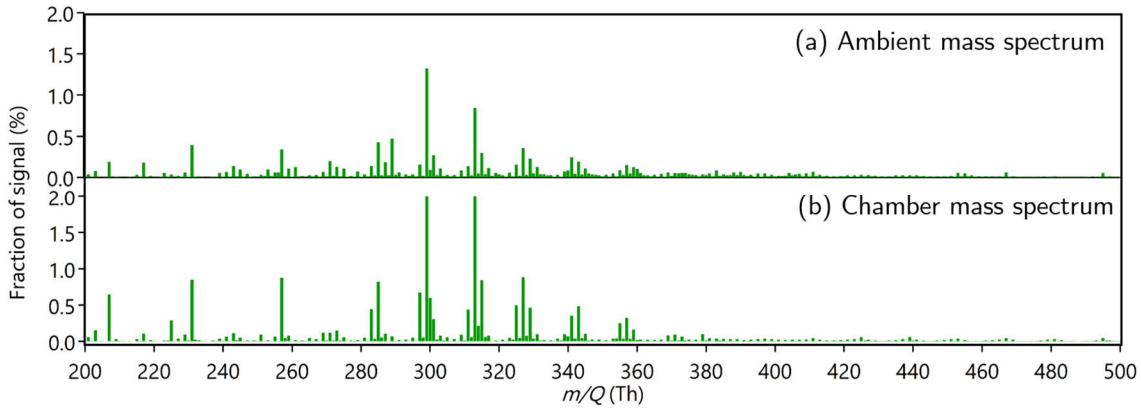

Figure 14. Mass spectra recorded by the FIGAERO-I⁻-CIMS at SMEAR II (panel **a**) and COALA chamber (panel **b**), both under the influence of acidic sulphate aerosol particles. The *y*-axis in panel b is cut. The peak at m/Q 299 Th reaches up to ca 12% and the peak at *m/Q* 313 Th reaches up to ca. 3%. Figure redrawn from data presented in **Paper V**.

Similar SOA transformations were also observed at SMEAR II in the presence of acidic sulphate aerosols, which likely originated from oil smelters refineries at Kola Peninsula (**Paper V**). In the case of acidic pollution episodes we observed again i) a decrease in HOM monomers and dimers in the particle phase with increasing sulphate loading, ii) higher contribution of signals at > *m/Q* 500 Th and iii) a strikingly similar mass spectrum to that recorded from the COALA experiments with ABS (**Paper V**; Fig. 14). While conclusion making from ambient data sets based on correlations is challenging, the results strongly suggest relevance of the phenomena studied in the COALA chamber.

Kourtchev et al. (2016) reported high oligomer contents at SMEAR II during summer 2014 using the summer of 2011 as a reference point. Due to a large difference between the temperatures between the two summers, also the OA loading between them was different, because less monoterpenes were emitted during the cold summer of 2011. The higher oligomer content in 2014 was therefore suggested to be a result of a higher mass loading and such results were later replicated via chamber experiments (Kourtchev et al., 2016). While the SOA yield was significantly higher when the highest production of oligomers took place at also at the experiments conducted in the COALA chamber, the phenomenon also occurred on deliquesced ABS particles in which case the SOA yield was close to the yield calculated for the AS system. Nonetheless, it remains an open question whether the projected increase in the warm summer frequencies would boost SOA oligomerisation reactions in the boreal environment even if the acidity of aerosol particles would decrease due to emission regulations regarding acidifying aerosol species.

6 Review of papers and the author's contribution

Paper I presents the inter- and intra-annual variability of aerosol chemical composition at SMEAR II utilising 7 years of measurement data. I performed the majority of the measurements from summer 2013 onwards, took a leading role in determining the content of the paper, performed the majority of the data analysis and data visualisation and wrote the paper with comments from co-authors.

Paper II presents an 8-year characterisation of organic aerosol mass spectra and its seasonal variability at SMEAR II by using a data-driven data analysis approach. I performed the majority of the measurements, determined the content and scope of the paper, performed the majority of the data analysis, methodology development and data visualisation. I wrote the paper with comments from co-authors.

Paper III investigates (anthropogenic) organic aerosol pollution episodes at the SMEAR II utilising a machine learning approach. I participated in the data analysis by data visualisation and by commenting and editing the manuscript.

Paper IV introduces an experimental method for exploring HOM volatilities. I had a major role executing the chamber experiments. I contributed to the data analysis by preparing the AMS data set utilised, and discussing the key results of the study. I contributed to the writing process by commenting and editing the manuscript.

Paper V explores the effect of aerosol acidity on HOM condensate and SOA (trans)formations. The study represents a combination of atmospheric simulation chamber and ambient studies. I had a major role in the experiment design and execution and I performed all the AMS and ACSM measurements and their data analysis. I actively participated in data visualisation and designing the content of the paper. I contributed to the writing process by commenting and editing the manuscript.

7 Conclusions and outlook

This thesis investigates the composition and (trans)formation of OA in the boreal environment using various observations gained via mass spectrometric techniques. The broad combinations of measurement equipment together with the mix of long-term field measurements, advanced statistical analysis techniques and environmental chamber studies helped to assess the following scientific goals (**1-5**) of this thesis:

(1) Develop a statistical analysis framework for OA classification in rural or remote regions (**Papers II** and **III**).
(2) Determine the driving constituents of boreal OA and their inter- and intra-annual variabilities in the boreal forest (**Papers I** and **II**).
(3) Assess the volatilities of condensable vapours in the boreal forest (**Paper IV**).
(4) Assess the influence of anthropogenic pollutants in boreal SOA formation (**Papers IV** and **V**).
(5) Determine the types of chemical transformations taking place in fresh boreal SOA with or without anthropogenic influence (**Paper V**).

The following paragraphs summarise the key results and outcomes of the thesis work. The number(s) in the beginning of each paragraph refers to the scientific goal addressed. The final paragraph provides future study prospects regarding boreal OA evolution.

(1) Long-term measurements (2012–2019) from SMEAR II station were utilised for achieving the first goals of the thesis. The development of an OA classification framework was an essential step needed for summarising the information held within the time-dependent mass spectra recorded over eight years. The developed data analysis procedure included exploration of a wealth of unconstrained PMF runs via K-Means clustering (**Paper II** and **III**), which was followed by constrained PMF runs using the compressed information yielded from the clustering analysis (**Paper II**). The methodology was proven successful via tests conducted on anthropogenic pollution episodes at SMEAR II (**Paper III**), and finally on the long-term data in which nearly 90% of the occurring OA variability at the station could be explained (**Paper II**). This developed data-driven method is most certainly suitable also for OA classification in other rural/remote environments and can possibly highly improve the information gain of the prevailing OA types in those areas. By using the developed methodology for the long-term SMEAR II data set, the bulk OA data could be split into three sub-categories: SV-OOA, LV-OOA and POA (**Paper II**), which enabled me to finally tackle the next scientific goal of the thesis.

(2) While the organic mass fraction expressed strong seasonality, having lowest mass fractions in winter and highest in summer (**Paper I**), the ubiquity of LV-OOA was evident throughout the year (**Paper II**). As LV-OOA has been shown to be yielded through photochemical aging of multiple OA types (Jimenez et al., 2009), it can be concluded that also the LV-OOA detected within this work resulted from photochemical aging of its fresh precursors. These LV-OOA precursors were most certainly season-dependent. POA, the concentration and mass fraction of which peaked in winter (**Paper II**), likely represented an important wintertime candidate. As the majority of wintertime POA can be linked to anthropogenic emissions from e.g. domestic wood burning, the wintertime LV-OOA was also

likely of anthropogenic origin. This is further supported by the reduced wintertime biogenic VOC emissions, which are highly dependent on temperature (Guenther et al., 1993), especially in the monoterpene-dominated boreal forest (Hakola et al., 2012). Upon the arrival of summer, the concentrations of SV-OOA increased (**Paper II**). This group of organics likely involved SOA produced from several biogenic pathways, which all potentially produced LV-OOA during the efficient summertime photochemical aging. The strong temperature dependence of OA mass concentration further spoke for the importance of biogenic SOA formation at the measurement site (**Paper I**). We estimated natural summertime SOA (LV-OOA) production of tens of ng m^{-3} h^{-1} over the boreal forest (**Paper II**). Due to the strong temperature dependence of boreal SOA formation and aging, it is possible that increasing summertime LV-OOA concentrations can be expected if the projected increase in the number of heatwaves come true in the boreal climate. Heatwaves, which took place during the measurement period, led to up to 70% increase in the OA concentration (**Paper I**).

(3-4) These long-term measurements conducted in the boreal environment describe mostly the composition, concentration and variability of the accumulated organics in the atmosphere. The initial steps of the SOA formation and aging taking place *in situ* are not easily extracted from such ambient data. Therefore, the experiments conducted in the laboratory environment provide useful insights into these phenomena. Using the COALA chamber at the University of Helsinki, we examined SOA formation via HOM condensation (**Paper IV**). HOMs, which in the boreal air originate from the autoxidation of monoterpenes, such as α-pinene, and have been suggested as an important source of boreal SOA (Ehn et al., 2014;Bianchi et al., 2019;Roldin et al., 2019). HOMs have been recognised as low volatility species, but their volatility has remained an open and challenging question due to high scatter in volatility estimates between different methods (Kurtén et al., 2016). The reason why accurate volatility estimation is much desired is that HOM volatility governs their SOA formation potential. The experiments conducted in the COALA chamber provided a possibility to experimentally explore HOM volatilities on a molecular level (**Paper IV**). The results obtained predicted HOM volatilities within the previously estimated ranges, giving confidence to the applied methodology. The methodology described in **Paper IV** could be further utilised with systems other than α-pinene ozonolysis to yield insight of volatility distributions of various HOMs generated over the boreal environment. HOM volatilities were predicted as low or extremely low for HOM dimers and low or semi-volatile for HOM monomers. The addition of NO_x did not influence the volatilities of non-nitrate HOMs. However, a clear difference was spotted between non-nitrate and organonitrate HOMs of same molecular mass, the organonitrates being more volatile (**Paper IV**). The volatility distribution of HOMs in the presence of NO_x contained more higher volatility products compared to scenarios in the absence of NO_x. It has also been proposed elsewhere and linked to size-dependent suppression of particle growth (Yan et al., 2020). In general, this means that in the presence of NO_x, the growth of the smallest particles is limited more than the growth of larger particles.

(4-5) As highlighted recently by Pospisilova et al. (2020), predicting SOA composition accurately needs accounting for particle phase fragmentation of HOM, which takes place during the first hours after HOM condensate formation. We in turn showed in **Paper V** how

these fragmentation reactions might speed up in the presence of acidic seed particles. Despite the success in actions reducing the amount of acid rain over the boreal environment, the acidic nature of aerosol has remained as a common feature describing atmospheric aerosol (Pye et al., 2020). Therefore, studies deployed within **Paper V**, which focused on acid-driven chemical transformations of biogenic boreal SOA, achieved high atmospheric relevance. This relevance was further demonstrated by the similarity between ambient observations in the boreal forest and the laboratory experiments (**Paper V**). Interestingly, not only did the aerosol acidity promote the fragmentation of several HOM monomers and dimers, it also enhanced SOA yields possibly via reactive uptake of carbonyls and initiated oligomerisation reactions. These processes lead to the formation of low-volatility SOA yet with relatively low degree of oxygenation (**Paper V**).

The combination of results obtained within the thesis work brings us to the conclusion that the fresh SOA including HOM condensate might undergo complicated reactions during the first hours after formation due to the highly reactive nature of fresh SOA. However, the importance of accounting for photochemical aging through functionalisation is undeniably important in order to achieve the highly oxidised forms of SOA observed in the (boreal) atmosphere. Therefore, further work should be conducted in exploring photochemical aging via the recently developed state-of-the-art mass spectrometric techniques in both chamber and long-term field studies. Due to the increasing amounts of data these measurements provide, utilisation of machine learning techniques, similar to the ones developed within this work, could be useful. These methods could provide insight into the production mechanisms and mechanism-dependent chemical variability of LV-OOA. Such understanding could ultimately ease OA source apportionment and yield perceptivity of the OA evolution in the boreal environment. Concurrently to the state-of-the-art mass spectrometric measurements, comparisons between the boreal long-term measurement data and global/chemical transport model outputs should be made. These assessments can further help to evaluate the strengths and weaknesses of the modelling efforts, which can further improve our understanding of fundamental aerosol reactions in climate models.

References

Albrecht, B.: Aerosols, Cloud Microphysics, and Fractional Cloudiness, Science, 245, 1227-1230, 10.1126/science.245.4923.1227, 1989.

Alfarra, M. R., Prevot, A. S., Szidat, S., Sandradewi, J., Weimer, S., Lanz, V. A., Schreiber, D., Mohr, M., and Baltensperger, U.: Identification of the mass spectral signature of organic aerosols from wood burning emissions, Environmental Science & Technology, 41, 5770-5777, 2007.

Allan, J. D., Jimenez, J. L., Williams, P. I., Alfarra, M. R., Bower, K. N., Jayne, J. T., Coe, H., and Worsnop, D. R.: Quantitative sampling using an Aerodyne aerosol mass spectrometer 1. Techniques of data interpretation and error analysis, Journal of Geophysical Research: Atmospheres, 108, 10.1029/2002jd002358, 2003.

Allan, J. D., Delia, A. E., Coe, H., Bower, K. N., Alfarra, M. R., Jimenez, J. L., Middlebrook, A. M., Drewnick, F., Onasch, T. B., Canagaratna, M. R., Jayne, J. T., and Worsnop, D. R.: A generalised method for the extraction of chemically resolved mass spectra from Aerodyne aerosol mass spectrometer data, Journal of Aerosol Science, 35, 909-922, 2004.

Ariya, P. A., Sun, J., Eltouny, N. A., Hudson, E. D., Hayes, C. T., and Kos, G.: Physical and chemical characterization of bioaerosols – Implications for nucleation processes, International Reviews in Physical Chemistry, 28, 1-32, 10.1080/01442350802597438, 2009.

Arthur, D., and Vassilvitskii, S.: K-Means++: The Advantages of Careful Seeding, In Proceedings of the 18th Annual ACM-SIAM Symposium on Discrete Algorithms, 1027-1035 pp., 2007.

Atkinson, R., and Arey, J.: Atmospheric Degradation of Volatile Organic Compounds, Chemical Reviews, 103, 4605-4638, 10.1021/cr0206420, 2003.

Ball, G. H., and Hall, D. J.: ISODATA, a novel method of analysis and pattern classification, DTIC Document, Technical report, Stanford research institute, Menlo Park, CA, USA, 1965.

Barsanti, K., Kroll, J., and Thornton, J. A.: Formation of Low-Volatility Organic Compounds in the Atmosphere: Recent Advancements and Insights, The Journal of Physical Chemistry Letters, 8 7, 1503-1511, 2017.

Berndt, T., Scholz, W., Mentler, B., Fischer, L., Herrmann, H., Kulmala, M., and Hansel, A.: Accretion Product Formation from Self- and Cross-Reactions of RO2 Radicals in the Atmosphere, Angewandte Chemie International Edition, 57, 3820-3824, 10.1002/anie.201710989, 2018.

Bianchi, F., Kurtén, T., Riva, M., Mohr, C., Rissanen, M. P., Roldin, P., Berndt, T., Crounse, J. D., Wennberg, P. O., Mentel, T. F., Wildt, J., Junninen, H., Jokinen, T., Kulmala, M., Worsnop, D. R., Thornton, J. A., Donahue, N., Kjaergaard, H. G., and Ehn, M.: Highly Oxygenated Organic Molecules (HOM) from Gas-Phase Autoxidation Involving Peroxy Radicals: A Key Contributor to Atmospheric Aerosol, Chemical Reviews, 119, 3472-3509, 10.1021/acs.chemrev.8b00395, 2019.

Bond, T. C., Streets, D. G., Yarber, K. F., Nelson, S. M., Woo, J. H., and Klimont, Z.: A technology-based global inventory of black and organic carbon emissions from combustion, Journal of Geophysical Research: Atmospheres, 109, 2004.

Boucher, O., Randall, D., Artaxo, P., Bretherton, C., Feingold, G., Forster, P., Kerminen, V.-M., Kondo, Y., Liao, H., and Lohmann, U.: Clouds and aerosols, in: Climate change 2013: the physical science basis. Contribution of Working Group I to the Fifth Assessment Report of the Intergovernmental Panel on Climate Change, Cambridge University Press, 571-657, 2013.

Canagaratna, M. R., Jayne, J. T., Jimenez, J. L., Allan, J. D., Alfarra, M. R., Zhang, Q., Onasch, T. B., Drewnick, F., Coe, H., Middlebrook, A., Delia, A., Williams, L. R., Trimborn, A. M., Northway, M. J., DeCarlo, P. F., Kolb, C. E., Davidovits, P., and Worsnop, D. R.: Chemical and microphysical characterization of ambient aerosols with the aerodyne aerosol mass spectrometer, Mass Spectrometry Reviews, 26, 185-222, 10.1002/mas.20115, 2007.

Canagaratna, M. R., Onasch, T. B., Wood, E. C., Herndon, S. C., Jayne, J. T., Cross, E. S., Miake-Lye, R. C., Kolb, C. E., and Worsnop, D. R.: Evolution of Vehicle Exhaust Particles in the Atmosphere, Journal of the Air & Waste Management Association, 60, 1192-1203, 10.3155/1047-3289.60.10.1192, 2010.

Canagaratna, M. R., Jimenez, J. L., Kroll, J. H., Chen, Q., Kessler, S. H., Massoli, P., Hildebrandt Ruiz, L., Fortner, E., Williams, L. R., Wilson, K. R., Surratt, J. D., Donahue, N. M., Jayne, J. T., and Worsnop, D. R.: Elemental ratio measurements of organic compounds using aerosol mass spectrometry: characterization, improved calibration, and implications, Atmospheric Chemistry and Physics, 15, 253-272, 10.5194/acp-15-253-2015, 2015.

Canonaco, F., Crippa, M., Slowik, J. G., Baltensperger, U., and Prévôt, A. S. H.: SoFi, an IGOR-based interface for the efficient use of the generalized multilinear engine (ME-2) for the source

apportionment: ME-2 application to aerosol mass spectrometer data, Atmospheric Measurement Techniques, 6, 3649-3661, 10.5194/amt-6-3649-2013, 2013.
Canonaco, F., Tobler, A., Chen, G., Sosedova, Y., Slowik, J. G., Bozzetti, C., Daellenbach, K. R., ElHaddad, I., Crippa, M., Huang, R. J., Furger, M., Baltensperger, U., and Prévôt, A. S. H.: A new method for long-term source apportionment with time-dependent factor profiles and uncertainty assessment using SoFi Pro: application to one year of organic aerosol data, Atmospheric Measurement Techniques Discussions, 2020, 1-39, 10.5194/amt-2020-204, 2020.
Cappa, C. D., and Jimenez, J. L.: Quantitative estimates of the volatility of ambient organic aerosol, Atmospheric Chemistry and Physics, 10, 5409-5424, 10.5194/acp-10-5409-2010, 2010.
Cappa, C. D., and Wilson, K. R.: Evolution of organic aerosol mass spectra upon heating: implications for OA phase and partitioning behavior, Atmospheric Chemistry and Physics, 11, 1895-1911, 10.5194/acp-11-1895-2011, 2011.
Chacon-Madrid, H. J., and Donahue, N. M.: Fragmentation vs. functionalization: chemical aging and organic aerosol formation, Atmospheric Chemistry and Physics, 11, 10553-10563, 10.5194/acp-11-10553-2011, 2011.
Chacon-Madrid, H. J., Henry, K. M., and Donahue, N. M.: Photo-oxidation of pinonaldehyde at low NOx: from chemistry to organic aerosol formation, Atmospheric Chemistry and Physics, 13, 3227-3236, 10.5194/acp-13-3227-2013, 2013.
Claflin, M. S., Krechmer, J. E., Hu, W., Jimenez, J. L., and Ziemann, P. J.: Functional Group Composition of Secondary Organic Aerosol Formed from Ozonolysis of α-Pinene Under High VOC and Autoxidation Conditions, ACS Earth and Space Chemistry, 2, 1196-1210, 10.1021/acsearthspacechem.8b00117, 2018.
Coggon, M. M., Veres, P. R., Yuan, B., Koss, A., Warneke, C., Gilman, J. B., Lerner, B. M., Peischl, J., Aikin, K. C., Stockwell, C. E., Hatch, L. E., Ryerson, T. B., Roberts, J. M., Yokelson, R. J., and de Gouw, J. A.: Emissions of nitrogen-containing organic compounds from the burning of herbaceous and arboraceous biomass: Fuel composition dependence and the variability of commonly used nitrile tracers, Geophysical Research Letters, 43, 9903-9912, 10.1002/2016gl070562, 2016.
Collins, M., Knutti, R., Arblaster, J., Dufresne, J.-L., Fichefet, T., Friedlingstein, P., Gao, X., Gutowski, W. J., Johns, T., Krinner, G., Shongwe, M., Tebaldi, A., Weaver, J., and Wehner, M.: Long-term climate change: projections, commitments and irreversibility, in: Climate Change 2013-The Physical Science Basis: Contribution of Working Group I to the Fifth Assessment Report of the Intergovernmental Panel on Climate Change, Cambridge University Press, 1029-1136, 2013.
Crounse, J. D., Nielsen, L. B., Jørgensen, S., Kjaergaard, H. G., and Wennberg, P. O.: Autoxidation of Organic Compounds in the Atmosphere, The Journal of Physical Chemistry Letters, 4, 3513-3520, 10.1021/jz4019207, 2013.
Cubison, M., Ortega, A., Hayes, P., Farmer, D., Day, D., Lechner, M., Brune, W. H., Apel, E., Diskin, G., Fisher, J., Hecobian, A., Knapp, D., Mikoviny, T., Riemer, D., Sache, G., Sessions, W., Weber, R., Weinheimer, A., Wisthaler, A., and Jimenez, J. L.: Effects of aging on organic aerosol from open biomass burning smoke in aircraft and laboratory studies, Atmospheric Chemistry and Physics, 11, 12049-12064, 2011.
Czoschke, N. M., Jang, M., and Kamens, R. M.: Effect of acidic seed on biogenic secondary organic aerosol growth, Atmospheric Environment, 37, 4287-4299, https://doi.org/10.1016/S1352-2310(03)00511-9, 2003.
De Gouw, J., and Jimenez, J. L.: Organic Aerosols in the Earth's Atmosphere, Environmental Science & Technology, 43, 7614-7618, 10.1021/es9006004, 2009.
Donahue, N. M., Robinson, A. L., Stanier, C. O., and Pandis, S. N.: Coupled Partitioning, Dilution, and Chemical Aging of Semivolatile Organics, Environmental Science & Technology, 40, 2635-2643, 10.1021/es052297c, 2006.
Donahue, N. M., Henry, K. M., Mentel, T. F., Kiendler-Scharr, A., Spindler, C., Bohn, B., Brauers, T., Dorn, H. P., Fuchs, H., Tillmann, R., Wahner, A., Saathoff, H., Naumann, K.-H., Möhler, O., Leisner, T., Müller, L., Reinnig, M.-C., Hoffmann, T., Salo, K., Hallquist, M., Frosch, M., Bilde, M., Tritscher, T., Barmet, P., Praplan, A. P., DeCarlo, P. F., Dommen, J., Prévôt, A. S. H., and Baltensperger, U.: Aging of biogenic secondary organic aerosol via gas-phase OH radical reactions, Proceedings of the National Academy of Sciences, 109, 13503-13508, 10.1073/pnas.1115186109, 2012a.
Donahue, N. M., Kroll, J. H., Pandis, S. N., and Robinson, A. L.: A two-dimensional volatility basis set – Part 2: Diagnostics of organic-aerosol evolution, Atmospheric Chemistry and Physics, 12, 615-634, 10.5194/acp-12-615-2012, 2012b.
Drewnick, F., Hings, S. S., DeCarlo, P., Jayne, J. T., Gonin, M., Fuhrer, K., Weimer, S., Jimenez, J. L., Demerjian, K. L., Borrmann, S., and Worsnop, D.: A new time-of-flight aerosol mass spectrometer

(TOF-AMS)—Instrument description and first field deployment, Aerosol Science and Technology, 39, 637-658, 2005.

Drewnick, F., Diesch, J. M., Faber, P., and Borrmann, S.: Aerosol mass spectrometry: particle–vaporizer interactions and their consequences for the measurements, Atmospehric Measurement Techniques, 8, 3811-3830, 10.5194/amt-8-3811-2015, 2015.

Dusek, U., Frank, G. P., Hildebrandt, L., Curtius, J., Schneider, J., Walter, S., Chand, D., Drewnick, F., Hings, S., Jung, D., Borrmann, S., and Andreae, M. O.: Size Matters More Than Chemistry for Cloud-Nucleating Ability of Aerosol Particles, Science, 312, 1375-1378, 10.1126/science.1125261, 2006.

Ehn, M., Kleist, E., Junninen, H., Petäjä, T., Lönn, G., Schobesberger, S., Dal Maso, M., Trimborn, A., Kulmala, M., Worsnop, D. R., Wahner, A., Wildt, J., and Mentel, T. F.: Gas phase formation of extremely oxidized pinene reaction products in chamber and ambient air, Atmospheric Chemistry and Physics, 12, 5113-5127, 10.5194/acp-12-5113-2012, 2012.

Ehn, M., Thornton, J. A., Kleist, E., Sipilä, M., Junninen, H., Pullinen, I., Springer, M., Rubach, F., Tillmann, R., Lee, B., Lopez-Hilfiker, F., Andres, S., Acir, I.-H., Rissanen, M., Jokinen, T., Schobesberger, S., Kangasluoma, J., Kontkanen, J., Nieminen, T., Kurtén, T., Nielsen, L. B., Jørgensen, S., Kjaergaard, H. G., Canagaratna, M., Maso, M. D., Berndt, T., Petäjä, T., Wahner, A., Kerminen, V.-M., Kulmala, M., Worsnop, D. R., Wildt, J., and Mentel, T. F.: A large source of low-volatility secondary organic aerosol, Nature, 506, 476-479, 10.1038/nature13032, 2014.

Eisele, F. L., and Tanner, D. J.: Measurement of the gas phase concentration of H2SO4 and methane sulfonic acid and estimates of H2SO4 production and loss in the atmosphere, Journal of Geophysical Research: Atmospheres, 98, 9001-9010, 10.1029/93jd00031, 1993.

Epstein, S. A., Riipinen, I., and Donahue, N. M.: A Semiempirical Correlation between Enthalpy of Vaporization and Saturation Concentration for Organic Aerosol, Environmental Science & Technology, 44, 743-748, 10.1021/es902497z, 2010.

Faust, J. A., Wong, J. P. S., Lee, A. K. Y., and Abbatt, J. P. D.: Role of Aerosol Liquid Water in Secondary Organic Aerosol Formation from Volatile Organic Compounds, Environmental Science & Technology, 51, 1405-1413, 10.1021/acs.est.6b04700, 2017.

Finlayson-Pitts, B. J., and Pitts Jr, J. N.: Chemistry of the upper and lower atmosphere: theory, experiments, and applications, Elsevier, 1999.

Fröhlich, R., Cubison, M. J., Slowik, J. G., Bukowiecki, N., Prévôt, A. S. H., Baltensperger, U., Schneider, J., Kimmel, J. R., Gonin, M., Rohner, U., Worsnop, D. R., and Jayne, J. T.: The ToF-ACSM: a portable aerosol chemical speciation monitor with TOFMS detection, Atmospheric Measurement Techniques, 6, 3225-3241, 10.5194/amt-6-3225-2013, 2013.

Fröhlich, R., Crenn, V., Setyan, A., Belis, C. A., Canonaco, F., Favez, O., Riffault, V., Slowik, J. G., Aas, W., Äijälä, M., Alastuey, A., Artiñano, B., Bonnaire, N., Bozzetti, C., Bressi, M., Carbone, C., Coz, E., Croteau, P. L., Cubison, M. J., Esser-Gietl, J. K., Green, D. C., Gros, V., Heikkinen, L., Herrmann, H., Jayne, J. T., Lunder, C. R., Minguillón, M. C., Močnik, G., O'Dowd, C. D., Ovadnevaite, J., Petralia, E., Poulain, L., Priestman, M., Ripoll, A., Sarda-Estève, R., Wiedensohler, A., Baltensperger, U., Sciare, J., and Prévôt, A. S. H.: ACTRIS ACSM intercomparison – Part 2: Intercomparison of ME-2 organic source apportionment results from 15 individual, co-located aerosol mass spectrometers, Atmospheric Measurement Techniques, 8, 2555-2576, 10.5194/amt-8-2555-2015, 2015.

Gao, S., Keywood, M., Ng, N. L., Surratt, J., Varutbangkul, V., Bahreini, R., Flagan, R. C., and Seinfeld, J. H.: Low-Molecular-Weight and Oligomeric Components in Secondary Organic Aerosol from the Ozonolysis of Cycloalkenes and α-Pinene, The Journal of Physical Chemistry A, 108, 10147-10164, 10.1021/jp047466e, 2004.

Gauthier, S., Bernier, P., Kuuluvainen, T., Shvidenko, A., and Schepaschenko, D.: Boreal forest health and global change, Science, 349, 819-822, 2015.

George, I. J., and Abbatt, J. P. D.: Heterogeneous oxidation of atmospheric aerosol particles by gas-phase radicals, Nature Chemistry, 2, 713-722, 10.1038/nchem.806, 2010.

Ghan, S. J., and Schwartz, S. E.: Aerosol Properties and Processes: A Path from Field and Laboratory Measurements to Global Climate Models, Bulletin of the American Meteorological Society, 88, 1059-1084, 10.1175/BAMS-88-7-1059, 2007.

Glasius, M., Calogirou, A., Jensen, N. R., Hjorth, J., and Nielsen, C. J.: Kinetic study of gas-phase reactions of pinonaldehyde and structurally related compounds, International Journal of Kinetics, 29, 527-533, 10.1002/(sici)1097-4601(1997)29:7<527::Aid-kin7>3.0.Co;2-w, 1997.

Goldstein, A. H., and Galbally, I. E.: Known and Unexplored Organic Constituents in the Earth's Atmosphere, Environmental Science & Technology, 41, 1514-1521, 10.1021/es072476p, 2007.

Govender, P., and Sivakumar, V.: Application of k-means and hierarchical clustering techniques for analysis of air pollution: A review (1980–2019), Atmospheric Pollution Research, 11, 40-56, https://doi.org/10.1016/j.apr.2019.09.009, 2020.

Graedel, T., and Franey, J.: Field measurements of submicron aerosol washout by snow, Geophysical Research Letters, 2, 325-328, 1975.

Grieshop, A., Donahue, N., and Robinson, A.: Laboratory investigation of photochemical oxidation of organic aerosol from wood fires 2: analysis of aerosol mass spectrometer data, Atmospheric Chemistry and Physics, 9, 2227-2240, 2009.

Guenther, A. B., Zimmerman, P. R., Harley, P. C., Monson, R. K., and Fall, R.: Isoprene and monoterpene emission rate variability: model evaluations and sensitivity analyses, Journal of Geophysical Research: Atmospheres, 98, 12609-12617, 1993.

Guenther, A. B., Jiang, X., Heald, C. L., Sakulyanontvittaya, T., Duhl, T., Emmons, L. K., and Wang, X.: The Model of Emissions of Gases and Aerosols from Nature version 2.1 (MEGAN2.1): an extended and updated framework for modeling biogenic emissions, Geoscientific Model Development, 5, 1471-1492, 10.5194/gmd-5-1471-2012, 2012.

Hakola, H., Hellén, H., Hemmilä, M., Rinne, J., and Kulmala, M.: In situ measurements of volatile organic compounds in a boreal forest, Atmospheric Chemistry and Physics, 12, 11665-11678, 2012.

Hallquist, M., Wenger, J. C., Baltensperger, U., Rudich, Y., Simpson, D., Claeys, M., Dommen, J., Donahue, N. M., George, C., Goldstein, A. H., Hamilton, J. F., Herrmann, H., Hoffmann, T., Iinuma, Y., Jang, M., Jenkin, M. E., Jimenez, J. L., Kiendler-Scharr, A., Maenhaut, W., McFiggans, G., Mentel, T. F., Monod, A., Prévôt, A. S. H., Seinfeld, J. H., Surratt, J. D., Szmigielski, R., and Wildt, J.: The formation, properties and impact of secondary organic aerosol: current and emerging issues, Atmospheric Chemistry and Physics, 9, 5155-5236, 10.5194/acp-9-5155-2009, 2009.

Hansen, J., and Nazarenko, L.: Soot climate forcing via snow and ice albedos, Proceedings of the National Academy of Sciences, 101, 423-428, 10.1073/pnas.2237157100 2004.

Hari, P., and Kulmala, M.: Station for measuring ecosystem-atmosphere relations (SMEAR II), Boreal Environment Research, 10, 315-322, 2005.

Hatakeyama, S., Izumi, K., Fukuyama, T., Akimoto, H., and Washida, N.: Reactions of OH with α-pinene and β-pinene in air: Estimate of global CO production from the atmospheric oxidation of terpenes, Journal of Geophysical Research: Atmospheres, 96, 947-958, 10.1029/90jd02341, 1991.

Hennigan, C. J., Miracolo, M. A., Engelhart, G. J., May, A. A., Presto, A. A., Lee, T., Sullivan, A. P., McMeeking, G. R., Coe, H., Wold, C. E., Hao, W. M., Gilman, J. B., Kuster, W. C., de Gouw, J., Schichtel, B. A., Collett Jr, J. L., Kreidenweis, S. M., and Robinson, A. L.: Chemical and physical transformations of organic aerosol from the photo-oxidation of open biomass burning emissions in an environmental chamber, Atmospheric Chemistry and Physics, 11, 7669-7686, 10.5194/acp-11-7669-2011, 2011.

Henry, K. M., and Donahue, N. M.: Photochemical Aging of α-Pinene Secondary Organic Aerosol: Effects of OH Radical Sources and Photolysis, The Journal of Physical Chemistry A, 116, 5932-5940, 10.1021/jp210288s, 2012.

Herrmann, H., Schaefer, T., Tilgner, A., Styler, S. A., Weller, C., Teich, M., and Otto, T.: Tropospheric Aqueous-Phase Chemistry: Kinetics, Mechanisms, and Its Coupling to a Changing Gas Phase, Chemical Reviews, 115, 4259-4334, 10.1021/cr500447k, 2015.

Hyttinen, N., Kupiainen-Määttä, O., Rissanen, M. P., Muuronen, M., Ehn, M., and Kurtén, T.: Modeling the Charging of Highly Oxidized Cyclohexene Ozonolysis Products Using Nitrate-Based Chemical Ionization, The Journal of Physical Chemistry A, 119, 6339-6345, 10.1021/acs.jpca.5b01818, 2015.

Isaacman-VanWertz, G., Massoli, P., O'Brien, R., Lim, C., Franklin, J. P., Moss, J. A., Hunter, J. F., Nowak, J. B., Canagaratna, M. R., Misztal, P. K., Arata, C., Roscioli, J. R., Herndon, S. T., Onasch, T. B., Lambe, A. T., Jayne, J. T., Su, L., Knopf, D. A., Goldstein, A. H., Worsnop, D. R., and Kroll, J. H.: Chemical evolution of atmospheric organic carbon over multiple generations of oxidation, Nature Chemistry, 10, 462-468, 10.1038/s41557-018-0002-2, 2018.

Iyer, S., Lopez-Hilfiker, F., Lee, B. H., Thornton, J. A., and Kurtén, T.: Modeling the Detection of Organic and Inorganic Compounds Using Iodide-Based Chemical Ionization, The Journal of Physical Chemistry A, 120, 576-587, 10.1021/acs.jpca.5b09837, 2016.

Jain, A. K.: Data clustering: 50 years beyond K-means, Pattern Recognition Letters, 31, 651-666, 2010.

Jang, M., Czoschke, N. M., Lee, S., and Kamens, R. M.: Heterogeneous Atmospheric Aerosol Production by Acid-Catalyzed Particle-Phase Reactions, Science, 298, 814-817, 10.1126/science.1075798, 2002.

Jayne, J. T., Leard, D. C., Zhang, X., Davidovits, P., Smith, K. A., Kolb, C. E., and Worsnop, D. R.: Development of an Aerosol Mass Spectrometer for Size and Composition Analysis of Submicron Particles, Aerosol Science and Technology, 33, 49-70, 10.1080/027868200410840, 2000.

Jiang, J., Aksoyoglu, S., El-Haddad, I., Ciarelli, G., Denier van der Gon, H. A. C., Canonaco, F., Gilardoni, S., Paglione, M., Minguillón, M. C., Favez, O., Zhang, Y., Marchand, N., Hao, L., Virtanen, A., Florou, K., O'Dowd, C., Ovadnevaite, J., Baltensperger, U., and Prévôt, A. S. H.: Sources of organic aerosols in Europe: a modeling study using CAMx with modified volatility basis set scheme, Atmospheric Chemistry and Physics, 19, 15247-15270, 10.5194/acp-19-15247-2019, 2019.

Jimenez, J. L., Canagaratna, M. R., Donahue, N. M., Prevot, A. S. H., Zhang, Q., Kroll, J. H., DeCarlo, P. F., Allan, J. D., Coe, H., Ng, N. L., Aiken, A. C., Docherty, K. S., Ulbrich, I. M., Grieshop, A. P., Robinson, A. L., Duplissy, J., Smith, J. D., Wilson, K. R., Lanz, V. A., Hueglin, C., Sun, Y. L., Tian, J., Laaksonen, A., Raatikainen, T., Rautiainen, J., Vaattovaara, P., Ehn, M., Kulmala, M., Tomlinson, J. M., Collins, D. R., Cubison, M. J., Dunlea, E. J., Huffman, J. A., Onasch, T. B., Alfarra, M. R., Williams, P. I., Bower, K., Kondo, Y., Schneider, J., Drewnick, F., Borrmann, S., Weimer, S., Demerjian, K., Salcedo, D., Cottrell, L., Griffin, R., Takami, A., Miyoshi, T., Hatakeyama, S., Shimono, A., Sun, J. Y., Zhang, Y. M., Dzepina, K., Kimmel, J. R., Sueper, D., Jayne, J. T., Herndon, S. C., Trimborn, A. M., Williams, L. R., Wood, E. C., Middlebrook, A. M., Kolb, C. E., Baltensperger, U., and Worsnop, D. R.: Evolution of Organic Aerosols in the Atmosphere, Science, 326, 1525-1529, 10.1126/science.1180353, 2009.

Jimenez, J. L., Canagaratna, M. R., Drewnick, F., Allan, J. D., Alfarra, M. R., Middlebrook, A. M., Slowik, J. G., Zhang, Q., Coe, H., Jayne, J. T., and Worsnop, D. R.: Comment on “The effects of molecular weight and thermal decomposition on the sensitivity of a thermal desorption aerosol mass spectrometer”, Aerosol Science and Technology, 50, i-xv, 10.1080/02786826.2016.1205728, 2016.

Jokinen, T., Sipilä, M., Junninen, H., Ehn, M., Lönn, G., Hakala, J., Petäjä, T., Mauldin Iii, R. L., Kulmala, M., and Worsnop, D. R.: Atmospheric sulphuric acid and neutral cluster measurements using CI-APi-TOF, Atmospheric Chemistry and Physics, 12, 4117-4125, 10.5194/acp-12-4117-2012, 2012.

Jokinen, T., Berndt, T., Makkonen, R., Kerminen, V.-M., Junninen, H., Paasonen, P., Stratmann, F., Herrmann, H., Guenther, A. B., Worsnop, D. R., Kulmala, M., Ehn, M., and Sipilä, M.: Production of extremely low volatile organic compounds from biogenic emissions: Measured yields and atmospheric implications, Proceedings of the National Academy of Sciences, 112, 7123-7128, 10.1073/pnas.1423977112, 2015.

Junninen, H., Ehn, M., Petäjä, T., Luosujärvi, L., Kotiaho, T., Kostiainen, R., Rohner, U., Gonin, M., Fuhrer, K., Kulmala, M., and Worsnop, D. R.: A high-resolution mass spectrometer to measure atmospheric ion composition, Atmospheric Measurement Techniques, 3, 1039-1053, 10.5194/amt-3-1039-2010, 2010.

Kalberer, M., Paulsen, D., Sax, M., Steinbacher, M., Dommen, J., Prevot, A. S. H., Fisseha, R., Weingartner, E., Frankevich, V., Zenobi, R., and Baltensperger, U.: Identification of Polymers as Major Components of Atmospheric Organic Aerosols, Science, 303, 1659-1662, 10.1126/science.1092185, 2004.

Kim, S., Sinclair, V. A., Räisänen, J., and Ruuhela, R.: Heat waves in Finland: Present and projected summertime extreme temperatures and their associated circulation patterns, International Journal of Climatology, 38, 1393-1408, 2018.

Kirkby, J., Duplissy, J., Sengupta, K., Frege, C., Gordon, H., Williamson, C., Heinritzi, M., Simon, M., Yan, C., Almeida, J., Tröstl, J., Nieminen, T., Ortega, I. K., Wagner, R., Adamov, A., Amorim, A., Bernhammer, A.-K., Bianchi, F., Breitenlechner, M., Brilke, S., Chen, X., Craven, J., Dias, A., Ehrhart, S., Flagan, R. C., Franchin, A., Fuchs, C., Guida, R., Hakala, J., Hoyle, C. R., Jokinen, T., Junninen, H., Kangasluoma, J., Kim, J., Krapf, M., Kürten, A., Laaksonen, A., Lehtipalo, K., Makhmutov, V., Mathot, S., Molteni, U., Onnela, A., Peräkylä, O., Piel, F., Petäjä, T., Praplan, A. P., Pringle, K., Rap, A., Richards, N. A. D., Riipinen, I., Rissanen, M. P., Rondo, L., Sarnela, N., Schobesberger, S., Scott, C. E., Seinfeld, J. H., Sipilä, M., Steiner, G., Stozhkov, Y., Stratmann, F., Tomé, A., Virtanen, A., Vogel, A. L., Wagner, A. C., Wagner, P. E., Weingartner, E., Wimmer, D., Winkler, P. M., Ye, P., Zhang, X., Hansel, A., Dommen, J., Donahue, N. M., Worsnop, D. R., Baltensperger, U., Kulmala, M., Carslaw, K. S., and Curtius, J.: Ion-induced nucleation of pure biogenic particles, Nature, 533, 521-526, 10.1038/nature17953, 2016.

Knopf, D. A., Forrester, S. M., and Slade, J. H.: Heterogeneous oxidation kinetics of organic biomass burning aerosol surrogates by O3, NO2, N2O5, and NO3, Physical Chemistry Chemical Physics, 13, 21050-21062, 10.1039/C1CP22478F, 2011.

Kourtchev, I., Giorio, C., Manninen, A., Wilson, E., Mahon, B., Aalto, J., Kajos, M., Venables, D., Ruuskanen, T., Levula, J., Loponen, M., Connors, S., Harris, N., Zhao, D., Kiendler-Scharr, A., Mentel, T., Rudich, Y., Hallquist, M., Doussin, J.-F., Maenhaut, W., Bäck, J., Petäjä, T., Wenger, J., Kulmala, M., and Kalberer, M.: Enhanced volatile organic compounds emissions and organic aerosol mass increase the oligomer content of atmospheric aerosols, Scientific reports, 6, 35038, 2016.

Krapf, M., El Haddad, I., Bruns, Emily A., Molteni, U., Daellenbach, Kaspar R., Prévôt, André S. H., Baltensperger, U., and Dommen, J.: Labile Peroxides in Secondary Organic Aerosol, Chem, 1, 603-616, https://doi.org/10.1016/j.chempr.2016.09.007, 2016.

Kroll, J. H., Smith, J. D., Che, D. L., Kessler, S. H., Worsnop, D. R., and Wilson, K. R.: Measurement of fragmentation and functionalization pathways in the heterogeneous oxidation of oxidized organic aerosol, Physical Chemistry Chemical Physics, 11, 8005-8014, 10.1039/B905289E, 2009.

Kroll, J. H., Donahue, N. M., Jimenez, J. L., Kessler, S. H., Canagaratna, M. R., Wilson, K. R., Altieri, K. E., Mazzoleni, L. R., Wozniak, A. S., Bluhm, H., Mysak, E. R., Smith, J. D., Kolb, C. E., and Worsnop, D. R.: Carbon oxidation state as a metric for describing the chemistry of atmospheric organic aerosol, Nature Chemistry, 3, 133-139, 10.1038/nchem.948, 2011.

Kroll, J. H., Lim, C. Y., Kessler, S. H., and Wilson, K. R.: Heterogeneous Oxidation of Atmospheric Organic Aerosol: Kinetics of Changes to the Amount and Oxidation State of Particle-Phase Organic Carbon, The Journal of Physical Chemistry A, 119, 10767-10783, 10.1021/acs.jpca.5b06946, 2015.

Kulmala, M.: Build a global Earth observatory, Nature, 553, 21-23, 10.1038/d41586-017-08967-y, 2018.

Kurtén, T., Petäjä, T., Smith, J., Ortega, I. K., Sipilä, M., Junninen, H., Ehn, M., Vehkamäki, H., Mauldin, L., Worsnop, D. R., and Kulmala, M.: The effect of H2SO4-amine clustering on chemical ionization mass spectrometry (CIMS) measurements of gas-phase sulfuric acid, Atmospheric Chemistry and Physics, 11, 3007-3019, 10.5194/acp-11-3007-2011, 2011.

Kurtén, T., Tiusanen, K., Roldin, P., Rissanen, M., Luy, J.-N., Boy, M., Ehn, M., and Donahue, N.: α-Pinene Autoxidation Products May Not Have Extremely Low Saturation Vapor Pressures Despite High O:C Ratios, The Journal of Physical Chemistry A, 120, 2569-2582, 10.1021/acs.jpca.6b02196, 2016.

Köhler, H.: The nucleus in and the growth of hygroscopic droplets, Transactions of the Faraday Society, 32, 1152-1161, 10.1039/TF9363201152, 1936.

Lambe, A. T., Miracolo, M. A., Hennigan, C. J., Robinson, A. L., and Donahue, N. M.: Effective Rate Constants and Uptake Coefficients for the Reactions of Organic Molecular Markers (n-Alkanes, Hopanes, and Steranes) in Motor Oil and Diesel Primary Organic Aerosols with Hydroxyl Radicals, Environmental Science & Technology, 43, 8794-8800, 10.1021/es901745h, 2009.

Lambe, A. T., Onasch, T. B., Croasdale, D. R., Wright, J. P., Martin, A. T., Franklin, J. P., Massoli, P., Kroll, J. H., Canagaratna, M. R., Brune, W. H., Worsnop, D. R., and Davidovits, P.: Transitions from Functionalization to Fragmentation Reactions of Laboratory Secondary Organic Aerosol (SOA) Generated from the OH Oxidation of Alkane Precursors, Environmental Science & Technology, 46, 5430-5437, 10.1021/es300274t, 2012.

Lane, T. E., Donahue, N. M., and Pandis, S. N.: Simulating secondary organic aerosol formation using the volatility basis-set approach in a chemical transport model, Atmospheric Environment, 42, 7439-7451, https://doi.org/10.1016/j.atmosenv.2008.06.026, 2008.

Le Treut, H., Somerville, R., Cubasch, U., Ding, Y., Mauritzen, C., Moskssit, A., Peterson, T., and Prather, M.: Historical Overview of Climate Change, Climate Change 2007: The Physical Science Basis. Contribution of Working Group I to the Fourth Assessment Report of the Intergovernmental Panel on Climate Change. [Solomon, S., D. Qin, M. Manning, Z. Chen, M. Marquis, K.B. Averyt, M. Tignor and H.L. Miller (eds.)]. Cambridge University Press, Cambridge, United Kingdom and New York, NY, USA., 2007.

Lee, B. H., Lopez-Hilfiker, F. D., Mohr, C., Kurtén, T., Worsnop, D. R., and Thornton, J. A.: An Iodide-Adduct High-Resolution Time-of-Flight Chemical-Ionization Mass Spectrometer: Application to Atmospheric Inorganic and Organic Compounds, Environmental Science & Technology, 48, 6309-6317, 10.1021/es500362a, 2014.

Lee, B. H., Mohr, C., Lopez-Hilfiker, F. D., Lutz, A., Hallquist, M., Lee, L., Romer, P., Cohen, R. C., Iyer, S., Kurtén, T., Hu, W., Day, D. A., Campuzano-Jost, P., Jimenez, J. L., Xu, L., Ng, N. L., Guo, H., Weber, R. J., Wild, R. J., Brown, S. S., Koss, A., de Gouw, J., Olson, K., Goldstein, A. H., Seco, R., Kim, S., McAvey, K., Shepson, P. B., Starn, T., Baumann, K., Edgerton, E. S., Liu, J., Shilling, J. E., Miller, D. O., Brune, W., Schobesberger, S., D'Ambro, E. L., and Thornton, J. A.: Highly functionalized organic nitrates in the southeast United States: Contribution to secondary organic aerosol and reactive nitrogen budgets, Proceedings of the National Academy of Sciences, 113, 1516-1521, 10.1073/pnas.1508108113, 2016.

Li, H., Canagaratna, M. R., Riva, M., Rantala, P., Zhang, Y., Thomas, S., Heikkinen, L., Flaud, P. M., Villenave, E., Perraudin, E., Worsnop, D., Kulmala, M., Ehn, M., and Bianchi, F.: Source identification of atmospheric organic vapors in two European pine forests: Results from Vocus PTR-TOF observations, Atmospheric Chemistry and Physics Discussions, 2020, 1-39, 10.5194/acp-2020-648, 2020a.

Li, H., Riva, M., Rantala, P., Heikkinen, L., Daellenbach, K., Krechmer, J. E., Flaud, P. M., Worsnop, D., Kulmala, M., Villenave, E., Perraudin, E., Ehn, M., and Bianchi, F.: Terpenes and their oxidation products in the French Landes forest: insights from Vocus PTR-TOF measurements, Atmos. Chem. Phys., 20, 1941-1959, 10.5194/acp-20-1941-2020, 2020b.

Liao, L., Dal Maso, M., Taipale, R., Rinne, J., Ehn, M., Junninen, H., Äijälä, M., Nieminen, T., Alekseychik, P., Hulkkonen, M., Worsnop, D., Kerminen, V.-M., and Kulmala, M.: Monoterpene pollution episodes in a forest environment: indication of anthropogenic origin and association with aerosol particles, Boreal Environment Research, 16, 288-303, 2011.

Liggio, J., and Li, S.-M.: Reactive uptake of pinonaldehyde on acidic aerosols, Journal of Geophysical Research: Atmospheres, 111, 10.1029/2005jd006978, 2006.

Likens, G. E., Bormann, F. H., and Johnson, N. M.: Acid Rain, Environment: Science and Policy for Sustainable Development, 14, 33-40, 10.1080/00139157.1972.9933001, 1972.

Liu, P. S., Deng, R., Smith, K. A., Williams, L. R., Jayne, J. T., Canagaratna, M. R., Moore, K., Onasch, T. B., Worsnop, D. R., and Deshler, T.: Transmission efficiency of an aerodynamic focusing lens system: Comparison of model calculations and laboratory measurements for the Aerodyne Aerosol Mass Spectrometer, Aerosol Science and Technology, 41, 721-733, 2007.

Liu, X., Day, D. A., Krechmer, J. E., Brown, W., Peng, Z., Ziemann, P. J., and Jimenez, J. L.: Direct measurements of semi-volatile organic compound dynamics show near-unity mass accommodation coefficients for diverse aerosols, Communications Chemistry, 2, 98, 10.1038/s42004-019-0200-x, 2019.

Lohmann, U., and Feichter, J.: Global indirect aerosol effects: a review, Atmospheric Chemistry and Physics, 5, 715-737, 10.5194/acp-5-715-2005, 2005.

Lopez-Hilfiker, F. D., Mohr, C., Ehn, M., Rubach, F., Kleist, E., Wildt, J., Mentel, T. F., Lutz, A., Hallquist, M., Worsnop, D., and Thornton, J. A.: A novel method for online analysis of gas and particle composition: description and evaluation of a Filter Inlet for Gases and AEROsols (FIGAERO), Atmos. Meas. Tech., 7, 983-1001, 10.5194/amt-7-983-2014, 2014.

Lopez-Hilfiker, F. D., Mohr, C., Ehn, M., Rubach, F., Kleist, E., Wildt, J., Mentel, T. F., Carrasquillo, A. J., Daumit, K. E., Hunter, J. F., Kroll, J. H., Worsnop, D. R., and Thornton, J. A.: Phase partitioning and volatility of secondary organic aerosol components formed from α-pinene ozonolysis and OH oxidation: the importance of accretion products and other low volatility compounds, Atmos. Chem. Phys., 15, 7765-7776, 10.5194/acp-15-7765-2015, 2015.

Lopez-Hilfiker, F. D., Pospisilova, V., Huang, W., Kalberer, M., Mohr, C., Stefenelli, G., Thornton, J. A., Baltensperger, U., Prevot, A. S. H., and Slowik, J. G.: An extractive electrospray ionization time-of-flight mass spectrometer (EESI-TOF) for online measurement of atmospheric aerosol particles, Atmospheric Measurement Techniques, 12, 4867-4886, 10.5194/amt-12-4867-2019, 2019.

Luoma, K., Niemi, J. V., Helin, A., Aurela, M., Timonen, H., Virkkula, A., Rönkkö, T., Kousa, A., Fung, P. L., Hussein, T., and Petäjä, T.: Spatiotemporal variation and trends of equivalent black carbon in the Helsinki metropolitan area in Finland, Atmospheric Chemistry and Physics Discussions, 2020, 1-30, 10.5194/acp-2020-201, 2020.

MacQueen, J.: Some methods for classification and analysis of multivariate observations, Proceedings of the fifth Berkeley symposium on mathematical statistics and probability, 21 June–18 July 1965 and 27 December 1965–7 January 1966, Statistical Laboratory of the University of California, Berkeley, USA, 281–297, 1967.

Marais, E. A., Jacob, D. J., Jimenez, J. L., Campuzano-Jost, P., Day, D. A., Hu, W., Krechmer, J., Zhu, L., Kim, P. S., Miller, C. C., Fisher, J. A., Travis, K., Yu, K., Hanisco, T. F., Wolfe, G. M., Arkinson, H. L., Pye, H. O. T., Froyd, K. D., Liao, J., and McNeill, V. F.: Aqueous-phase mechanism for secondary organic aerosol formation from isoprene: application to the southeast United States and co-benefit of SO2 emission controls, Atmospheric Chemistry and Physics, 16, 1603-1618, 10.5194/acp-16-1603-2016, 2016.

McFiggans, G., Artaxo, P., Baltensperger, U., Coe, H., Facchini, M. C., Feingold, G., Fuzzi, S., Gysel, M., Laaksonen, A., Lohmann, U., Mentel, T. F., Murphy, D. M., O'Dowd, C. D., Snider, J. R., and Weingartner, E.: The effect of physical and chemical aerosol properties on warm cloud droplet activation, Atmos. Chem. Phys., 6, 2593-2649, 10.5194/acp-6-2593-2006, 2006.

McFiggans, G., Mentel, T. F., Wildt, J., Pullinen, I., Kang, S., Kleist, E., Schmitt, S., Springer, M., Tillmann, R., Wu, C., Zhao, D., Hallquist, M., Faxon, C., Le Breton, M., Hallquist, Å. M., Simpson, D., Bergström, R., Jenkin, M. E., Ehn, M., Thornton, J. A., Alfarra, M. R., Bannan, T. J., Percival, C. J., Priestley, M., Topping, D., and Kiendler-Scharr, A.: Secondary organic aerosol reduced by mixture of atmospheric vapours, Nature, 565, 587-593, 10.1038/s41586-018-0871-y, 2019.

Mentel, T. F., Springer, M., Ehn, M., Kleist, E., Pullinen, I., Kurtén, T., Rissanen, M., Wahner, A., and Wildt, J.: Formation of highly oxidized multifunctional compounds: autoxidation of peroxy radicals formed in the ozonolysis of alkenes – deduced from structure–product relationships, Atmospheric Chemistry and Physics, 15, 6745-6765, 10.5194/acp-15-6745-2015, 2015.

Middlebrook, A. M., Bahreini, R., Jimenez, J. L., and Canagaratna, M. R.: Evaluation of composition-dependent collection efficiencies for the aerodyne aerosol mass spectrometer using field data, Aerosol Science and Technology, 46, 258-271, 2012.

Mikhailov, E. F., Mironova, S., Mironov, G., Vlasenko, S., Panov, A., Chi, X., Walter, D., Carbone, S., Artaxo, P., Heimann, M., Lavric, J., Pöschl, U., and Andreae, M.: Long-term measurements (2010–2014) of carbonaceous aerosol and carbon monoxide at the Zotino Tall Tower Observatory (ZOTTO) in central Siberia, Atmospheric Chemistry and Physics, 17, 14365-14392, 2017.

Mohr, C., Lopez-Hilfiker, F. D., Yli-Juuti, T., Heitto, A., Lutz, A., Hallquist, M., D'Ambro, E. L., Rissanen, M. P., Hao, L., Schobesberger, S., Kulmala, M., Mauldin III, R. L., Makkonen, U., Sipilä, M., Petäjä, T., and Thornton, J. A.: Ambient observations of dimers from terpene oxidation in the gas phase: Implications for new particle formation and growth, Geophysical Research Letters, 44, 2958-2966, 10.1002/2017gl072718, 2017.

Mohr, C., Thornton, J. A., Heitto, A., Lopez-Hilfiker, F. D., Lutz, A., Riipinen, I., Hong, J., Donahue, N. M., Hallquist, M., Petäjä, T., Kulmala, M., and Yli-Juuti, T.: Molecular identification of organic vapors driving atmospheric nanoparticle growth, Nature Communications, 10, 4442, 10.1038/s41467-019-12473-2, 2019.

Murphy, D. M., Cziczo, D. J., Froyd, K. D., Hudson, P. K., Matthew, B. M., Middlebrook, A. M., Peltier, R. E., Sullivan, A., Thomson, D. S., and Weber, R. J.: Single-particle mass spectrometry of tropospheric aerosol particles, Journal of Geophysical Research: Atmospheres, 111, 10.1029/2006jd007340, 2006.

Ng, N. L., Canagaratna, M. R., Zhang, Q., Jimenez, J. L., Tian, J., Ulbrich, I. M., Kroll, J. H., Docherty, K. S., Chhabra, P. S., Bahreini, R., Murphy, S. M., Seinfeld, J. H., Hildebrandt, L., Donahue, N. M., DeCarlo, P. F., Lanz, V. A., Prévôt, A. S. H., Dinar, E., Rudich, Y., and Worsnop, D. R.: Organic aerosol components observed in Northern Hemispheric datasets from Aerosol Mass Spectrometry, Atmospheric Chemistry and Physics, 10, 4625-4641, 10.5194/acp-10-4625-2010, 2010.

Ng, N. L., Canagaratna, M. R., Jimenez, J. L., Chhabra, P. S., Seinfeld, J. H., and Worsnop, D. R.: Changes in organic aerosol composition with aging inferred from aerosol mass spectra, Atmospheric Chemistry and Physics, 11, 6465-6474, 10.5194/acp-11-6465-2011, 2011a.

Ng, N. L., Herndon, S. C., Trimborn, A., Canagaratna, M. R., Croteau, P. L., Onasch, T. B., Sueper, D., Worsnop, D. R., Zhang, Q., Sun, Y. L., and Jayne, J. T.: An Aerosol Chemical Speciation Monitor (ACSM) for Routine Monitoring of the Composition and Mass Concentrations of Ambient Aerosol, Aerosol Science and Technology, 45, 780-794, 2011b.

O'Brien, R. E., and Kroll, J. H.: Photolytic Aging of Secondary Organic Aerosol: Evidence for a Substantial Photo-Recalcitrant Fraction, The Journal of Physical Chemistry Letters, 10, 4003-4009, 10.1021/acs.jpclett.9b01417, 2019.

Oke, T. R., Mills, G., Christen, A., and Voogt, J. A.: Urban Climates, Cambridge University Press, Cambridge, 2017.

Orlando, J. J., Tyndall, G. S., and Wallington, T. J.: The Atmospheric Chemistry of Alkoxy Radicals, Chemical Reviews, 103, 4657-4690, 10.1021/cr020527p, 2003.

Paatero, P.: Least squares formulation of robust non-negative factor analysis, Chemometrics and Intelligent Laboratory Systems, 37, 23-35, https://doi.org/10.1016/S0169-7439(96)00044-5, 1997.

Paatero, P., and Hopke, P. K.: Rotational tools for factor analytic models, Journal of Chemometrics, 23, 91-100, 10.1002/cem.1197, 2009.

Pai, S. J., Heald, C. L., Pierce, J. R., Farina, S. C., Marais, E. A., Jimenez, J. L., Campuzano-Jost, P., Nault, B. A., Middlebrook, A. M., Coe, H., Shilling, J. E., Bahreini, R., Dingle, J. H., and Vu, K.: An evaluation of global organic aerosol schemes using airborne observations, Atmospheric Chemistry and Physics, 20, 2637-2665, 10.5194/acp-20-2637-2020, 2020.

Paramonov, M.: Life cycle of a cloud condensation nucleus, CCN, Report Series in Aerosol Science, 2015.

Parworth, C., Fast, J., Mei, F., Shippert, T., Sivaraman, C., Tilp, A., Watson, T., and Zhang, Q.: Long-term measurements of submicrometer aerosol chemistry at the Southern Great Plains (SGP) using an Aerosol Chemical Speciation Monitor (ACSM), Atmospheric Environment, 106, 43-55, https://doi.org/10.1016/j.atmosenv.2015.01.060, 2015.

Patokoski, J., Ruuskanen, T. M., Kajos, M. K., Taipale, R., Rantala, P., Aalto, J., Ryyppö, T., Nieminen, T., Hakola, H., and Rinne, J.: Sources of long-lived atmospheric VOCs at the rural boreal forest site, SMEAR II, Atmospheric Chemistry and Physics, 15, 13413-13432, 2015.

Peräkylä, O.: Production of Condensible Vapours from Monoterpene Oxidation, Report Series in Aerosol Science, 2020.

Petters, M. D., and Kreidenweis, S. M.: A single parameter representation of hygroscopic growth and cloud condensation nucleus activity, Atmospheric Chemistry and Physics, 7, 1961-1971, 10.5194/acp-7-1961-2007, 2007.

Pospisilova, V., Lopez-Hilfiker, F. D., Bell, D. M., El Haddad, I., Mohr, C., Huang, W., Heikkinen, L., Xiao, M., Dommen, J., Prevot, A. S. H., Baltensperger, U., and Slowik, J. G.: On the fate of oxygenated organic molecules in atmospheric aerosol particles, Science Advances, 6, eaax8922, 10.1126/sciadv.aax8922, 2020.

Poulain, L., Spindler, G., Grüner, A., Tuch, T., Stieger, B., van Pinxteren, D., Herrmann, H., and Wiedensohler, A.: Multi-Year ACSM measurements at the Central European Research Station Melpitz (Germany) Part I: Instrument Robustness, Quality Assurance, and Impact of Upper Size Cut-Off Diameter, Atmospheric Measurement Techniques, 2019, 1-32, 10.5194/amt-2019-361, 2019.

Prăvălie, R.: Major perturbations in the Earth's forest ecosystems. Possible implications for global warming, Earth-Science Reviews, 185, 544-571, 2018.

Presto, A. A., Huff Hartz, K. E., and Donahue, N. M.: Secondary Organic Aerosol Production from Terpene Ozonolysis. 1. Effect of UV Radiation, Environmental Science & Technology, 39, 7036-7045, 10.1021/es050174m, 2005.

Pye, H. O. T., and Seinfeld, J. H.: A global perspective on aerosol from low-volatility organic compounds, Atmos. Chem. Phys., 10, 4377-4401, 10.5194/acp-10-4377-2010, 2010.

Pye, H. O. T., Nenes, A., Alexander, B., Ault, A. P., Barth, M. C., Clegg, S. L., Collett Jr, J. L., Fahey, K. M., Hennigan, C. J., Herrmann, H., Kanakidou, M., Kelly, J. T., Ku, I. T., McNeill, V. F., Riemer, N., Schaefer, T., Shi, G., Tilgner, A., Walker, J. T., Wang, T., Weber, R., Xing, J., Zaveri, R. A., and Zuend, A.: The acidity of atmospheric particles and clouds, Atmospheric Chemistry and Physics, 20, 4809-4888, 10.5194/acp-20-4809-2020, 2020.

Riipinen, I., Pierce, J. R., Yli-Juuti, T., Nieminen, T., Häkkinen, S., Ehn, M., Junninen, H., Lehtipalo, K., Petäjä, T., Slowik, J., Chang, R., Shantz, N. C., Abbatt, J., Leaitch, W. R., Kerminen, V. M., Worsnop, D. R., Pandis, S. N., Donahue, N. M., and Kulmala, M.: Organic condensation: a vital link connecting aerosol formation to cloud condensation nuclei (CCN) concentrations, Atmospheric Chemistry and Physics, 11, 3865-3878, 10.5194/acp-11-3865-2011, 2011.

Riipinen, I., Yli-Juuti, T., Pierce, J. R., Petäjä, T., Worsnop, D. R., Kulmala, M., and Donahue, N. M.: The contribution of organics to atmospheric nanoparticle growth, Nature Geoscience, 5, 453-458, 10.1038/ngeo1499, 2012.

Rinne, J., Bäck, J., and Hakola, H.: Biogenic volatile organic compound emissions from the Eurasian taiga: current knowledge and future directions, Boreal Environment Research, 14, 807-826, 2009.

Riuttanen, L., Hulkkonen, M., Maso, M. D., Junninen, H., and Kulmala, M.: Trajectory analysis of atmospheric transport of fine particles, SO2, NOx and O3 to the SMEAR II station in Finland in 1996–2008, Atmospheric Chemistry and Physics, 13, 2153-2164, 2013.

Riva, M.: Multiphase Chemistry of Highly Oxidized Molecules: The Case of Organic Hydroperoxides, Chem, 1, 526-528, https://doi.org/10.1016/j.chempr.2016.09.015, 2016.

Riva, M., Chen, Y., Zhang, Y., Lei, Z., Olson, N. E., Boyer, H. C., Narayan, S., Yee, L. D., Green, H. S., Cui, T., Zhang, Z., Baumann, K., Fort, M., Edgerton, E., Budisulistiorini, S. H., Rose, C. A., Ribeiro, I. O., e Oliveira, R. L., dos Santos, E. O., Machado, C. M. D., Szopa, S., Zhao, Y., Alves, E. G., de Sá, S. S., Hu, W., Knipping, E. M., Shaw, S. L., Duvoisin Junior, S., de Souza, R. A. F., Palm, B. B., Jimenez, J.-L., Glasius, M., Goldstein, A. H., Pye, H. O. T., Gold, A., Turpin, B. J., Vizuete, W., Martin, S. T., Thornton, J. A., Dutcher, C. S., Ault, A. P., and Surratt, J. D.: Increasing Isoprene Epoxydiol-to-Inorganic Sulfate Aerosol Ratio Results in Extensive Conversion of Inorganic Sulfate to Organosulfur Forms: Implications for Aerosol Physicochemical Properties, Environmental Science & Technology, 53, 8682-8694, 10.1021/acs.est.9b01019, 2019a.

Riva, M., Rantala, P., Krechmer, J. E., Peräkylä, O., Zhang, Y., Heikkinen, L., Garmash, O., Yan, C., Kulmala, M., Worsnop, D., and Ehn, M.: Evaluating the performance of five different chemical ionization techniques for detecting gaseous oxygenated organic species, Atmospheric Measurement Techniques, 12, 2403-2421, 10.5194/amt-12-2403-2019, 2019b.

Robinson, A. L., Donahue, N. M., Shrivastava, M. K., Weitkamp, E. A., Sage, A. M., Grieshop, A. P., Lane, T. E., Pierce, J. R., and Pandis, S. N.: Rethinking Organic Aerosols: Semivolatile Emissions and Photochemical Aging, Science, 315, 1259-1262, 10.1126/science.1133061 2007.

Roldin, P., Eriksson, A. C., Nordin, E. Z., Hermansson, E., Mogensen, D., Rusanen, A., Boy, M., Swietlicki, E., Svenningsson, B., Zelenyuk, A., and Pagels, J.: Modelling non-equilibrium secondary organic aerosol formation and evaporation with the aerosol dynamics, gas- and particle-phase chemistry

kinetic multilayer model ADCHAM, Atmospheric Chemistry and Physics, 14, 7953-7993, 10.5194/acp-14-7953-2014, 2014.
Roldin, P., Ehn, M., Kurtén, T., Olenius, T., Rissanen, M. P., Sarnela, N., Elm, J., Rantala, P., Hao, L., Hyttinen, N., Heikkinen, L., Worsnop, D. R., Pichelstorfer, L., Xavier, C., Clusius, P., Öström, E., Petäjä, T., Kulmala, M., Vehkamäki, H., Virtanen, A., Riipinen, I., and Boy, M.: The role of highly oxygenated organic molecules in the Boreal aerosol-cloud-climate system, Nature Communications, 10, 4370, 10.1038/s41467-019-12338-8, 2019.
Saleh, R., Donahue, N. M., and Robinson, A. L.: Time Scales for Gas-Particle Partitioning Equilibration of Secondary Organic Aerosol Formed from Alpha-Pinene Ozonolysis, Environmental Science & Technology, 47, 5588-5594, 10.1021/es400078d, 2013.
Sandler, S. I.: Chemical, biochemical, and engineering thermodynamics, John Wiley & Sons, 2017.
Schneider, J., Weimer, S., Drewnick, F., Borrmann, S., Helas, G., Gwaze, P., Schmid, O., Andreae, M., and Kirchner, U.: Mass spectrometric analysis and aerodynamic properties of various types of combustion-related aerosol particles, International Journal of Mass Spectrometry, 258, 37-49, 2006.
Schnell, R. C., and Vali, G.: Biogenic Ice Nuclei: Part I. Terrestrial and Marine Sources, Journal of the Atmospheric Sciences, 33, 1554-1564, 10.1175/1520-0469(1976)033<1554:BINPIT>2.0.CO;2, 1976.
Schutgens, N. A. J., and Stier, P.: A pathway analysis of global aerosol processes, Atmospheric Chemistry and Physics, 14, 11657-11686, 10.5194/acp-14-11657-2014, 2014.
Scott, C. E., Rap, A., Spracklen, D. V., Forster, P. M., Carslaw, K. S., Mann, G. W., Pringle, K. J., Kivekäs, N., Kulmala, M., Lihavainen, H., and Tunved, P.: The direct and indirect radiative effects of biogenic secondary organic aerosol, Atmospheric Chemistry and Physics, 14, 447-470, 10.5194/acp-14-447-2014, 2014.
Seinfeld, J. H., Bretherton, C., Carslaw, K. S., Coe, H., DeMott, P. J., Dunlea, E. J., Feingold, G., Ghan, S., Guenther, A. B., Kahn, R., Kraucunas, I., Kreidenweis, S. M., Molina, M. J., Nenes, A., Penner, J. E., Prather, K. A., Ramanathan, V., Ramaswamy, V., Rasch, P. J., Ravishankara, A. R., Rosenfeld, D., Stephens, G., and Wood, R.: Improving our fundamental understanding of the role of aerosol−cloud interactions in the climate system, Proceedings of the National Academy of Sciences, 113, 5781-5790, 10.1073/pnas.1514043113 2016.
Seinfeld, J. H., and Pandis, S. N.: Atmospheric chemistry and physics: from air pollution to climate change, John Wiley & Sons, 2016.
Settele, J., Scholes, R., Betts, R. A., Bunn, S., Leadley, P., Nepstad, D., Overpeck, J., Taboada, M. A., Fischlin, A., and Moreno, J. M.: Terrestrial and inland water systems, in: Climate Change 2014 Impacts, Adaptation and Vulnerability: Part A: Global and Sectoral Aspects, Cambridge University Press, 271-360, 2014.
Shiraiwa, M., and Seinfeld, J. H.: Equilibration timescale of atmospheric secondary organic aerosol partitioning, Geophysical Research Letters, 39, 10.1029/2012gl054008, 2012.
Shiraiwa, M., Yee, L. D., Schilling, K. A., Loza, C. L., Craven, J. S., Zuend, A., Ziemann, P. J., and Seinfeld, J. H.: Size distribution dynamics reveal particle-phase chemistry in organic aerosol formation, Proceedings of the National Academy of Sciences, 110, 11746-11750, 10.1073/pnas.1307501110 2013.
Shrivastava, M., Easter, R. C., Liu, X., Zelenyuk, A., Singh, B., Zhang, K., Ma, P.-L., Chand, D., Ghan, S., Jimenez, J. L., Zhang, Q., Fast, J., Rasch, P. J., and Tiitta, P.: Global transformation and fate of SOA: Implications of low-volatility SOA and gas-phase fragmentation reactions, Journal of Geophysical Research: Atmospheres, 120, 4169-4195, 10.1002/2014jd022563, 2015.
Shrivastava, M., Cappa, C. D., Fan, J., Goldstein, A. H., Guenther, A. B., Jimenez, J. L., Kuang, C., Laskin, A., Martin, S. T., Ng, N. L., Petaja, T., Pierce, J. R., Rasch, P. J., Roldin, P., Seinfeld, J. H., Shilling, J., Smith, J. N., Thornton, J. A., Volkamer, R., Wang, J., Worsnop, D. R., Zaveri, R. A., Zelenyuk, A., and Zhang, Q.: Recent advances in understanding secondary organic aerosol: Implications for global climate forcing, Reviews of Geophysics, 55, 509-559, 10.1002/2016rg000540, 2017.
Shrivastava, M. K., Lipsky, E. M., Stanier, C. O., and Robinson, A. L.: Modeling Semivolatile Organic Aerosol Mass Emissions from Combustion Systems, Environmental Science & Technology, 40, 2671-2677, 10.1021/es0522231, 2006.
Simoneit, B. R. T., Schauer, J. J., Nolte, C. G., Oros, D. R., Elias, V. O., Fraser, M. P., Rogge, W. F., and Cass, G. R.: Levoglucosan, a tracer for cellulose in biomass burning and atmospheric particles, Atmospheric Environment, 33, 173-182, https://doi.org/10.1016/S1352-2310(98)00145-9, 1999.
Stark, H., Yatavelli, R. L. N., Thompson, S. L., Kang, H., Krechmer, J. E., Kimmel, J. R., Palm, B. B., Hu, W., Hayes, P. L., Day, D. A., Campuzano-Jost, P., Canagaratna, M. R., Jayne, J. T., Worsnop, D. R., and Jimenez, J. L.: Impact of Thermal Decomposition on Thermal Desorption Instruments:

Advantage of Thermogram Analysis for Quantifying Volatility Distributions of Organic Species, Environmental Science & Technology, 51, 8491-8500, 10.1021/acs.est.7b00160, 2017.

Steinhaus, H.: Sur la division des corp materiels en parties, Bulletin de l'académie polonaise des sciences, 1, 801-804, 1956.

Stocker, T. F., Qin, D., Plattner, G.-K., Alexander, L. V., Allen, S. K., Bindoff, N. L., Bréon, F.-M., Church, J. A., Cubasch, U., Emori, S., Forster, P., Friedlingstein, P., Gillett, N., Gregory, J. M., Hartmann, D. L., Jansen, E., Kirtman, B., Knutti, R., Krishna Kumar, K., Lemke, P., Marotzke, J., Masson-Delmotte, V., Meehl, G. A., Mokhov, I. I., Piao, S., Ramaswamy, V., Randall, D., Rhein, M., Rojas, M., Sabine, C., Shindell, D., Talley, L. D., Vaughan, D. G., and Xie, S.-P. S.: Technical summary, in: Climate change 2013: the physical science basis. Contribution of Working Group I to the Fifth Assessment Report of the Intergovernmental Panel on Climate Change, Cambridge University Press, 33-115, 2013.

Stolzenburg, D., Fischer, L., Vogel, A. L., Heinritzi, M., Schervish, M., Simon, M., Wagner, A. C., Dada, L., Ahonen, L. R., Amorim, A., Baccarini, A., Bauer, P. S., Baumgartner, B., Bergen, A., Bianchi, F., Breitenlechner, M., Brilke, S., Buenrostro Mazon, S., Chen, D., Dias, A., Draper, D. C., Duplissy, J., El Haddad, I., Finkenzeller, H., Frege, C., Fuchs, C., Garmash, O., Gordon, H., He, X., Helm, J., Hofbauer, V., Hoyle, C. R., Kim, C., Kirkby, J., Kontkanen, J., Kürten, A., Lampilahti, J., Lawler, M., Lehtipalo, K., Leiminger, M., Mai, H., Mathot, S., Mentler, B., Molteni, U., Nie, W., Nieminen, T., Nowak, J. B., Ojdanic, A., Onnela, A., Passananti, M., Petäjä, T., Quéléver, L. L. J., Rissanen, M. P., Sarnela, N., Schallhart, S., Tauber, C., Tomé, A., Wagner, R., Wang, M., Weitz, L., Wimmer, D., Xiao, M., Yan, C., Ye, P., Zha, Q., Baltensperger, U., Curtius, J., Dommen, J., Flagan, R. C., Kulmala, M., Smith, J. N., Worsnop, D. R., Hansel, A., Donahue, N. M., and Winkler, P. M.: Rapid growth of organic aerosol nanoparticles over a wide tropospheric temperature range, Proceedings of the National Academy of Sciences, 115, 9122-9127, 10.1073/pnas.1807604115 2018.

Surratt, J. D., Kroll, J. H., Kleindienst, T. E., Edney, E. O., Claeys, M., Sorooshian, A., Ng, N. L., Offenberg, J. H., Lewandowski, M., Jaoui, M., Flagan, R. C., and Seinfeld, J. H.: Evidence for Organosulfates in Secondary Organic Aerosol, Environmental Science & Technology, 41, 517-527, 10.1021/es062081q, 2007.

Surratt, J. D., Chan, A. W. H., Eddingsaas, N. C., Chan, M., Loza, C. L., Kwan, A. J., Hersey, S. P., Flagan, R. C., Wennberg, P. O., and Seinfeld, J. H.: Reactive intermediates revealed in secondary organic aerosol formation from isoprene, Proceedings of the National Academy of Sciences, 107, 6640-6645, 10.1073/pnas.0911114107, 2010.

Swap, R., Garstang, M., Greco, S., Talbot, R., and Kållberg, P.: Saharan dust in the Amazon Basin, Tellus B, 44, 133-149, https://doi.org/10.1034/j.1600-0889.1992.t01-1-00005.x, 1992.

Tao, Y., and Murphy, J. G.: The sensitivity of PM2.5 acidity to meteorological parameters and chemical composition changes: 10-year records from six Canadian monitoring sites, Atmos. Chem. Phys., 19, 9309-9320, 10.5194/acp-19-9309-2019, 2019.

Thornton, J. A., Mohr, C., Schobesberger, S., D'Ambro, E. L., Lee, B. H., and Lopez-Hilfiker, F. D.: Evaluating Organic Aerosol Sources and Evolution with a Combined Molecular Composition and Volatility Framework Using the Filter Inlet for Gases and Aerosols (FIGAERO), Accounts of Chemical Research, 53, 1415-1426, 10.1021/acs.accounts.0c00259, 2020.

Tröstl, J., Chuang, W. K., Gordon, H., Heinritzi, M., Yan, C., Molteni, U., Ahlm, L., Frege, C., Bianchi, F., Wagner, R., Simon, M., Lehtipalo, K., Williamson, C., Craven, J. S., Duplissy, J., Adamov, A., Almeida, J., Bernhammer, A.-K., Breitenlechner, M., Brilke, S., Dias, A., Ehrhart, S., Flagan, R. C., Franchin, A., Fuchs, C., Guida, R., Gysel, M., Hansel, A., Hoyle, C. R., Jokinen, T., Junninen, H., Kangasluoma, J., Keskinen, H., Kim, J., Krapf, M., Kürten, A., Laaksonen, A., Lawler, M., Leiminger, M., Mathot, S., Möhler, O., Nieminen, T., Onnela, A., Petäjä, T., Piel, F. M., Miettinen, P., Rissanen, M. P., Rondo, L., Sarnela, N., Schobesberger, S., Sengupta, K., Sipilä, M., Smith, J. N., Steiner, G., Tomè, A., Virtanen, A., Wagner, A. C., Weingartner, E., Wimmer, D., Winkler, P. M., Ye, P., Carslaw, K. S., Curtius, J., Dommen, J., Kirkby, J., Kulmala, M., Riipinen, I., Worsnop, D. R., Donahue, N. M., and Baltensperger, U.: The role of low-volatility organic compounds in initial particle growth in the atmosphere, Nature, 533, 527-531, 10.1038/nature18271, 2016.

Tsimpidi, A. P., Karydis, V. A., Zavala, M., Lei, W., Molina, L., Ulbrich, I. M., Jimenez, J. L., and Pandis, S. N.: Evaluation of the volatility basis-set approach for the simulation of organic aerosol formation in the Mexico City metropolitan area, Atmospheric Chemistry and Physics, 10, 525-546, 10.5194/acp-10-525-2010, 2010.

Tunved, P., Hansson, H.-C., Kerminen, V.-M., Ström, J., Maso, M. D., Lihavainen, H., Viisanen, Y., Aalto, P. P., Komppula, M., and Kulmala, M.: High Natural Aerosol Loading over Boreal Forests, Science, 312, 261-263, 10.1126/science.1123052 2006.

Twomey, S.: Pollution and the planetary albedo, Atmospheric Environment, 8, 1251-1256, 1974.
Twomey, S.: The influence of pollution on the shortwave albedo of clouds, Journal of the Atmospheric Sciences, 34, 1149-1152, 1977.
Ulbrich, I. M., Canagaratna, M. R., Zhang, Q., Worsnop, D. R., and Jimenez, J. L.: Interpretation of organic components from Positive Matrix Factorization of aerosol mass spectrometric data, Atmospheric Chemistry and Physics, 9, 2891-2918, 10.5194/acp-9-2891-2009, 2009.
Wagstrom, K. M., and Pandis, S. N.: Determination of the age distribution of primary and secondary aerosol species using a chemical transport model, Journal of Geophysical Research: Atmospheres, 114, 10.1029/2009jd011784, 2009.
Wang, L., Khalizov, A. F., Zheng, J., Xu, W., Ma, Y., Lal, V., and Zhang, R.: Atmospheric nanoparticles formed from heterogeneous reactions of organics, Nature Geoscience, 3, 238-242, 10.1038/ngeo778, 2010.
Watson, J. G., Cooper, J. A., and Huntzicker, J. J.: The effective variance weighting for least squares calculations applied to the mass balance receptor model, Atmospheric Environment (1967), 18, 1347-1355, https://doi.org/10.1016/0004-6981(84)90043-X, 1984.
Weimer, S., Alfarra, M. R., Schreiber, D., Mohr, M., Prévôt, A. S. H., and Baltensperger, U.: Organic aerosol mass spectral signatures from wood-burning emissions: Influence of burning conditions and wood type, Journal of Geophysical Research: Atmospheres, 113, 10.1029/2007jd009309, 2008.
Went, F. W.: Blue Hazes in the Atmosphere, Nature, 187, 641-643, 10.1038/187641a0, 1960.
Vereecken, L., and Peeters, J.: Enhanced H-atom abstraction from pinonaldehyde, pinonic acid, pinic acid, and related compounds: theoretical study of C–H bond strengths, Physical Chemistry Chemical Physics, 4, 467-472, 10.1039/B109370C, 2002.
Vereecken, L., and Francisco, J. S.: Theoretical studies of atmospheric reaction mechanisms in the troposphere, Chemical Society Reviews, 41, 6259-6293, 10.1039/C2CS35070J, 2012.
Williams, B. J., Goldstein, A. H., Millet, D. B., Holzinger, R., Kreisberg, N. M., Hering, S. V., White, A. B., Worsnop, D. R., Allan, J. D., and Jimenez, J. L.: Chemical speciation of organic aerosol during the International Consortium for Atmospheric Research on Transport and Transformation 2004: Results from in situ measurements, Journal of Geophysical Research: Atmospheres, 112, 10.1029/2006jd007601, 2007.
Winiger, P., Andersson, A., Eckhardt, S., Stohl, A., Semiletov, I. P., Dudarev, O. V., Charkin, A., Shakhova, N., Klimont, Z., Heyes, C., and Gustafsson, Ö.: Siberian Arctic black carbon sources constrained by model and observation, Proceedings of the National Academy of Sciences, 114, E1054-E1061, 10.1073/pnas.1613401114, 2017.
Wolff, E. W., and Cachier, H.: Concentrations and seasonal cycle of black carbon in aerosol at a coastal Antarctic station, Journal of Geophysical Research: Atmospheres, 103, 11033-11041, https://doi.org/10.1029/97JD01363, 1998.
Xu, L., Guo, H., Boyd, C. M., Klein, M., Bougiatioti, A., Cerully, K. M., Hite, J. R., Isaacman-VanWertz, G., Kreisberg, N. M., Knote, C., Olson, K., Koss, A., Goldstein, A. H., Hering, S. V., de Gouw, J., Baumann, K., Lee, S.-H., Nenes, A., Weber, R. J., and Ng, N. L.: Effects of anthropogenic emissions on aerosol formation from isoprene and monoterpenes in the southeastern United States, Proceedings of the National Academy of Sciences, 112, 37-42, 10.1073/pnas.1417609112, 2015.
Xu, W., Croteau, P., Williams, L., Canagaratna, M., Onasch, T., Cross, E., Zhang, X., Robinson, W., Worsnop, D., and Jayne, J.: Laboratory characterization of an aerosol chemical speciation monitor with PM2.5 measurement capability, Aerosol Science and Technology, 51, 69-83, 10.1080/02786826.2016.1241859, 2017.
Yan, C., Nie, W., Äijälä, M., Rissanen, M. P., Canagaratna, M. R., Massoli, P., Junninen, H., Jokinen, T., Sarnela, N., Häme, S. A. K., Schobesberger, S., Canonaco, F., Yao, L., Prévôt, A. S. H., Petäjä, T., Kulmala, M., Sipilä, M., Worsnop, D. R., and Ehn, M.: Source characterization of highly oxidized multifunctional compounds in a boreal forest environment using positive matrix factorization, Atmospheric Chemistry and Physics, 16, 12715-12731, 10.5194/acp-16-12715-2016, 2016.
Yan, C., Nie, W., Vogel, A. L., Dada, L., Lehtipalo, K., Stolzenburg, D., Wagner, R., Rissanen, M. P., Xiao, M., Ahonen, L., Fischer, L., Rose, C., Bianchi, F., Gordon, H., Simon, M., Heinritzi, M., Garmash, O., Roldin, P., Dias, A., Ye, P., Hofbauer, V., Amorim, A., Bauer, P. S., Bergen, A., Bernhammer, A.-K., Breitenlechner, M., Brilke, S., Buchholz, A., Mazon, S. B., Canagaratna, M. R., Chen, X., Ding, A., Dommen, J., Draper, D. C., Duplissy, J., Frege, C., Heyn, C., Guida, R., Hakala, J., Heikkinen, L., Hoyle, C. R., Jokinen, T., Kangasluoma, J., Kirkby, J., Kontkanen, J., Kürten, A., Lawler, M. J., Mai, H., Mathot, S., Mauldin, R. L., Molteni, U., Nichman, L., Nieminen, T., Nowak, J., Ojdanic, A., Onnela, A., Pajunoja, A., Petäjä, T., Piel, F., Quéléver, L. L. J., Sarnela, N., Schallhart, S., Sengupta, K., Sipilä, M., Tomé, A., Tröstl, J., Väisänen, O., Wagner, A. C., Ylisirniö, A., Zha,

Q., Baltensperger, U., Carslaw, K. S., Curtius, J., Flagan, R. C., Hansel, A., Riipinen, I., Smith, J. N., Virtanen, A., Winkler, P. M., Donahue, N. M., Kerminen, V.-M., Kulmala, M., Ehn, M., and Worsnop, D. R.: Size-dependent influence of NOx on the growth rates of organic aerosol particles, Science Advances, 6, eaay4945, 10.1126/sciadv.aay4945, 2020.

Yttri, K. E., Simpson, D., Nøjgaard, J. K., Kristensen, K., Genberg, J., Stenström, K., Swietlicki, E., Hillamo, R., Aurela, M., Bauer, H., Offenberg, J. H., Jaoui, M., Dye, C., Eckhardt, S., Burkhart, J. F., Stohl, A., and Glasius, M.: Source apportionment of the summer time carbonaceous aerosol at Nordic rural background sites, Atmospheric Chemistry and Physics, 11, 13339-13357, 10.5194/acp-11-13339-2011, 2011.

Yu, H., Remer, L. A., Chin, M., Bian, H., Kleidman, R. G., and Diehl, T.: A satellite-based assessment of transpacific transport of pollution aerosol, Journal of Geophysical Research: Atmospheres, 113, https://doi.org/10.1029/2007JD009349, 2008.

Zhang, Q., Worsnop, D. R., Canagaratna, M. R., and Jimenez, J. L.: Hydrocarbon-like and oxygenated organic aerosols in Pittsburgh: insights into sources and processes of organic aerosols, Atmospheric Chemistry and Physics, 5, 3289-3311, 10.5194/acp-5-3289-2005, 2005.

Zhang, Q., Jimenez, J. L., Canagaratna, M., Allan, J., Coe, H., Ulbrich, I., Alfarra, M., Takami, A., Middlebrook, A., Sun, Y., Dzepina, K., Dunlea, E. J., Docherty, K. S., DeCarlo, P. F., Salcedo, D., Onasch, T., Borrmann, S., Weimer, S., Demerjian, K., Williams, P., Bower, K., Bahreini, R., Cottrell, L., Griffin, R., Rautiainen, J., Sun, J. Y., Zhang, Y. M., and Worsnop, D.: Ubiquity and dominance of oxygenated species in organic aerosols in anthropogenically-influenced Northern Hemisphere midlatitudes, Geophysical Research Letters, 34, 2007.

Zhang, X., McVay, R. C., Huang, D. D., Dalleska, N. F., Aumont, B., Flagan, R. C., and Seinfeld, J. H.: Formation and evolution of molecular products in α-pinene secondary organic aerosol, Proceedings of the National Academy of Sciences, 112, 14168-14173, 10.1073/pnas.1517742112, 2015.

Zhang, Y., Favez, O., Petit, J. E., Canonaco, F., Truong, F., Bonnaire, N., Crenn, V., Amodeo, T., Prévôt, A. S. H., Sciare, J., Gros, V., and Albinet, A.: Six-year source apportionment of submicron organic aerosols from near-continuous highly time-resolved measurements at SIRTA (Paris area, France), Atmospheric Chemistry and Physics, 19, 14755-14776, 10.5194/acp-19-14755-2019, 2019.

Ziemann, P. J., and Atkinson, R.: Kinetics, products, and mechanisms of secondary organic aerosol formation, Chemical Society Reviews, 41, 6582-6605, 2012.

Äijälä, M., Daellenbach, K. R., Canonaco, F., Heikkinen, L., Junninen, H., Petäjä, T., Kulmala, M., Prévôt, A. S., and Ehn, M.: Constructing a data-driven receptor model for organic and inorganic aerosol–a synthesis analysis of eight mass spectrometric data sets from a boreal forest site, Atmospheric Chemistry and Physics, 19, 3645-3672, 2019.

Öström, E., Putian, Z., Schurgers, G., Mishurov, M., Kivekäs, N., Lihavainen, H., Ehn, M., Rissanen, M. P., Kurtén, T., Boy, M., Swietlicki, E., and Roldin, P.: Modeling the role of highly oxidized multifunctional organic molecules for the growth of new particles over the boreal forest region, Atmospheric Chemistry and Physics, 17, 8887-8901, 10.5194/acp-17-8887-2017, 2017.